The Adhesion Force Study of Dairy Thermophile *Anoxybacillus flavithermus* CM with Atomic Force Microscopy

A thesis presented in partial fulfilment of the requirements for the degree of

Master of Engineering
in
Chemical & Nanotechnology

at Massey University, Manawatu,
New Zealand

Mohd Salihin Mohd Saidi

2014

Abstract

Anoxybacillus flavithermus is a common species of thermophilic bacteria discovered in most milk powder manufacturing plants through out New Zealand. The contamination of it's spores into the finished milk powder is an on-going problem as these spores are able to survive the sterilization process. Cheating death, *A. flavithermus* spores were then believed to attached on the stainless steel surface piping of the production line and germinate into a mature bacteria. A single surviving spore could grow to produce more spores that eventually dislodged from the colony and deposited together with the packaged milk powder. Over the storage time, the contaminated product will gives an off flavor as it deteriorates from bacterial action within.

Currently, the applied cleaning method is by rinsing the target section with 1% sodium hydroxide & acid solutions before being flushed out to remove any microorganisms attached on the interior surfaces. However, it is not very effective in removing spores and there is very little information on the value of the spore's adhesion force on a stainless steel surface. With that in mind, the aim of this study is to determine a proper adhesion force value between a dairy strain spore, *A.flavithermus* CM and stainless steel surface using the Atomic Force Microscopy (AFM) system. Meanwhile, *Geobacillus strearothermophilus* ATCC 2641 which is also a thermophilic organism was used over the study for comparison purpose.

To measure the adhesion force under an Atomic Force Microscopy (AFM), the crude suspension was first purified using two-phase separation method. Polyethylene glycol (PEG) and phosphate buffer were used as the phase separation chemicals while 0.1% polysorbate 20 was added to the freshly purified spores' suspension to aid the imaging sequence under the AFM. All AFM imaging and force measurements were done in air and conducted using the silicon type CSG 11/Au cantilever. The crucial Force-Volume imaging was done on a 32x32 grid scan size (1024 samples) on a scan rate of 0.5 Hz.

It was calculated that a single *A. flavithermus* CM spore has an adhesive force value of 16.8 μN when attached on a stainless steel surface. It has a stronger localize adhesive value of 3.9 nN than a *G.stearothermophilus* ATCC 2641 spore with just 3.6 nN. However, *G.stearothermophilus* ATCC 2641 has a larger adhesive force of 21.1 μN on a stainless steel surface due to it's larger spore size. It was also found that spore's hydrophobicity does not dictates the magnitude of it's adhesion on any surface.

The results from this study have provide the dairy industry an extra sight on the quantitative value of the adhesion force of thermophilic spores, particularly *A.flavithermus* CM. This will help the dairy industry to design strategies in preventing spores from adhering to its production lines.

Contents

Table of Figures

1 Introduction: Literature Review

1.1 Milk powder manufacture

Manufacturing milk powder involves the gentle removal of water to a product with high solubility (Baldwin, 2002) at the lowest possible cost with strict hygiene conditions (Pearce, 1996). The purpose is to convert the perishable raw milk to a product that can survive years of storage without substantial loss of its quality (Walstra, Geurts, Noomen, Jellema, & van Boekel, 1999). Raw milk is transferred from holding tanks in farms to storage silos at the milk powder's production plant. Roller drying and spray drying are two well utilized drying methods in the early development stages but dairy powders today are generally made by spray drying (Baldwin, 2002). Freeze-dried milk formed voluminous powder particles that easily dissolved and has minimal heat treatment's damages (Walstra *et al.*, 1999).

1.1.1 Milk powder manufacturing steps

The first treatment of raw milk involves separation, standardization and pasteurization. The basic of milk separation is using a centrifuge separator where skim milk and cream are discharged through centripetal pumps. Pasteurization provides the safety and enhanced the shelf life of the product. Meanwhile, standardization was done by re-adding either skim milk or cream in the storage tank based on legal requirements or manufacturer's standard. During storage in buffer silo, milk thermalized milk will be cooled at 7 ^{o}C to retard spoilage (Walstra *et al.*, 1999). The general milk powder manufacturing process is outlined in Figure 1.

Preheating is an efficient method to utilize the waste heat disposed from the warm air of the evaporator and spray dryer (Kristensen, 2010). Plate heat exchanger (PHE) or direct steam injections (DSI) are two common method of preheating which will heat the standardized milk to a temperature between 75 ^{o}C to 120 ^{o}C (Pearce, 1996).

Falling film evaporator is commonly used as it requires a short holding time and the concept of multi-stages greatly reduces the energy consumption. Meanwhile, using multiple effects evaporator will increase the water removal efficiency (Kristensen, 2010). Modern plant may have up to seven effects that removed up to 85% of the water in the milk (Pearce, 1996). A fine film of milk or concentrate is passed down the surface of a tube with steam in the other side which then recompressed in a vapour recompressor for a better efficient usage (Milk Powder Production, n.d.).

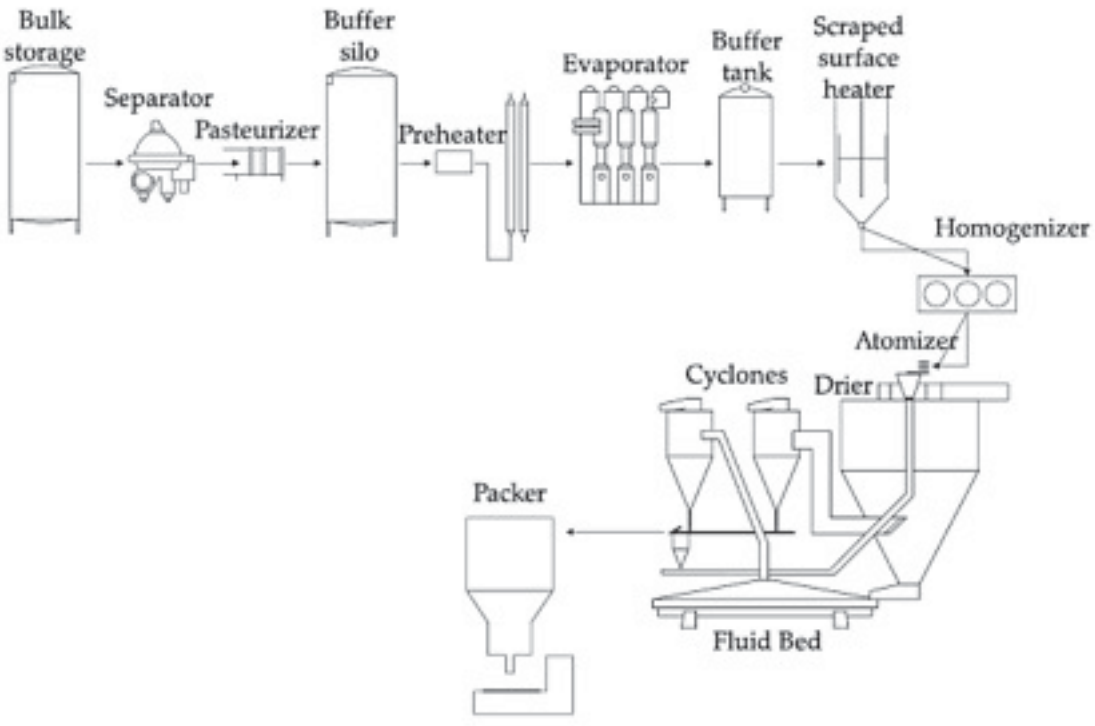

Figure 1: Schematic of milk powder manufacturing process (adapted from Pearce, 1996)

After evaporation stages, milk concentrate undergoes the next preheating & homogenization process followed by drying. The preheating lowers the drying heat load when passed through the spray dryer (Scott, 2005). It also controls the denaturation of the whey proteins and imparts heat stability of the milk (Pearce, 1996; Walstra *et al.*, 1999). Homogenization reduces the milk fat globule size which resulting in low free-fat content in the milk powder. Homogenization is not always necessary if the atomization during spray drying process will effectively disrupt the fat globules in the concentrated milk (Milk Powder Production, n.d.; Walstra *et al.,* 1999).

Roller drying and spray drying are two different production methods of milk powder in the early stages. Nowadays, spray drying was the universal norm while roller drying is used for specialty product (Baldwin, 2002) . Spray drying can be separated into three stages. Firstly, it is required to atomize the concentrated milk into a hot air stream up to 200 ^{o}C. It involves using either a spinning disc atomiser or a series of high pressure nozzles. Atomization via high pressure nozzle also removes the need of homogenization prior to spray drying. The fine droplets were mixed with hot air in the main drying chamber with a static fluid bed at the base of the chamber. The second stage is the second vibrating fluid bed dryer where powder leaves the dryer and enters the system of cyclones that simultaneously cools it (Milk Powder Production, n.d.; Pearce, 1996). Small particles or fines from cyclones are returned into the chamber to produce an agglomerated powder. Agglomerated powder formed when fines collided with atomised milk concentrate (Baldwin, 2002; Pearce, 1996). The milk powder was later packaged as a product that is small & easy to transport with a much longer shelf life than pasteurised milk.

1.1.2 Hygine in manufacturing plant – Clean-In-Place (CIP)

The main aim of cleaning is to remove any material that causes growth of microorganisms and deposits that impairs the production efficiency. Circulation cleaning or cleaning-in-place is primarily applied. The most applied method is pre-rinsing with water before 1% Sodium Hydroxide then acid rinse applied. Cleaning agents then flushed with water (Walstra *et al.*, 1999). Storage silos, separators and evaporators must be cleaned daily while large spray dryer is given an occasional rinse (Baldwin, 2002).

1.2 Thermophilic contamination of milk powder in manufacturing plant

The presence of high numbers (>10^4 cfu/g) of thermophiles in finished dairy products, like milk powders is an indicator of poor hygiene during processing. Obligate thermophiles are not known to be pathogenic(Burgess, Lindsay, & Flint, 2010). For example, *G. stearothermophilus* has been associated with 'flat-sour' spoilage in a variety of canned food products, including evaporated milk.(Ito, 1981; Kalogridou-Vassiliadou, 1992).

There are three factors that increase the survivability of microorganisms following the production of milk powder which are water activity, relative humidity and storage temperature (Higginbottom, 1953; Stapelfeldt, Nielsen, & Skibsted, 1997). Most dairy products are stored at temperature below 37 ^oC, in which obligate thermophiles will not grow(Burgess *et al.*, 2010).

1.2.1 Source of thermophiles

In a milk powder plant, the initial contamination of thermophiles is believed to arise from low numbers of spores present in the raw milk that survive pasteurization (Burgess, Brooks, Rakonjac, Walker, & Flint, 2009). The organism is characterized by the ability of its spores to survive pasteurization (73 ^oC, 15 s) and grow at 65 ^oC. The bacteria are present at low levels in raw milk, but may reach high levels in dairy products. This suggests that the bacteria grow during the manufacturing process (S. Flint, Palmer, Bloemen, Brooks, & Crawford, 2001). Few studies have the information as how thermophilic bacteria contaminated and forms biofilms within a milk powder plant (S. Flint *et al.*, 2001; Parkar, Flint, & Brooks, 2003; Parkar, Flint, Palmer, & Brooks, 2001). Although both vegetative cells and spores are found in the biofilms, it was shown that a greater amount of spores bind to stainless steel wall(S. Flint *et al.*, 2001)

1.2.2 Thermophilic spores \ endospores

Sporulation bacteria is a last ditch survival act which mainly triggered by nutritional starvation. Endospore formers usually induced its motility and even commit cannibalism before initiating sporulation. Even then, few factors must be met for a successful sporulation such as high cell density and chromosome integrity. These checklists ensure that once sporulation has started, it can be successfully completed (Grossman & Losick, 1988; Stephens, 1998).

(Russell, 1982) had compiles a sporulation cycles of an endospore forming bacteria that could be divided into seven stages as shown in Table 1. Figure 2 shows the development stages with red loop represents the DNA of the bacteria.

Table 1. Summary of stages in sporulation process (Russell, 1982)

Stage	Characteristics
0	Vegetative cell
1	Pre-septation: DNA in axial filament form. Extracellular products (amylase, proteases and antibiotics) appear
2	Septation: Separation of chromosmes resulting in asymmetric cell formation.
3	Engulfment of forespore: membrane of developing spore becomes completely detached from that of mother cell to give the spore protoplast. Appearance of characteristic enzymes
4	Cortex formation begins to be laid down between the two membranes of the protoplast. Refractility begins to develop, commencement of
5	peptidoglycan synthesis.
6	Synthesis of spore coat. DPA deposition, uptake of Ca2+. Development of resistance to organic solvents (octanol, chloroform).
7	Spora maturation: coat material becomes more dense, increase in refractility, development of heat resistance.
	Lysis of the mother cell, and liberation of mature spore

There are several other factors that influence spore formation besides starvation, high cell density and damage of DNA. These factors includes temperature, pH, oxygen's concentration, important minerals (manganese, carbon & nitrogenous compound) and type of sporulation media (Russell, 1982). Understanding the concept and requirement for sporulation is important as this knowledge could help in the prediction of spore occurrences.

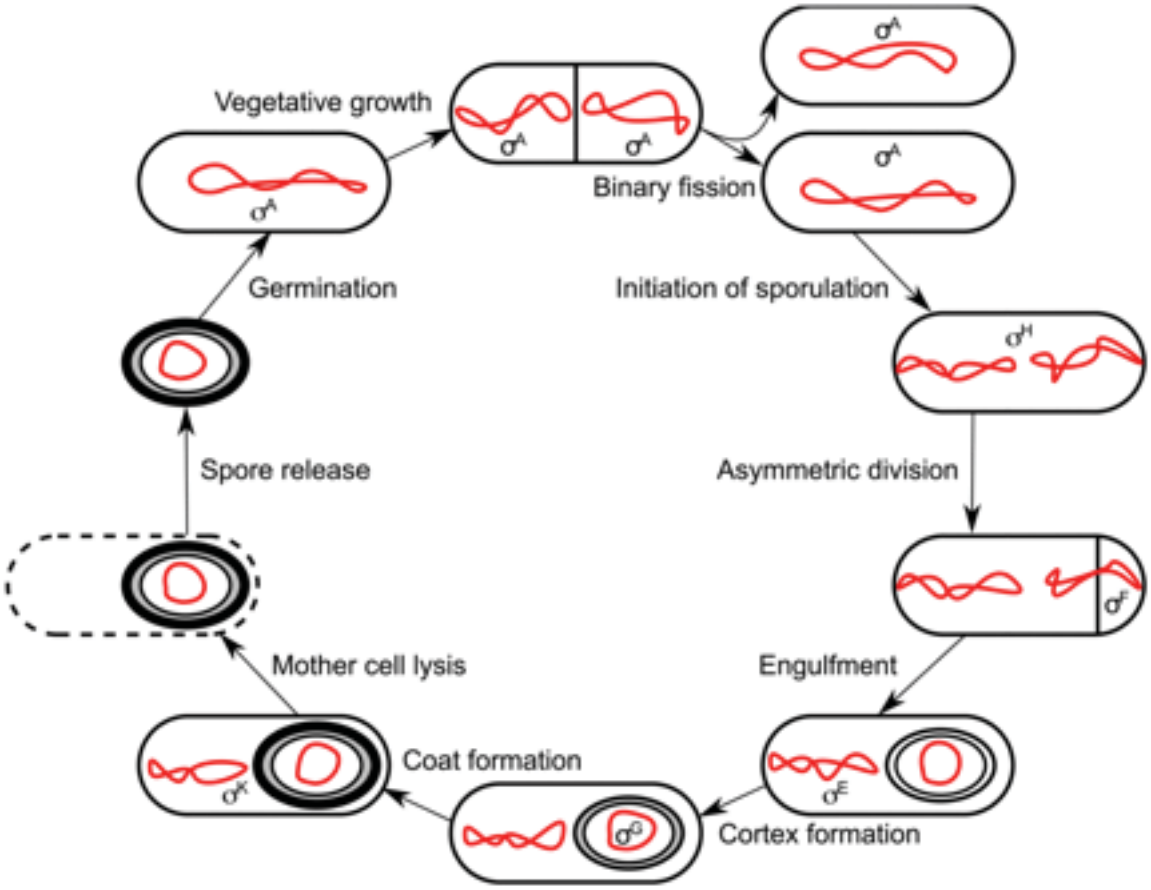

Figure 2: Stages in the development of bacterial spores (de Hoon, Eichenberger, & Vitkup, 2010)

A complete spore consist of four structures; protoplast, cortex, spore coat and exosporium. The major differences between species are the variation layers of spore coat and exosporium. Comparing the various structures, the cortex plays an important part in the heat resistance of spores and the coats usually imply in the chemical resistance region (Russell, 1982). Some bacteria such as *B. subtilis* does not has an exosporium while others such as the pathogenic *B. anthracis* and *B. cereus* are encased in exosporium after the coat (Adriano & Charles, 2007).

The two unique components of spores are dipicolinic acid (DPA) and peptidoglycan that contribute to the heat resistance status of spores (Church & Halvorson, 1959; Warth & Strominger, 1972) Other factors for its survivability are low permeability to toxic chemical and low water content of the core. Besides, binding the spore's DNA with a group of acid soluble proteins increases it's resistance to damage by radiation (Setlow, 1995).

1.2.3 Dairy fouling

The undesirable milk product that adheres to the surface is commonly associated with heating in evaporation & drying section. The foolant is removed by clean-in-place chemical cleaning method every 10 to 40 hours of operation (Baldwin, 2002). Fouled surfaces have higher number of vegetative cells and spores of *Geobacillus spp.* On fouled surface suggesting fouling may play a major role in the colonization of dairy manufacturing plant (S. Flint *et al.*, 2001).

1.2.4 Biofilms

Biofilm of thermophilic bacilli can develop rapidly to levels that cause significant contamination of milk passing the biofilm. Thus, represent a source of contamination of dairy products (S. Flint *et al.*, 2001). The biofilms could develop from spores and release vegetative cells at 8 h and spores at 14 h post-inoculation. Similar behaviour was observes in the manufacturing environment. Results showed that spores comprised as much as 10-50% of an 8 h *A. flavithermus* biofilms (Burgess *et al.*, 2009) . Meanwhile, *Geobacillus spp.* was able to form biofilm after a 6 hour incubation period (S. Flint *et al.*, 2001).

1.2.5 Pasteurization

Studies had showed that thermophilic bacteria spores like *Geobacillus spp* has heat resistance ability up to 126.6 ^{o}C (Yildiz & Westhoff, 1989). In the dairy industry, heat is the most likely mechanism of thermophilic spore activation, because of the extensive use of heat as a preservation technology. Hence, the act of pasteurization does not destroy the heat resistance endospores and might behave as a double edge sword. Although it destroys any living bacteria, pasteurization heat also activates any existing spores in the milk which are already encouraged by the availability of crucial minerals that induced sporulation (Burgess *et al.*, 2010).

Making things worst, endospores are also resistance to other treatments such as cooling, irradiation, hydrostatic pressure, and chemicals. The feasibility of bacteriocin/ enterocin treatment to heat resistance endospores has been surfacing in literature years back. This biopreservation shows that it could decrease the heat resistance or even deactivated the endospores (Galvez, Abriouel, Lopez, & Ben Omar, 2007). As concrete as a reality it could be, this is where it gets dicey. As biopreservation is in its early stages, food safety requirements is still a massive challenge to overcome and not to mention the production hurdle of bacteriocin itself (Gautam & Sharma, 2009; Holo *et al.*, 2002).

1.3 The phylogeny of genus Bacillus

Anoxybacillus flavithermus and *Geobacillus spp*. are the most common thermophilic contaminants found in milk powder. *Bacillus licheniformis* and *Bacillus subtilis* are the minor contaminants in milk powder (Burgess *et al.*, 2010; Ron S. Ronimus *et al.*, 2003; Seale, Flint, McQuillan, & Bremer, 2008). Eventhough they are common, *A. flavithermus* and *G. stearothermophilus* are relatively a newly discovered bacteria. Eventhough, it is suggested that both species did not survive a long-term storage based on samples from 1907's British Antarctic Expedition (Ron S Ronimus, Rueckert, & Morgan, 2006).

1.3.1 Anoxybacillus *flavithermus*

Formerly known as *Bacillus flavothermus*, this first isolated facultative thermophile was from hot spring in northern island of New Zealand (Heinen, Lauwers, & Mulders, 1982). Other isolates later immerged from Yellowstone National Park (Nold, Kopczynski, & Ward, 1996), Turkey (Beldüz, Dülger, Demirbağ, & Ertürk, 2000) and China (Dai *et al.*, 2011). It is also reported present in gelatine extract (De Clerck *et al.*, 2004) and milk powder (Ron S. Ronimus *et al.*, 2003). It was then revised to

Anoxybacillus species when another strain, A. *pushchinoensis* immerged as strict anaerobe similar to *A. flavithermus* (Pikuta *et al.*, 2000). This species since had been revised of being aerotolerant anaerobe or facultative anaerobes (Pikuta, Cleland, & Tang, 2003).

A.flavithermus can be characterised with rod shaped structure, 0.85 x 2.3-7.1 μm that forms a dark yellow colony at warm to high temperature up to 70 degrees Celsius (Pikuta *et al.*, 2000). The bacteria is observed as motile, facultative anaerobic with gram positive coating upon its first isolation. It is able to grow in condition richer than normal hot spring environment while its optimum growth temperature varies between strains. The New Zealand's hot spring isolate has a growth range between 30 and 70 degree Celsius while isolated from milk powder range between 50 and 65 degrees Celsius (Burgess *et al.*, 2010; Heinen *et al.*, 1982; Ron S. Ronimus *et al.*, 2003).

1.3.2 Geobacillus genus: *G. stearothermophilus* and *G. thermoleovorans*

Formely known as *Bacillus stearothermophilus* and was extensively studied (S. Flint *et al.*, 2001; Ron S. Ronimus *et al.*, 2003). Previously classified in Group 5 of *Bacillus* genus with other species (Ash, Farrow, Wallbanks, & Collins, 1991), this group had later been revised into a new validly-described genus called *Geobacillus* . Various strains have been isolated in various environments throughout the world such as central Asia's oilfield (Nazina *et al.*, 2001), geothermal system of Antartica (Nicolaus *et al.*, 1996), sugar refineries (Tai, Lin, Kuo, & Liu, 2004) and dairy plant (Prickett, 1928) .

G. stearothermophilus is a fat and heat loving bacterium that can be isolated from dairy milk, rotting wood and sometimes natural hot spring. Meanwhile, *G. thermoleovans* is capable on utilizing hydrocarbons as a carbon source (Zeigler & Daniel, 2001). The majority of *Geobacillus* species isolated from dairy plant or milk powder can be related to *G. stearothermophilus* (S. Flint *et al.*, 2001; Ron S. Ronimus *et al.*, 2003). The optimum growth temperature for dairy isolates is between 55 – 70 ^{o}C (Ron S. Ronimus *et al.*, 2003).

1.4 Adhesion forces between bacterial spores & dryer bed

Bacteria adhesion to solid surfaces occurs in a variety of system in dairy plant and mostly causes problems such as fouling and contamination. Hence, it should be in great interest to study the mechanism underlying adhesion.

It was found that the germinating spores have higher adhesion forces compared to their dormant counterpart. Strong adhesion forces measured at the surface of germinating spores may come from the increase of surface polysaccharide and also increase in cell surface hydrophocity (Dufrêne, Boonaert, van der Mei, Busscher, & Rouxhet, 2001).

1.4.1 Hydrophilic and hydrophobic surfaces

Most studies on hydrophobicity of spores to substrate uses hydrophobic interaction chromatography (HIC) and microbial adhesion to hydrocarbon (MATH) test (Husmark & Rönner, 1992; Palmer, Flint, Schmid, & Brooks, 2010; Seale *et al.*, 2008). Many studies have mixed reviews regarding either spores are hydrophobic (Koshikawa *et*

al., 1989; Wiencek, Klapes, & Foegeding, 1990) or hydrophilic (Seale *et al.*, 2008). However, the relative hydrophobicity measured was between 10 to 58% and decent amount of spores are still found adhered on the surfaces tested.

Besides the spores, the substrate itself could behave as either hydrophilic or hydrophobic surface. Relative surface hydrophobicity can be measured using water contact angle method with a hydrophilic surface has a small contact angle while a very hydrophobic surface is at the high end scale (Rosenberg & Kjelleberg, 1986). A hydrophilic stainless steel surface has a water contact angle of 25^{o} while when treated with strong acid or oxidized turns it into a hydrophobic surface with a water contact angle value of 60^{o} and 82^{o} respectively. Meanwhile, a very clean glass surface is highly hydrophilic and turns highly hydrophobic when treated with methyl silane showing water contact angle value of 5^{o} and 90^{o} respectively (Rönner, Husmark, & Henriksson, 1990).

1.4.2 Ionic charges / surface charges

The net-surface charge varies between spores and adhesion of spore to hydrophobic substrate shows species with less surface charge has higher adhesion success (Husmark & Rönner, 1992). However, spores with stronger negative charge also has greater ability to adhere to substrate due to existence of positively charged domains that mediated attachment despite existing electrostatic repulsion (Palmer *et al.*, 2010).

1.4.3 Cell-surface proteins

Some studies also pointed that cell-surface protein plays the role in the attachment to surfaces (S. H. Flint, Brooks, & Bremer, 1997; Parkar *et al.*, 2001). Earlier studies shows no correlation between removal of spore coat proteins to the adhesion or attachment ability (Parkar *et al.*, 2001). However, *A.flavithermus* has less ability to attach on the stainless steel surface once the removal of its surface proteins (Palmer *et al.*, 2010). Meanwhile, some studies also pointed at polysaccharide layers that aide the adhesion (Dufrêne *et al.*, 2001; Faille *et al.*, 2010; Wiencek *et al.*, 1990) and appendages on spore's exosporium (Faille *et al.*, 2010; Husmark & Rönner, 1992).

Various studies on this field had only reinforced the fact that there is no simple relationship between individual physicochemical interactions with the adhesion and attachment capabilities of spores. Meanwhile, there are also variables of the substrate itself.

1.4.4 Force on stainless steel

As a substrate, stainless steel usually has a net-negative charge at neutral pH (Palmer *et al.*, 2010). It was reported that *Geobacillus spp.* Spores are preferably attached to stainless steel than the vegetative cells. (S. Flint *et al.*, 2001). Meanwhile, spores also tend to adhere more to a hydrophobic surface than to the hydrophilic surface (Husmark & Rönner, 1992) and adsorbed milk proteins on the surface of hydrophobic stainless steel reduce the adhesion of spores on it (Parkar *et al.*, 2001).

Discussing all these factors, adhesion and attachment is dependent on a complex and poorly defined relationship. Spores of different species will have different

characteristic in adhesion factor (Faille *et al.*, 2002; Parkar *et al.*, 2001) and even species of different strains varies (Palmer *et al.*, 2010).

1.4.5 Existing methods on removing or preventing spores in dairy product

It is demonstrated that it is feasible to control the thermophilic biofilms by lowering the temperature of the growth environment to 48 ^{o}C by preventing the formation of spores of *A. flavithermus* (Burgess *et al.*, 2009). It is believed that the future development in preventing biofilms in dairy plants are likely to focus on altering the manufacturing conditions, reducing bacterial attachment by manipulating stainless steel's surface and developing novel sanitizer (Bremer *et al.*, 2009).

1.5 The Atomic Force Microscopy (AFM)

1.5.1 Background and AFM today

In 1987, Gerd Binnig and Calvin Quate of Standord University and Christoph Gerber from IBM proposed a force measurement method to investigate a surface of interest on an atomic scale. It involves monitoring the deformation of spring with the existing Scanning Tunneling Microscope (Binnig, Quate, & Gerber, 1986) creating a new type of Scanning Probe Microscope.

Ultimately, it is about measuring forces or interaction between a sharp probing tip and a sample surface.It is a marriage of a mechanical profilometer with a piezoelectric transducers (Meyer, 1992). In other words an AFM images by 'feeling' the surface it's sampling. On that note, a person without eyesight is basically an AFM?

A year later, the first set of atomic resolution images were published on graphite (Binnig, Gerber, Stoll, Albrecht, & Quate, 1987) and a non-conductor element (Albrecht & Quate, 1987).

The basic principle of AFM is using a sharp probing tip mounted on a cantilever type spring which forces the tip to deflect when in contact with sample. This deflection is monitored by photodiode sensor connected to piezoelectric scanner with the aid of a feedback-loop. In equiforce mode, the feedback loop will keep the deflection constant. Figure 3 shows the basic of an AFM.

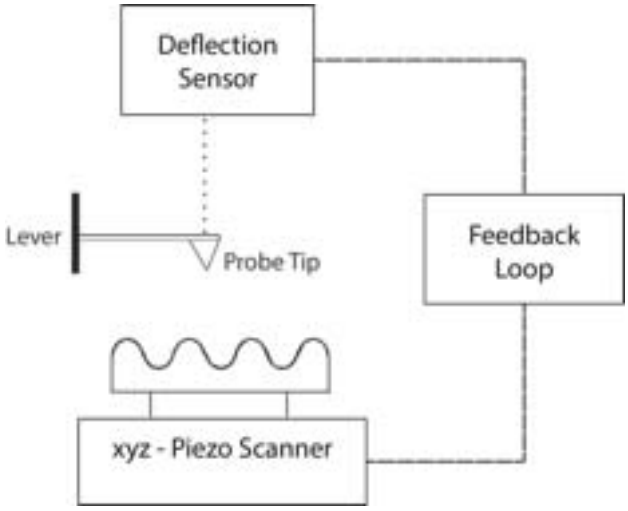

Figure 3 : Basic principle of AFM (adapted from Meyer 1992)

During force microscopy, the probing tip which attached to a lever is scanned over a sample relative to the probing tip. The deflection of the lever or the z-movement of the piezo relative to the lateral position of x,y is monitored and digitized into images. Two types of force microscopy are possible: Contact and non-contact mode.

Non-contact mode is normally used to sense forces such as electrostatic, van der Waals or capillary. Meanwhile, contact mode allows a high resolution trace of surface topography. In addition, various types of deformation could also be implemented and measured on sample using an AFM to determine its characteristic.

The existing wide field of SPM techniques had resulted in the tendency to combine different methods such as Scanning Tunnelling Microscope (STM), Magnetic Force Microscopy (MFM) and Fluorescence Microscopy (FM). The close similarity of the functioning procedure of SPM methods gives the advantage to obtain better information on a sample than the separate application of a single method.

1.5.2 Biological Application of AFM

Before the birth of AFM, investigation techniques in field of microbiology were limited to a subcellular level. The existing Scanning Tunneling Microscopy of biomaterial is unreliable and the closest imaging available was limited to the metal graininess resolution of Transmission Electron Microscope (TEM) (Firtel & Beveridge, 1995). With the advance of AFM, high molecular resolution imaging of cells and its cellular processes (Tripathi *et al.*, 2012; Yamashita *et al.*, 2012), membranes with its proteins (Fotiadis, 2012) and even smaller scale molecules such as DNA (Li, Cassell, & Dai, 1999) is possible. Although AFM is designed for imaging hard and flat surfaces which is impossible in biological sample, substantial information can still be obtained with a resolution at a lower level (Gad & Ikai, 1995).

There are numerous & diverse potential applications of AFM in microbiology such as responses to chemical properties (Dupres, Alsteens, Pauwels, & Dufrene, 2009) , biological/growth processes (Touhami, Jericho, & Beveridge, 2004) and the studies of the substructures of the microbe itself (Touhami, Jericho, Boyd, & Beveridge, 2006). With rapid advance in miniaturization, latest AFM is a lot faster and upgrading

its status to high-speed atomic force microscopy that can further the study the dynamic behaviour of biomolecules (Ando *et al.*, 2002; Ando *et al.*, 2001).

Meanwhile, AFM also can be use significantly to study the interface region between two surfaces. It is important to various applications particularly in food safety (Faille *et al.*, 2002) and biomaterial sterilization (Emerson & Camesano, 2004). AFM provides an efficient tool in measuring the adhesive interaction between surfaces at nano- and sometimes pico-newton (J. Helenius, C. P. Heisenberg, H. E. Gaub, & D. J. Muller, 2008). This so called force spectroscopy technique is used to measure interfacial forces such as surface charge densities, elasticity and hydrophobicity (Cappella & Dietler, 1999). For better information during imaging, AFM can be integrated with complimentary techniques such laser scanning microscopy (Lau, Lindhout, Beveridge, Dutcher, & Lam, 2009) , fluorescence microscopy (Chaudhuri, Parekh, Lam, & Fletcher, 2009) or transmission electron microscopy (Ubbink & Schär-Zammaretti, 2005).

1.5.3 AFM for imaging

Differ to imaging modes, imaging type is the different ways of displaying data and can be combined during a single scan mode. Selection of imaging type depends on specific properties of the samples ones are measuring.

Topographical measurement is the most used image recording for the AFM. This is ideally done by programming the piezoelectric tube's vertical movement to keep the cantilever at a constant bend and hence constant force between the tip and sample. By scanning the area of interest with a constant applied force, it creates a map of height measurements of the sample. Topographic imaging type can be implemented in both contact and non-contact mode depending on the variability and condition. Contact mode will provide a sharp topographic images but tends to drift or damage soft samples while non-contact highly preserve the sample in the exchange of less resolution images.

Beside topography, area of different friction can also be imaged using AFM and this operation known as lateral force imaging. Done in contact mode, this measurement can be useful is that it contains information about the mechanical interaction the tip with the sample surface. Hence, it is possible to obtain quantitative information about variation in sample properties.

Another common used mechanical property imaging in biological samples is phase imaging. This method will show the different in contrast between different adhesion or viscoelastic properties. It uses the concept of energy dissipation from an oscillating tip of intermitten-contact mode scan when it touches the sample. Besides differentiating mechanical properties, the oscillating tips also produce topometric differences images due to slopes within the sample.

By monitoring the deflection of the cantilever as it approaches, touches and withdraws from a sample, a force-distance curve is obtained. With this technique, the AFM directly measures the force between the contacting atoms or molecules at the end of the probe which opens the possibility of single-molecular interaction studies.

Compared to the topography imaging which represents the reflection of the sample surface, force-distance imaging adds on the material properties of the sample such as charge density, Adhesion or elasticity. Different type of interaction can lead to differences in contrast and the details is sensitive in the force-distance curve leading to increasing interest in this measurements and interpretation for soft biological system. Figure 4 shows the correlation discussed.

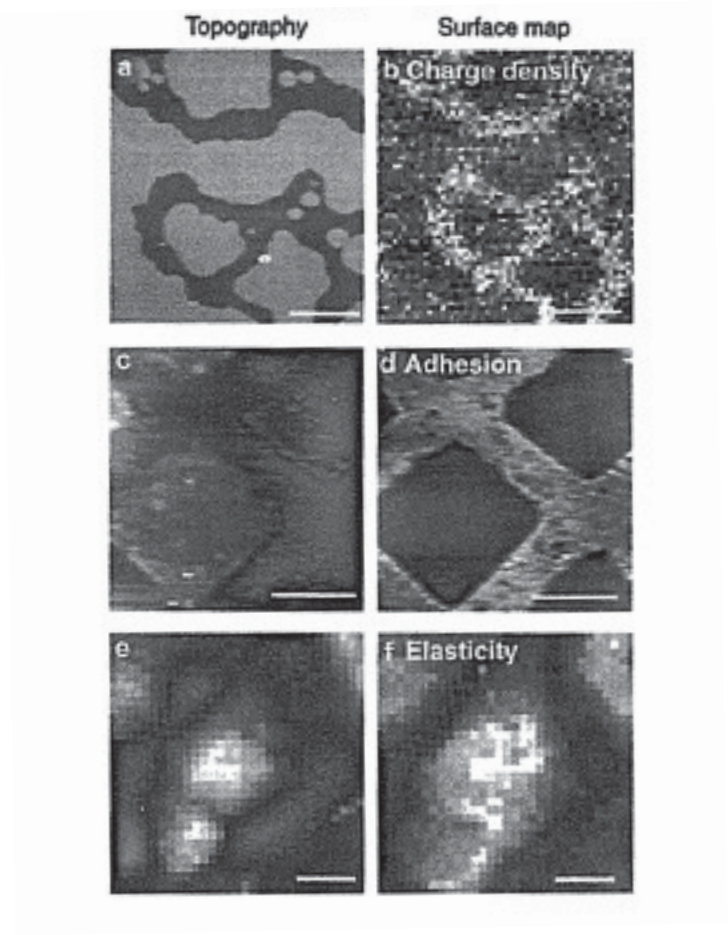

Figure 4. Topographical image and Surface map image of similar sample ((Morris, Kirby, & Gunning, 1999)

1.5.4 Imaging Substrates

Samples to be images under AFM need to be secured into a rigid substrate to ensure a high resolution imaging without any sample drift or accurate quantitative measurement on a fixed sample. Table 2 summarizes some properties commonly used substrates for AFM.

Table 2 : Properties of commonly used substrates for AFM . Adapted from (Eaton & West, 2010)

Material	Preparation	Roughness	Common samples	Notes
Mica	cleaving	<Å (atomically flat)	All, single molecules	Cleaved material stable in storage, Hydrophilic
HOPG	cleaving	<Å (atomically flat)	All, single molecules	Cleaved material stable in storage. Conductive. Hydrophilic
Silicon	cleaning or oxide removal	<Å to a few nm	Lithography, electronic applications	Best for conducting application
Quarts/ Glass slides	cleaning	1-10nm	Larger samples or film, cells	Not fully flat but easy to work with & cheap
Gold	Flame annealing	<Å to a few nm	Chemically modifies surfaces	Easy to chemically modify. Large atomically flat terraces
	Template stripping	<Å to a few nm	Chemically modified surfaces	Easy to chemically modify. Stable in storage

1.5.5 Imaging in air and liquid

For imaging in air, the sample is simply mounted on a small metal disc fixed to the piezo scanner. However, imaging in air is not generally the best option for biological sample and liquid cell is used instead (Morris *et al.*, 1999). Imaging in liquid also provide an important biological applications on which studies can be done in the samples' native state, the reproducibility of scanning environment and minimizing water contact angle force between tip and sample. Although higher resolution is usually obtained in air, dried biological samples usually have a small fraction of their hydrated height (Eaton & West, 2010).

1.6 Adhesion force measurement with AFM

Cell-to-cell adhesion is essential for development of organisms. A cell may carry several adhesion molecules (Kennedy & Thorley, 2000) in-situ or ex-situ of its surface. With the development of new instrumentation based on AFM technology, the precision of scanning & piconewton force resolution have allowed the measurements at the single-molecule level (Müller, Baumeister, & Engel, 1999). In determining the cell adhesion, many techniques are available such as optical tweezers (Choquet, Felsenfeld, & Sheetz, 1997) and functionalized beads (Suter, Errante, Belotserkovsky, & Forscher, 1998). AFM Force curve technique is still used today to determine the adhesion forces between substrate (Benoit, 2002; Touhami *et al.*, 2006). Recently, cell adhesion measurements with AFM technology had evolved again with force volume technique (Arnal *et al.*, 2012; Domke *et al.*, 2000).

1.6.1 Force spectroscopy

There are two major ways in which force spectroscopy can be carried out: in one or in three dimensions. The one-dimentional (1-D) force technique is used where the

interest is measuring the specific intermolecular force rather than spatial distribution of the measured forces. A small selection of the interaction that have been studied with this technique include biotin-avidin binding (Allen *et al.*, 1996), carbohydrate interaction (Misevic, Karamanos, & Misevic, 2008) and cell-cell interaction (J. Helenius, C.-P. Heisenberg, H. E. Gaub, & D. J. Muller, 2008)

Meanwhile, three-dimensional force spectroscopy or force-mapping is used to determine the location of specific molecule on the sample surface by mapping every interaction forces on the specified surface in a grid pattern. Also known as force volume imaging, it requires no receptor labelling on the sample prior to imaging and gain higher resolution than optical technique. It can be used in a broad range of application particularly in mapping of various molecules on the outer membrane of biological structure (Verbelen *et al.*, 2009) or its surface nano-mechanical properties (Arnal *et al.*, 2012; Medalsy, Hensen, & Muller, 2011). Figure 5 shows the comparison on three-dimensional force mapping of adhesion force and normal topography of mixed layer of group A and O cells. The topography image has less clarity on the sample compares to adhesion force-mapping.

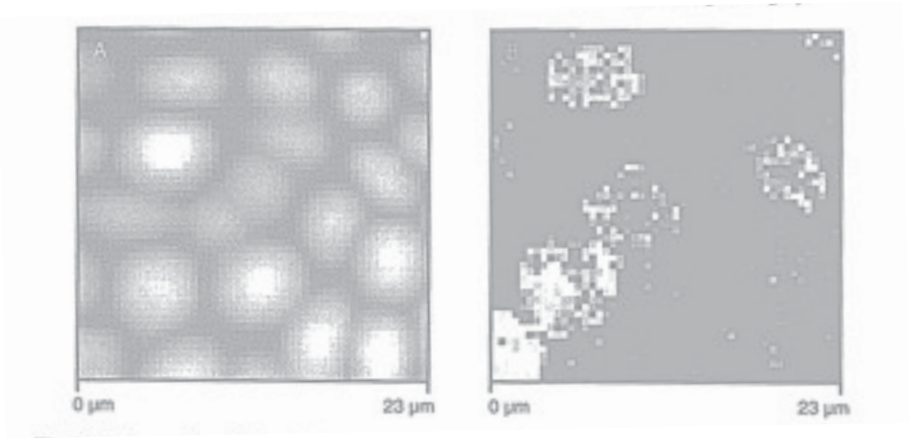

Figure 5 : Example of biological force spectroscopy.Total adhesion image (left) and topography image (right) of a mixed ayer of group A and O cells (Eaton & West, 2010).

1.6.2 AFM application in endospore studies

Apart on its initial application for high resolution topography imaging (Binnig *et al.*, 1986) , AFM is also a valuable technique to measure local physical properties and interaction forces (Ohnesorge & Binnig, 1993). Thanks to the invention of AFM back in 1986, vast amount of literature exist today in either imaging small endospores or surface characterization of spores. In fact, recent technology had advanced into high resolution imaging and rapid characterization of samples enabling studies on the dynamics behind survivability of spores (Dague, Alsteens, Latgé, & Dufrêne, 2008).

Most AFM studied regarding spore is the mechanics of its surface-to-surface interaction particularly its ability to adhere and attach to a surface. There are different techniques in finding & determining the interaction mechanisms such as functionalized probes (Dufrêne, 2000), implementing spore as the probe (Bowen, Fenton, Lovitt, & Wright, 2002; Bowen, Lovitt, & Wright, 2000) and even using tip's lateral force (Boyd, Verran, Jones, & Bhakoo, 2002).

AFM-based sensors also enable a rapid, ultra-sensitive detection of spores without requiring any labelling or external probe. This window of possibilities is achieved using bespoke functionalized for specific biomolecular recognition by monitoring either cantilever bending or the resonance frequency shift (Dufrene, 2008). Spore detection methods using AFM also were developed for fast detection either in a much diluted sample(Nugaeva *et al*., 2007) and specific spore detection in a cocktail of various species (Campbell & Mutharasan, 2006).

1.7 Research Objectives: Atomic Force Microscopy on *Anoxybacillus flavithermus* & *Geobacillus stearothermophilus*

Contamination in milk powder with non-pathogenic thermophilic spores continues to be a constant cliff-hanger problem for the New Zealand dairy industry. The two major thermophilic contaminants found in New Zealand produced milk powder have been identified as *Geobacillus spp*. and *A. flavithermus*.

These organisms have shown their ability to survive sterilization process which later formed into colonies, also known as biofilms within the manufacturing lines of milk powder plant. The major source of contamination in milk powders appears to be from the detachment of thermophilic cells and the releases of their endospores from the colonies thriving within the biofilms.

A majority of previous studies focused on the growth of these organisms within the biofilm and how it happens. Meanwhile, few studies agreed that the survived activated endospores of these species could adhere to the hydrophilic stainless steel. However, little have been done on quantitatively measures the adhesion force of the spore belongs to these organisms.

The purpose of this study was to determine the initial adhesion force of these endospores on the stainless steel surface in the dairy plant. This was achieved by measuring the adhesion forces of the spores using an Atomic Force Microscopy.

The specific objectives of this study were as follows:

1. **Determine the best methodology & workflow applicable for a precise and accurate AFM imaging and force measurements.**
2. **Determine a quantitative value on the adhesion force that exist between an *Anoxybacillus flavithermus*'s spore and stainless steel surface.**
3. **Extend the existing knowledge and investigate some of the conditions that involved in the adhesion factor and compare the adhesion forces with other dairy thermophile or equivalent.**

2 Materials and Methods

2.1 Source of bacterial isolates

Crude spore isolates were prepared by the research team at Fonterra Research and Development Centre, Dairy Farm Road, Palmerston North. Table 3 shows the required species for this study.

Table 3 : Various thermophilic species obtained

Species	Strain No.	Source
Anoxybacillus flavithermus	CM	Waikato University (Te Awamutu)
Geobacillus stearothermophilus	ATCC 2641	
Geobacillus stearothermophilus	D1	
Geobacillus stearothermophilus	P3	
Bacillus subtilis	str 168	

2.2 Bacteriological methods

2.2.1 Media preparation and storage

All media were made up with distilled water and sterilized by autoclaving at 121^{o}C for 15 min. Solid media were cooled to 47 ^{o}C before poured into growth container. Liquid media were cooled to ambient temperature before used. Sterilized storage media were stored at 4 ^{o}C.

2.2.2 Spore preparation and crude spore suspension

Geobacillus stearothermophilus, Bacillus subtilis and *Anoxybacillus flavithermus* were inoculated into Tryptone Soy Broth and grown for 6-8 hours to mid exponential phase at 55°C.

100 ml of the broth culture is then spread plated onto Sporulation Agar (SA) (Sporulation Agar- 0.25g MgSO4, 0.97g KCl, 0.15g CaCl2, 0.002g/L (10ml of 0.2g/10 ml solution) MnCl2, 0.0003g/L (1ml of 0.3g/10ml solution) FeSO4, 8g Nutrient Broth, 30g Agar (Oxoid), 1L water) and incubated at 55°C for 7 days. Surface growth was harvested and suspended in 10 ml of sterile distilled water.The spore suspension was heated at 100°C for 30 min to inactivate vegetative cells, and re-plated onto SA. Plates were again incubated at 55°C for 7 days, spores harvested as before and the suspension went to separation process (section 2.2.3).

2.2.3 Spore isolation

Freshly harvested spore suspension was centrifuged at 12000 rpm for 5 minutes. After the supernatant was discarded, 1 ml of sterile water was added to the spores, and centrifuged again. This rinsing procedure was repeated twice. The final spores collected were re-suspended in 5 ml of sterile distilled water and stored at 4 ^{o}C for at least 1 week before use as this step aids in removing remaining vegetative cells.

Final spore suspensions were purified by extensive washing with sterile distilled water at 4 ^{o}C.

2.2.4 Spore management and storage

All suspensions were diluted using sterilized Milli-Q water (deionised water using the Milli-Q® water purification system, Millipore®). All suspensions were stored at 4 ^{o}C when not in use and a required volume was pipetted out prior to usage (purification, fixation & imaging).

Spores were further purified using a two-phase polyethylene glycol (PEG) system (Sacks & Alderton, 1961). The system was created by dissolving 0.72 gram of PEG 4000 in 4ml of 3 M Phosphate buffer (pH 7.4). After phase separation, the crude spore suspension was carefully layered on the gradient. The sample was centrifuged at 1500xg for 3 minutes at 20^{o}C. Debris migrated to the lower phase, while spores concentrated in a layer above PEG phase. Figure 6 shows the region of interest where most of the spores are concentrated. Spores were carefully recovered and washed five times at 20^{o}C in water. A small amount of 0.1% Tween 20 was added into the purified spores' suspension to avoid adhering with other spores or cell debris. The effectiveness of the separation was determined by visual examination using light microscopy (section 2.3).

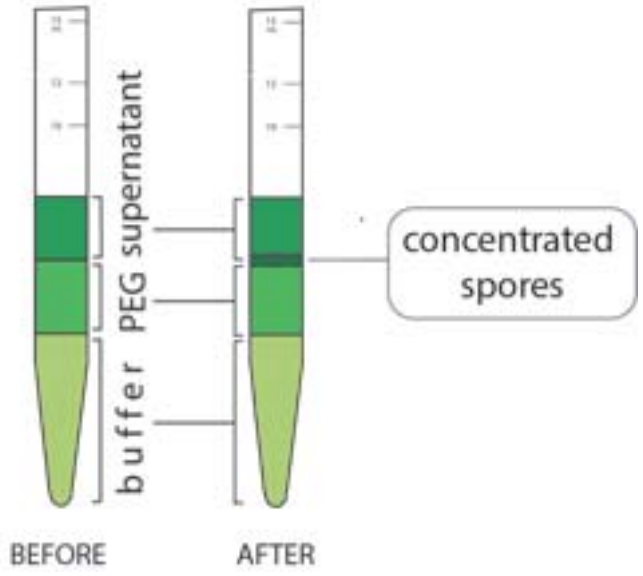

Figure 6 : Layer of highly concentrated spores between the PEG and crude suspension phase appears after centrifugation.

2.3 Light Microscopy

Prior to imaging, purified spores were air dried & heat fixed on the glass slide and stained using Schouffer-Foulton staining method. Fixed samples were steam dye with Malachite green stain for 5 minutes before it was rinsed with tap water. Samples were then counterstained with Safranin solution for 30 seconds, rinsed and dried. Spores will hold the Malachite green stain while vegetative and cell debris will have the Safranin counterstain.

The stained samples were imaged using Olympus BX53 System Microscope equipped with Olympus XC50 Digital Colour Camera. Light microscopy imaging was done under oil immersion lens for highest magnification (x100). Olympus cellSens Dimension ver. 1.5 was use as the imaging software and spores' sizes were measured using the on-board Scale Bar application.

2.4 Atomic Force Microscopy

All imaging were done using Digital Instruments Multimode Scanning Probe Microscope (Veeco, Santa Barbara, Ca). The AFM consists of a Scanning Probe Microscope (SPM) unit, Nanoscope® E controller, Nanoscope ® lll ver. 5.31R1 processing software, and control &display monitor (Figure 7).

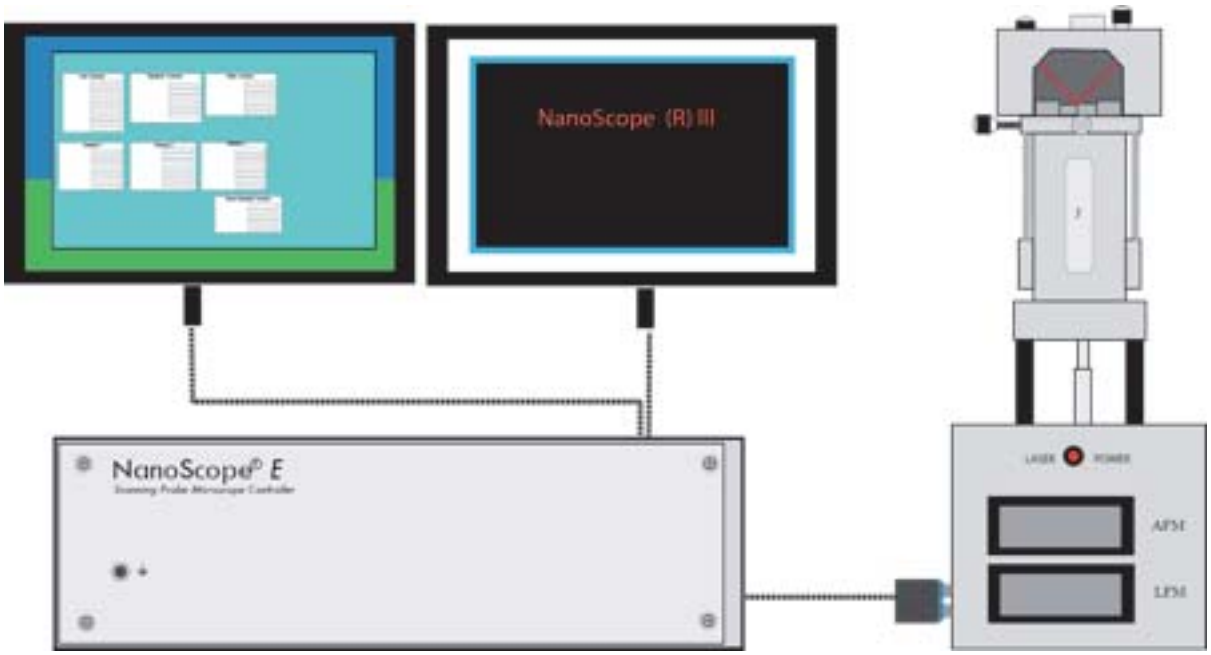

Figure 7 : A complete set of an AFM unit

In this particular study, Type 'J' scanner was used with the SPM. Last but not least, contact silicon cantilevers, model CSG 11 (NT-MDT, Moscow) were used in all imaging. Each unit contains two tips (A & B) with different value of spring constant of 0.1 N/m and 0.03 N/m respectively. Figure 8 shows a representation of the silicon cantilever and its probing tip. These two variations were used in initial run then narrowed to a tip that's best suited for the particular imaging technique.

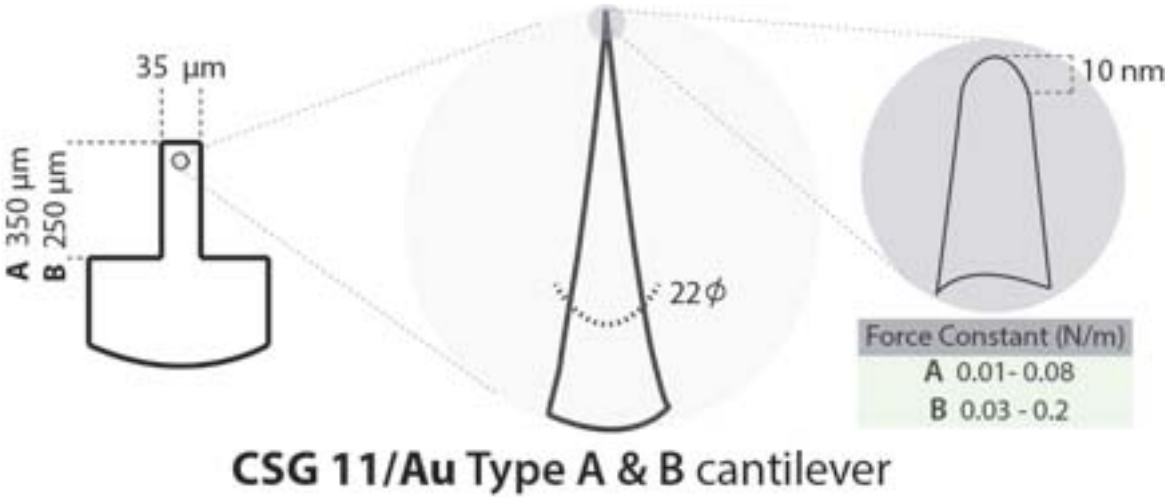

Figure 8 : The anatomy of a silicon cantilever probe.

2.4.1 Sample fixation

Purified spores suspension was air dried and heat fixed on a chosen substrate (stainless steel or glass slide) that was later fixed on a sample puck using a sticky tape. The sample puck was later mounted on the top of AFM's scanner tube. This method will be the same throughout other imaging techniques (section 2.4.2 - 2.4.4).

2.4.2 Height and deflection imaging

Imaging was done in normal Contact Image mode that provides both height and deflection images. Each image are pre-set for 512 scan lines with a scan rate between 2 Hz to 5 Hz which depends on the scan size, higher scan rate for a small scan size. The Feedback Control of Integral and Proportional gain is set between 2 to 5 depending to the sensitivity required during a scan. Microscope mode was set into Contact with a maximum Z limit of 5.5μm. Channel 1 was set for Height while Channel 2 for Deflection option in the Control Monitor to obtain the desired Height and Deflection images in the Display monitor.

Sample attached on a substrate (stainless steel or glass) is fixed on a magnetic sample puck with a sticky tape. Depending on the condition of imaging, cantilever was mounted on a normal holder for in air imaging while special liquid container holder for imaging under liquid.

Image was later edited using the same Nanoscope III software before converted to a Tagged Image File Format (TIFF) file. Figure 9 shows an example on both height and deflection images.

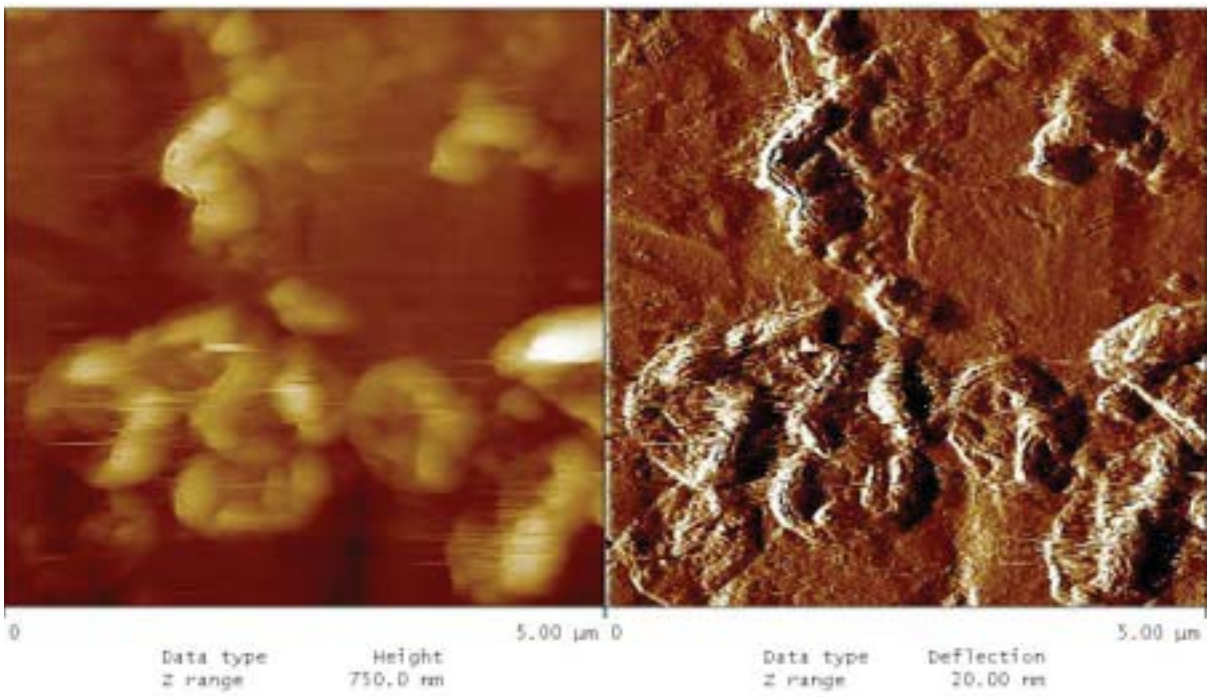

Figure 9 : Height & Deflection images of *B.subtilis* spores using a sharp end probe.

2.4.3 Force-Distance imaging

Force-distance (F-D) curve was obtained using software's Force Advance mode in the Nanoscope III software. In the Main Control tab, Ramp channel Z was set to maximum range of 2.75 μm at a scan rate of 0.5 Hz for a 1536 recorded values on every force curve measured. Spring constant value was set using the value of the cantilever used. In the Scan Mode tab, Trigger mode was set to Relative and Deflection in Trigger Chanel with a threshold of 150 nm.

Channel 1 Data type was set to Deflection in the Control Monitor to obtain a Force plot image in the Display monitor. Figure 10 shows an example of a force-curve from a sample. Display images were converted into raw American Standard Code for Information Interchange (ASCII) format.

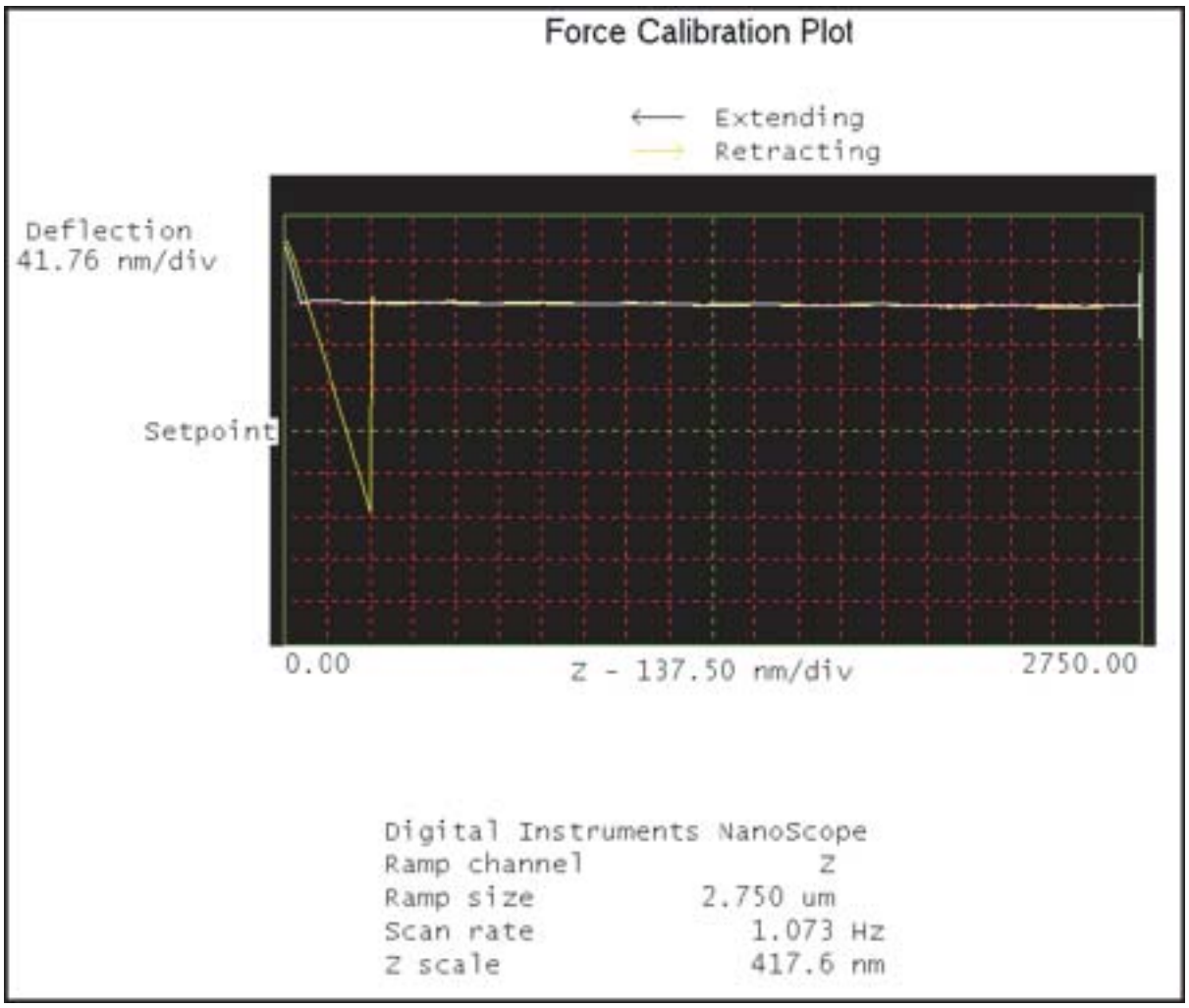

Figure 10 : A force-curve plot generated in the Display monitor

2.4.4 Force-Volume imaging

Prior to this imaging, spore sample was first located by raster-scan with the normal imaging technique (section 2.4.2).

Force-Volume (F-V) imaging then was done using software's Force Volume mode. The Ramp size in Scan Controls tab was set to 2.75 μm on a medium FV scan rate or 0.404 Hz. In the Feedback Controls tab, the maximum tip deflection was set to 150 nm and Trigger channel on Deflection to avoid excessive force on the tip.

Imaging was done in 32 x 32 scanning plots on both Image & FV channels. The Z direction of FV Channel was set to Extend to obtain an electrostatic or Retract for elasticity values in the Display monitor. Meanwhile, Force Channel tab was set to give the deflection data that records 512 values for each force curve measured. Figure 11 shows the images during the procedure to locate a spore sample and the FV image displayed in the Display Monitor.

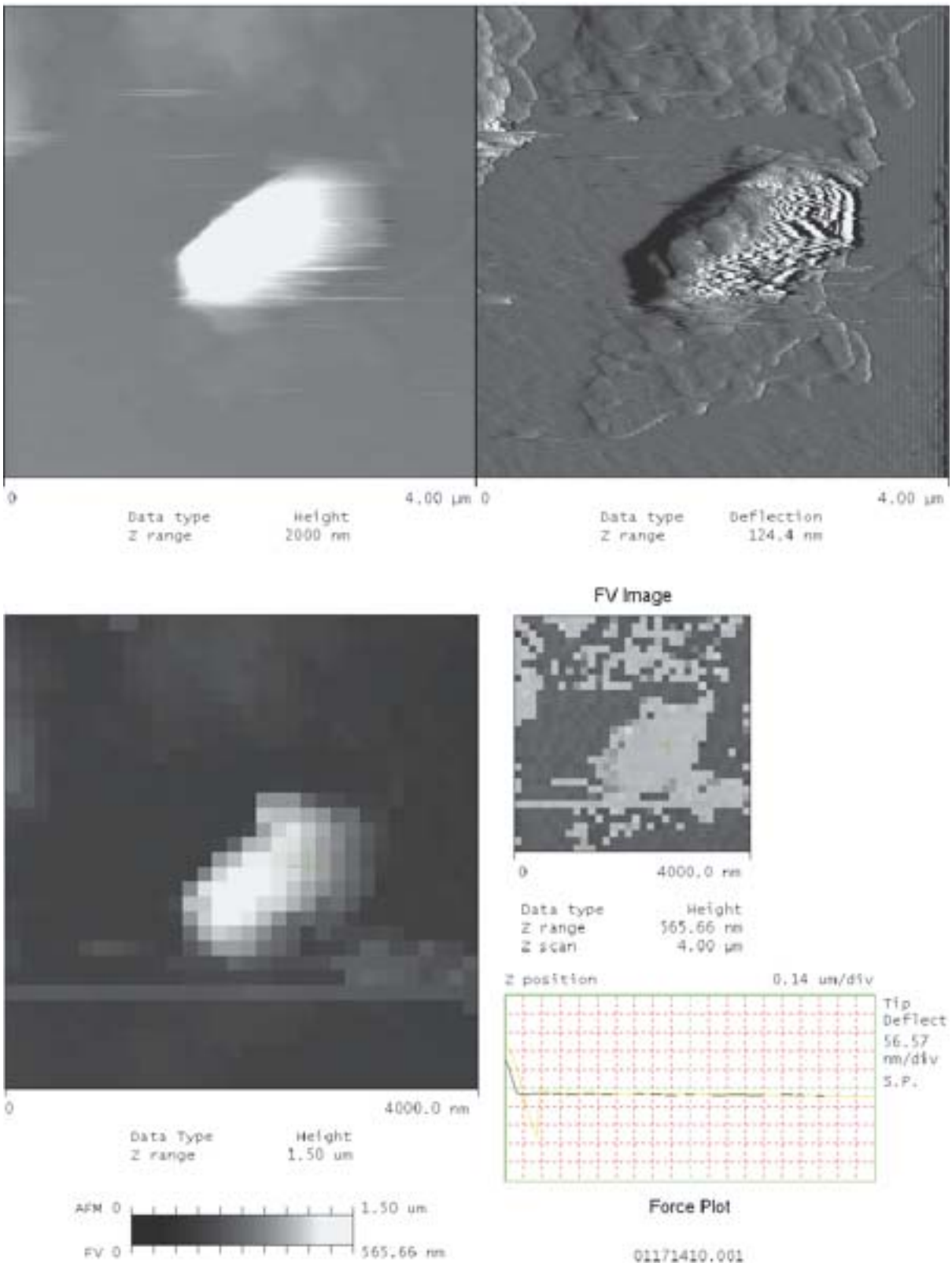

Figure 11 : Top image shows the raster-scan of a targeted spore and the bottom image is its Height & FV of 32x32 grids image.

In this mode, a probe keeps approaches into contact with the surface, and then retracts it away until out of contact. The approach-retracts manoeuvres are repeated

in a grid pattern defined by the AFM user. In the end, this technique provide a compilation of well-defined individual force curves

These collections of force curves were converted into ASCII format for further processing. Later on, adhesion force values were extracted from each plot and mapped representing the adhesion forces in the scanned area. Samples elasticity was also mapped.

2.5 Data analysis and statistics

All data analysis was done with Microsoft® Office Excel 2010 and Sigmaplot® 12. A minimum of 10 spore samples were collected for each species and statistical validation was done using t-test analysis on a 98% confidence interval.

2.5.1 Measuring the adhesion force

Figure 12 shows a model of force-distance curve. In Force-Volume mode, the software could only convert the voltage into deflection not a further step into force value. Ideally, the value of adhesion force is at the 'pull-off' point when the cantilever overcomes the interaction between tip and sample.

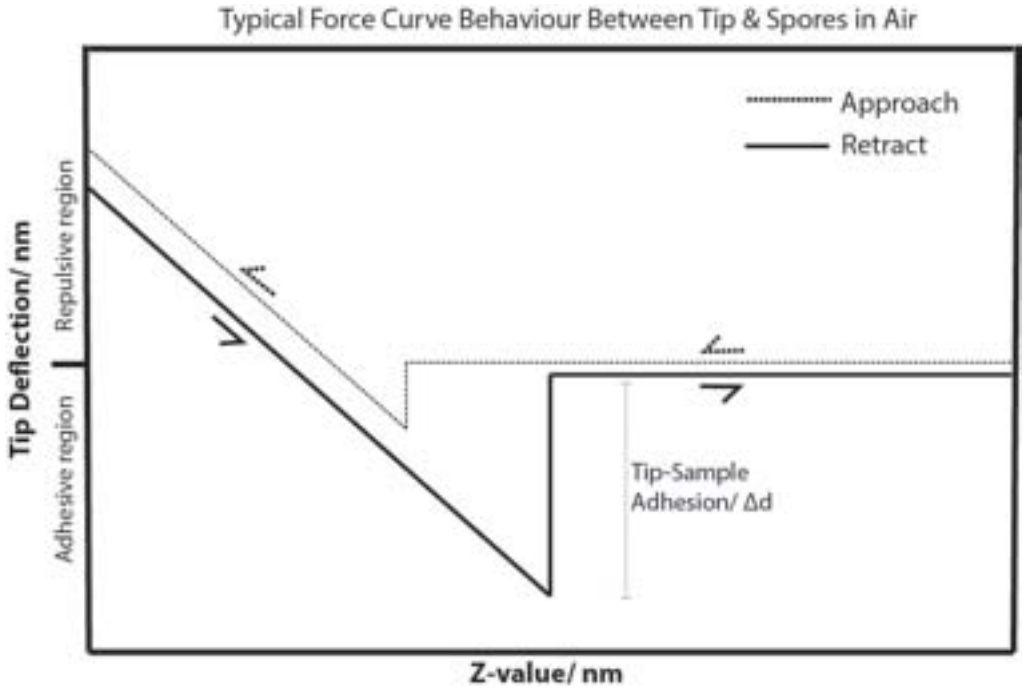

Figure 12 : A model of force-distance curve. Dotted line is recorded value during the approach while the solid line is the retraction data.

Hence, the adhesion force from a force curve is measured from the product of cantilever's deflection during retraction (Δd) and the effective cantilever spring constant (k) according to Hooke's law (F_{AD} = k Δd).

However, large adhesion force values sometimes do not recorded in the measured force curve and this could happens in both force curve & force volume imaging. This is due to the probe is outside the detection circle of the photodiodes. In this case, the Δd value can be calculated based on the horizontal distance (Δz) between the zero

deflection point and the ‘pull-off’ point. Figure 13 shows the correlation of the situation using an image will full data and another with a higher deflection.

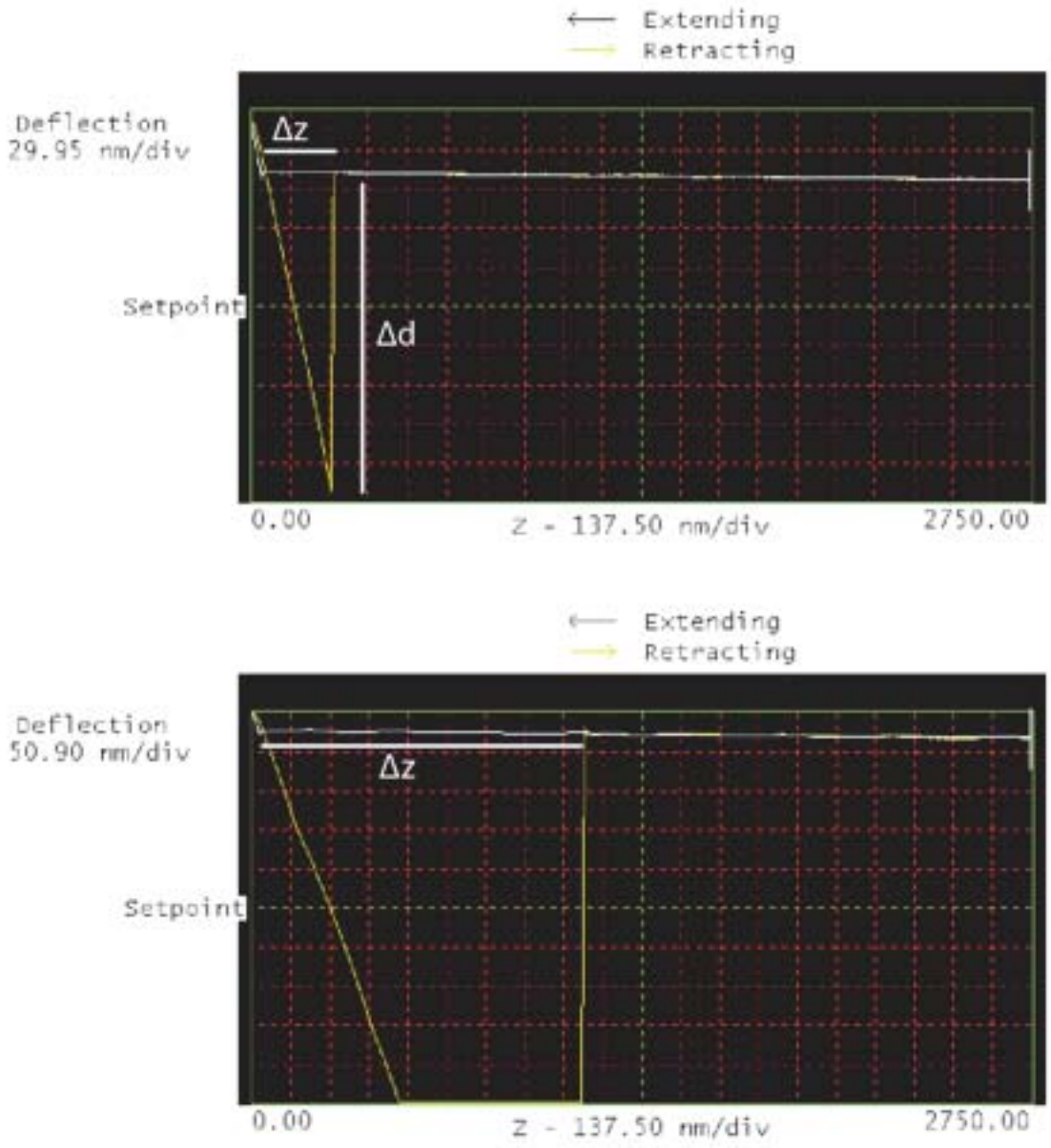

Figure 13 : two different sets of force-distance curve from a glass sample.(top) Δd is similar value to Δz. (bottom) Only Δz is salvageable since the values upon retraction is clipped.

This data extraction method is extremely useful when measuring a very high interaction such as hydrophilic-hydrophilic surfaces or both surfaces are hydrophobic. This side approach is originally suggested by Willing. *et. al* (2000).

3 Trials study – Results and discussion

These early trials were done to scope the most suitable method that would optimize the imaging and force measurement under the Atomic Force Microscopy.

3.1 AFM study of *B.subtilis* on stainless steel

Two experiment setups were planned for this trial. The aim of Trial 1 was to prepare and observe the stability of a monolayer (single layer) spore lawn for AFM imaging. *B.subtilis* will be the control sample in this experiment. For the first run, the methodology will be further refined until a technique that produce a stable spore lawn for AFM imaging was developed. Meanwhile, the second run was set up to get a preliminary result on how the spore lawn behave during an AFM run and finally to obtain a set of force-curve results.

3.1.1 Preparing monolayer spore lawn on substrate

This preparation method was refined from (Bowen *et al.*, 2002) for its simplicity. Three different concentration of *B.Subtilis*' spore suspensions (10^8, 10^4, & 10^2 cfu/ml) were prepared via fold dilution from it's original sample. Circular stainless steel SAE 316 substrate was immersed in each suspension from one hour. Suspensions were kept cold (4-5^{o}C) in ice to avoid germination during the immersion period. After immersion, samples were rinsed four times by dipping in deionized water to emulate a shear force that removes loosely attached spores. Samples were air dried between rinses. Similar samples were duplicated with the only change is to immersion time of two hours.

Initial observation shows that samples which were prepared longer have a whiter surface than the original setup. However, those spores tend to tear-off from the stainless steel substrate during rinsing procedure. Most of the spores were completely removed from the substrate and it was not usable for AFM imaging.

The spore layer that appears whiter on the substrate suggests that more spores managed to attach, covering more of the surface of the stainless steel substrate. Samples that were immersed in higher spore concentration or immersed longer have a thicker layer. Initially, spores that were loosely attached on the stainless steel could be removed by a small sheer force as dipping in the liquid leaving the rigidly adhered spores on the substrate. When an increased amount of spores adhered, these spores are not supposedly only adhered to the substrate but also with the neighbouring spores. The amount of spore surface area in contact with the surface substrate will be smaller than a well spread monolayer surface as the clustered arrangement does not provide the optimum surface for each spore to attach efficiently.

These loosely bound spores tend to pull along their neighbouring spores that had adhered firmly on the substrate. Applying a repetitive sheer force eventually exceeded the limit the spore-substrate's adhesion force thus detached the whole layer from the stainless steel substrate. Figure 14 shows a representation on how surface area affects the stability of the spore lawn under sheer force.

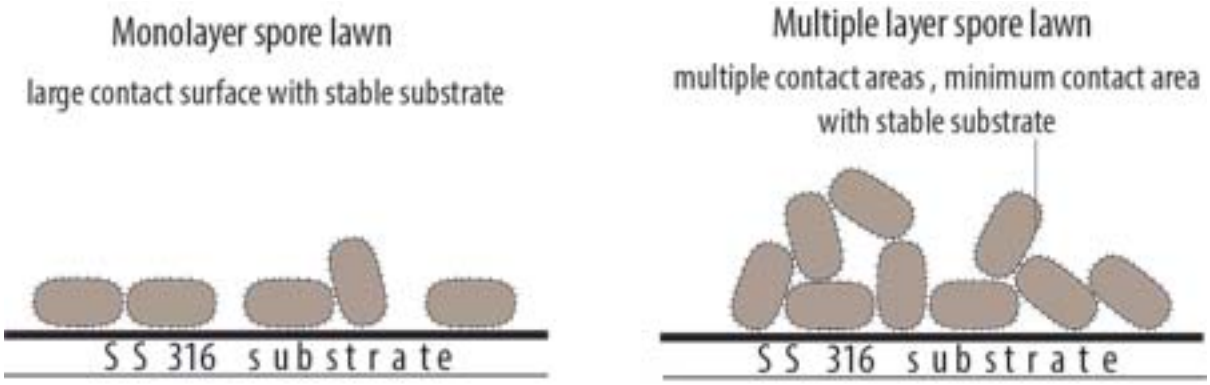

Figure 14 : Representation on surface interaction affecting spore lawn's stability. Left image is when most spores adhered fully to the SS substrate while only partially adhered on the substrate on the Right image.

In the literature, the average length of a *B. subtilis* spores is 1.07 ± 0.09*μ*m (Carrera, Zandomeni, Fitzgibbon, & Sagripanti, 2007; Faille *et al.*, 2010). This value is used during the AFM imaging of the samples as reference to determine the result of the developed spore lawn. Figure 15 shows both height and deflection images of the spore lawn on the stainless steel substrate. It shows that the amount of adhered spores' decreases as the concentration of spore suspension lowered, both for normal and longer immersion time.

In identifying if each procedure produces a single layer lawn, the height image was set at one micron as any image that exceeds the setup height has multiple layered spore surfaces. AFM height images in Figure 15 show that a longer immersion time tends to have a multiple layered surface. Samples that were prepared within a shorter time showed a more evenly spread monolayer surface while the other samples tend to have a clustered layer of spores that could lead to difficulties in observing and measuring the properties of a single spores later during the project.

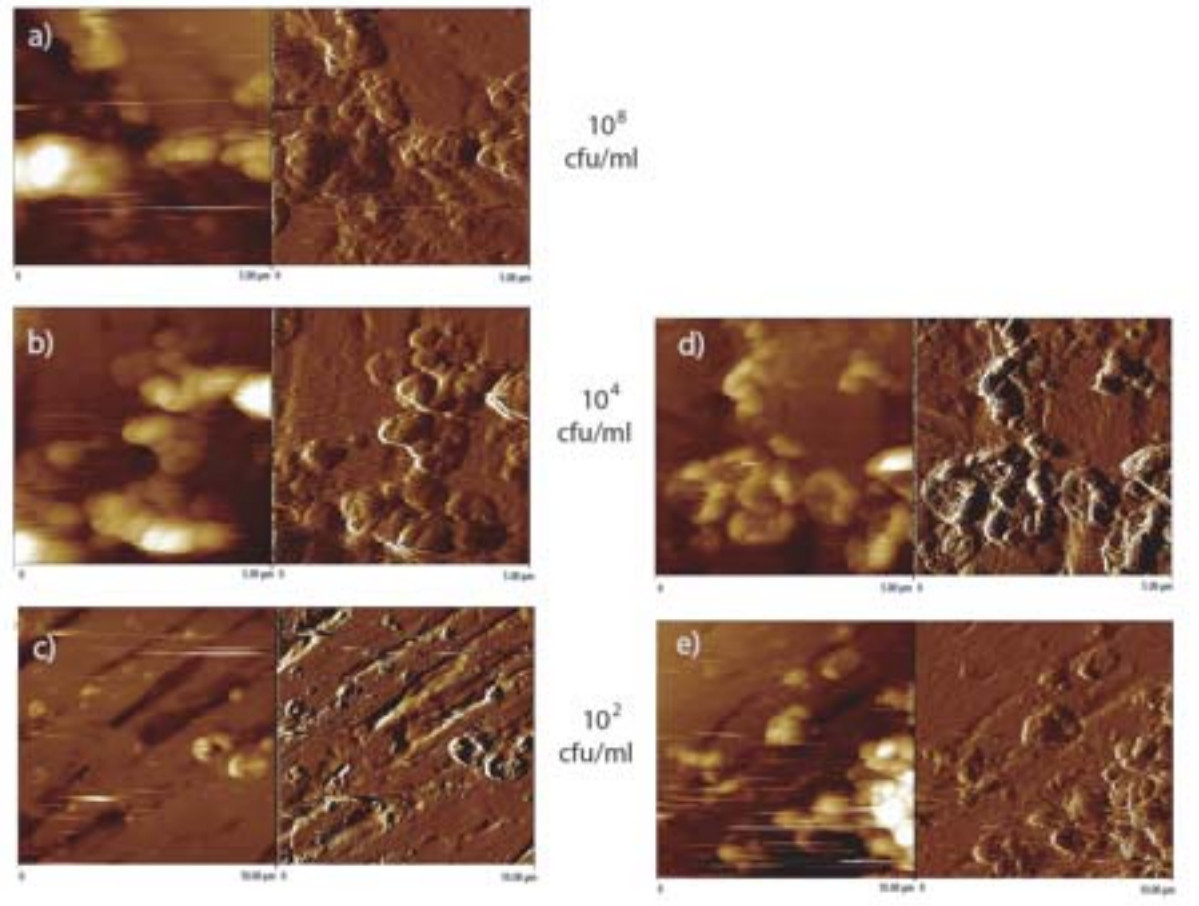

Figure 15 : Height and deflection images of spore lawn on SS substrate. Samples were prepared using spores suspension under different concentration; a (10^8 cfu/ml), b & d (10^4 cfu/ml), c&e 10^2 cfu/ml). Sample a, b & c was immersed for 1 hour while d & e were immersed for 2 hours. Each image varies from 5x5 μm to 10x10 μm.

3.1.2 Observing the stability of spore lawn under imaging condition

Samples were imaged with AFM in liquid environment. Milli-Q water was used as the liquid media and normal contact scanning was done repetitively at the same 10x10 μm area. High frequency (5 Hz) scanning was done prior to imaging until final image remain unchanged. Simple force-curves were obtained on selected attached spores. Data analysis was conducted to determine any changes in spores' stability over time.

Previous setup shows the most suitable spore lawn was prepared using 10^4 cfu/ml crude spore suspension with one hour immersion time. It was also found that if the crude suspension is halved but doubling the immersion time will gives a similar quality of layer. Figure 16 shows a clean stainless steel substrate imaged under a liquid environment.

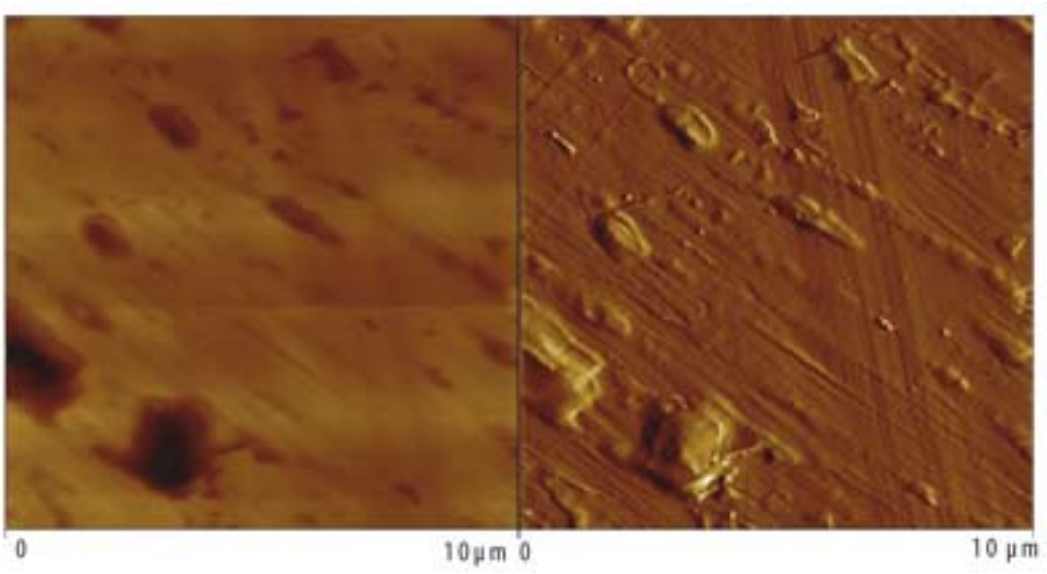

Figure 16 : Height (left) & Deflection (right) images of clean SS 316 substrate under a liquid environment. Each image is 10x10 µm.

During the initial sweep of the spore lawn, most spores have little adhesive stability as the initial spore count keeps decreasing and changing over each scan pass. The spores were potentially detached by the lateral force made by the scanning AFM tip. Given enough time with the scanning, the probe eventually removed most of the large spores from the substrate. The percentage of monolayer spores that had detached could not be determined.

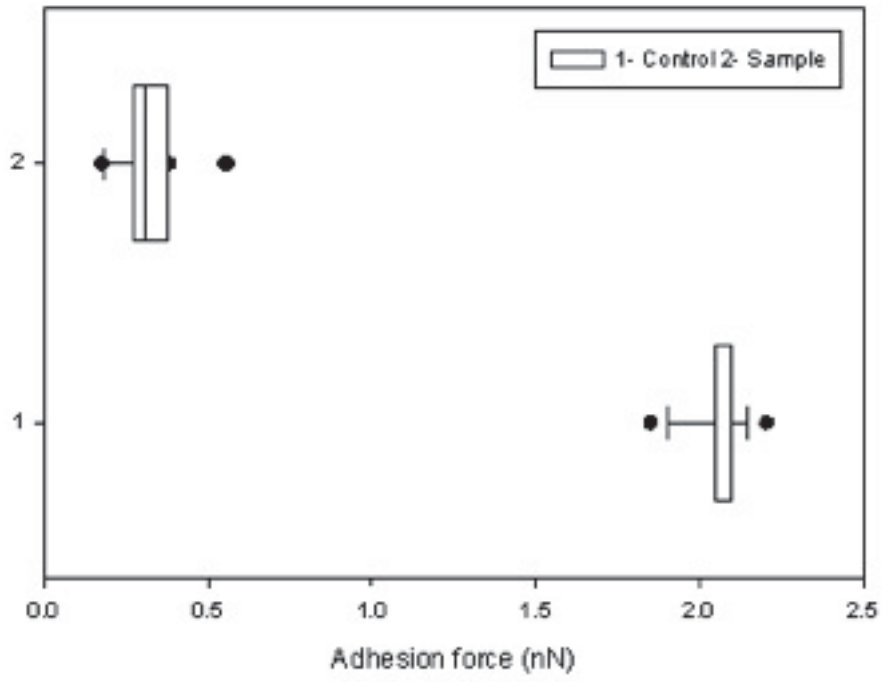

Figure 17 : Boxplot - Adhesion force of stainless steel substrate (1) and B.*subtilis* spores (2)

The average adhesion force values using the silicon tip are 2.06±0.09 nN and 0.3±0.09 nN for stainless steel substrate and *B.subtilis* spores respectively.Figure 17 shows a boxplot of adhesion force on both samples. Statistical analysis on the adhesion forces reveals that the adhesion regime between silicon tip and stainless steel substrate is significantly higher compared to the interaction between tip and spores (t-stat = -87.708, df 79, t-crit <0.001).

This significantly difference in interaction suggest that spores are hydrophobic while the stainless steel substrate is hydrophilic in relative to the hydrophilic silicon tip. It also suggest that the more hydrophobic spores would only loosely adhere to the hydrophilic stainless steel and the detachment of the spores with a small lateral force of the tip proves it.

For AFM imaging purposes, glass (Table 2) is also acknowledged as a suitable substrate and a trial run shows that it provides a stable surface to fix the spore suspension. A significant amount of spores remains fixed on the surface after a significant scan passes. All AFM images in Chapter 4 are spores fixed on glass substrates.

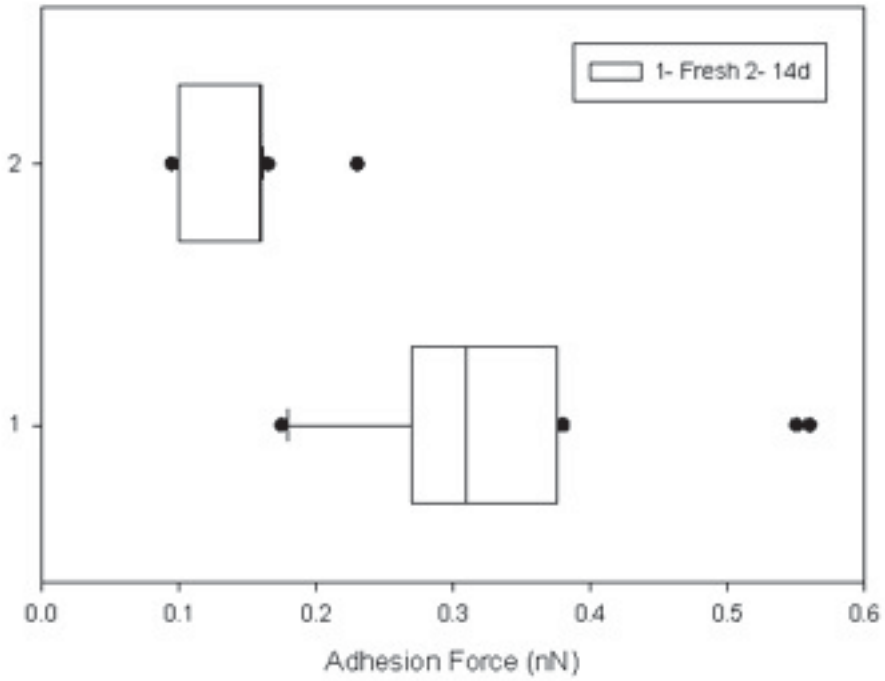

Figure 18 : Boxplot - Adhesion force of fresh (1) and old (2)

Meanwhile, time also plays a significant role in the adhesion behaviour of *B.subtilis* spores. Duplicate samples that were left in a dry storage at a room temperature for 14 days showed a less adhesive force with the silicon tip with an average force of 0.14±0.03 nN. Figure 18 shows a boxplot between fresh and old sample. Again, statistical analysis shows that it is significantly low compare to fresh samples (t-stat =11.975, df = 92, t-crit <0.001). Since *B.subtilis* spore's outer layer is mainly composed of thick saccharide; rhamnose and quivose (Faille *et al.*, 2010), the oxidation or dessication of these might be the reason to the increase in

hydrophobicity of the spores. This interaction forces regarding oxidation and dessication has yet to be determined.

3.2 Purification of bacterial spores

In the past trials, it was observed that there are a lot of debris that does not represent the size or shape of spores. Thus, obtaining a good clean image of spores is a challenge and yet measuring the independent force acting on the spore. This section will be discussing about the purity of the crude spore suspensions and the technique used to further purify these samples for a good AFM imaging.

3.2.1 Initial observation of crude spore suspension

To visualize and differentiate the spores from cell debris or other material, spores were stained with malachite green while other materials were counterstained with safranin. This initial microscopy is purposely to determine the quality of the suspension. Thus, the scale of the images is not significant. Spores were seen in four out of five samples supplied; *A.flavithermus* CM, *B.subtilis*, *G. stearothermophilus* D1 & ATCC 2641. Figure 19 shows the images of spores from different species and strains under light microscope.

Comparing the quality of the suspensions visually shows that both *B.subtilis* and *G.stearothermophilus* ATCC 2641 have the best amount of spores while *A.flavithermus* has a slightly better count than *G.stearothermophilus* D1. Meanwhile, *G.stearothermophilus* P3 strain does not shows any visible spores and full vegetative cells are visible.

Different species or even strains have their preferred trigger condition in producing spores such as magnesium, calcium and potassium. In addition, the time period for a successful spore formation also varies widely among thermophilic bacilli (Burgess *et al.*, 2010). In the case of *G.stearothermophilus* P3, the spore formation period might be longer than the expected 7 days resulting in the absence of spores in the sample. It is also worth mentioning that *G.stearothermophilus* D1, P3 and *A.flavithermus* CM are dairy isolates. On that note, producing spores might not be the priority of these dairy isolates as starvation is uncommon in a dairy processing plant.

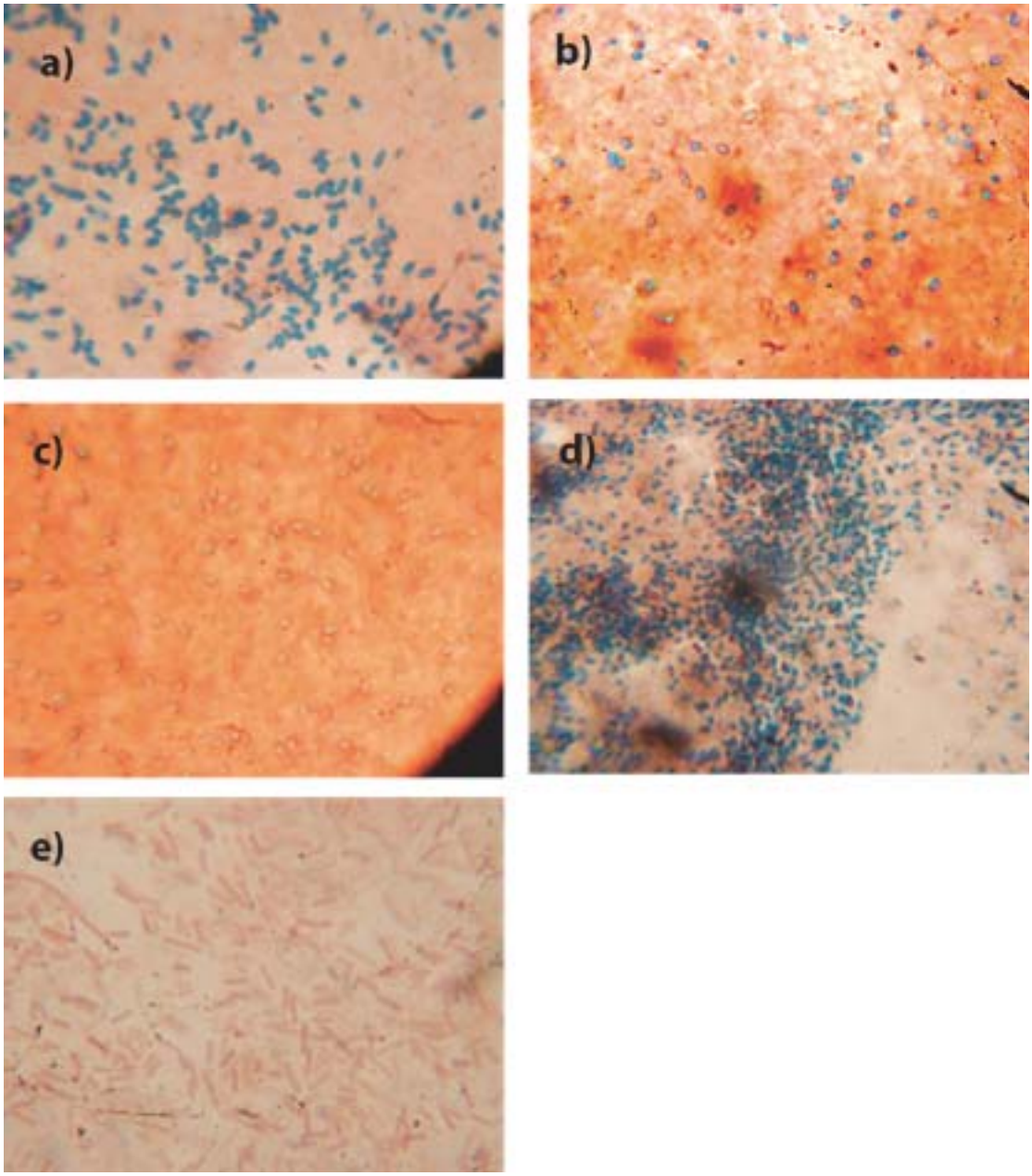

Figure 19 : Stained spores under light microscopy. *G.stearothermophilus* ATCC 2641 b) *A.flavithermus* CM c) *G.stearothermophilus* D1 d) *B.subtilis* e) *G.stearothermophilus* P3.

3.2.2 Purification: Two-phase separation process

A.flavithermus CM and *B.subtilis* spores were purified from a crude suspension of 10^8 cfu/ml while *G.stearothermophilus* ATCC 2641 & D1 were from crude suspension of 10^2 cfu/ml instead. Since *G.stearothermophilus* P3 does not produce any spores, it was not included in the spore purification for an obvious reason. After the purification, spores were stained and viewed under light microscope to observe the effectiveness of the procedure. The two-phase purification & staining for microscopy methods are described in section 2.2.5 & 2.3 respectively.

A.flavithermus CM, *B.subtilis* and *G.stearothermophilus* ATCC 2641 purified suspensions have a significant reduction in cell debris while *G.steatorhermophilus* P3

still shows a decent amount of vegetative cells. Figure 20 shows the microscopy images of purifies spores on each species.

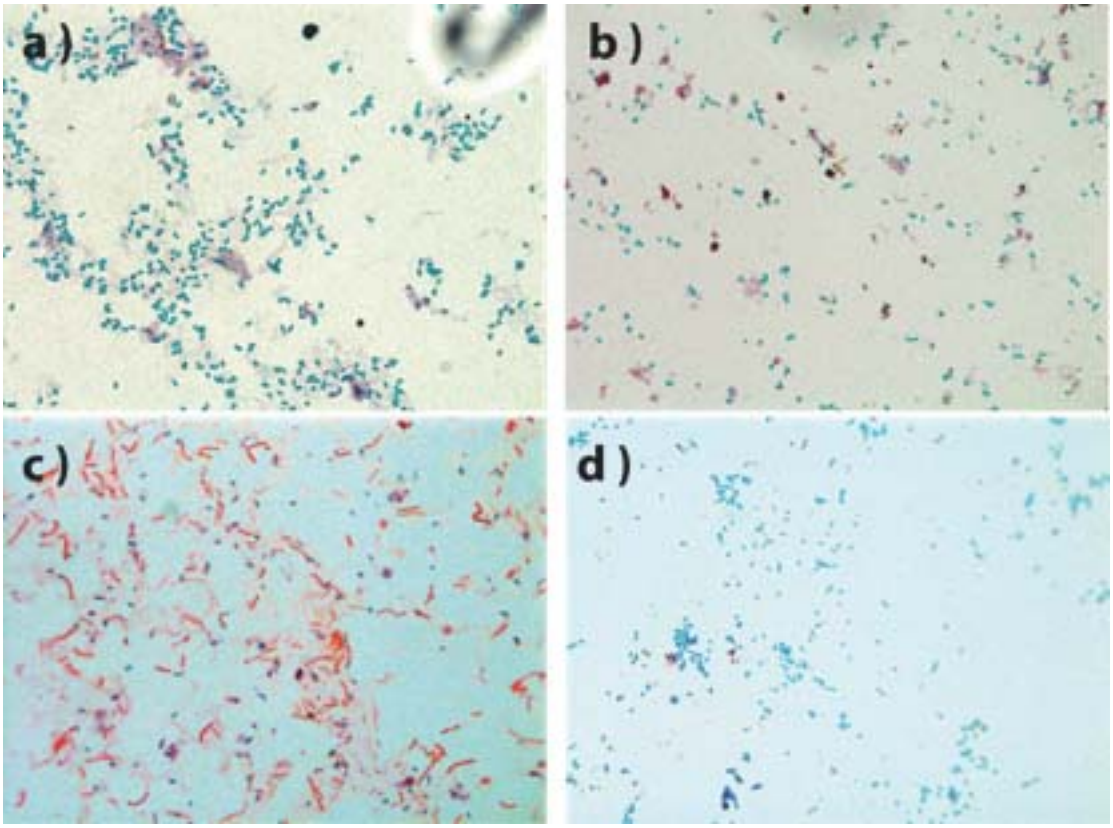

Figure 20 : Purified spores from two=phase separation; a) *G.stearothermophilus* ATCC 2641 b) *A.flavithermus* CM c) *G.stearothermophilus* P3 d) *B.subtilis*.

Although pure spores are collected in a thin layer between PEG and original crude suspension, a decent amount of spores somehow managed to move further down along with the debris into the PEG and phosphate buffer. This presumably happened due to the high speed centrifugation procedure during the purification. A small amount of spores are also still available in the original suspension phase. This is proven by imaging all these layers under light microscopy similar to the pure suspension collected. Figure 21 shows the images *of A.flavithermus* CM samples collected at different layers and phases.

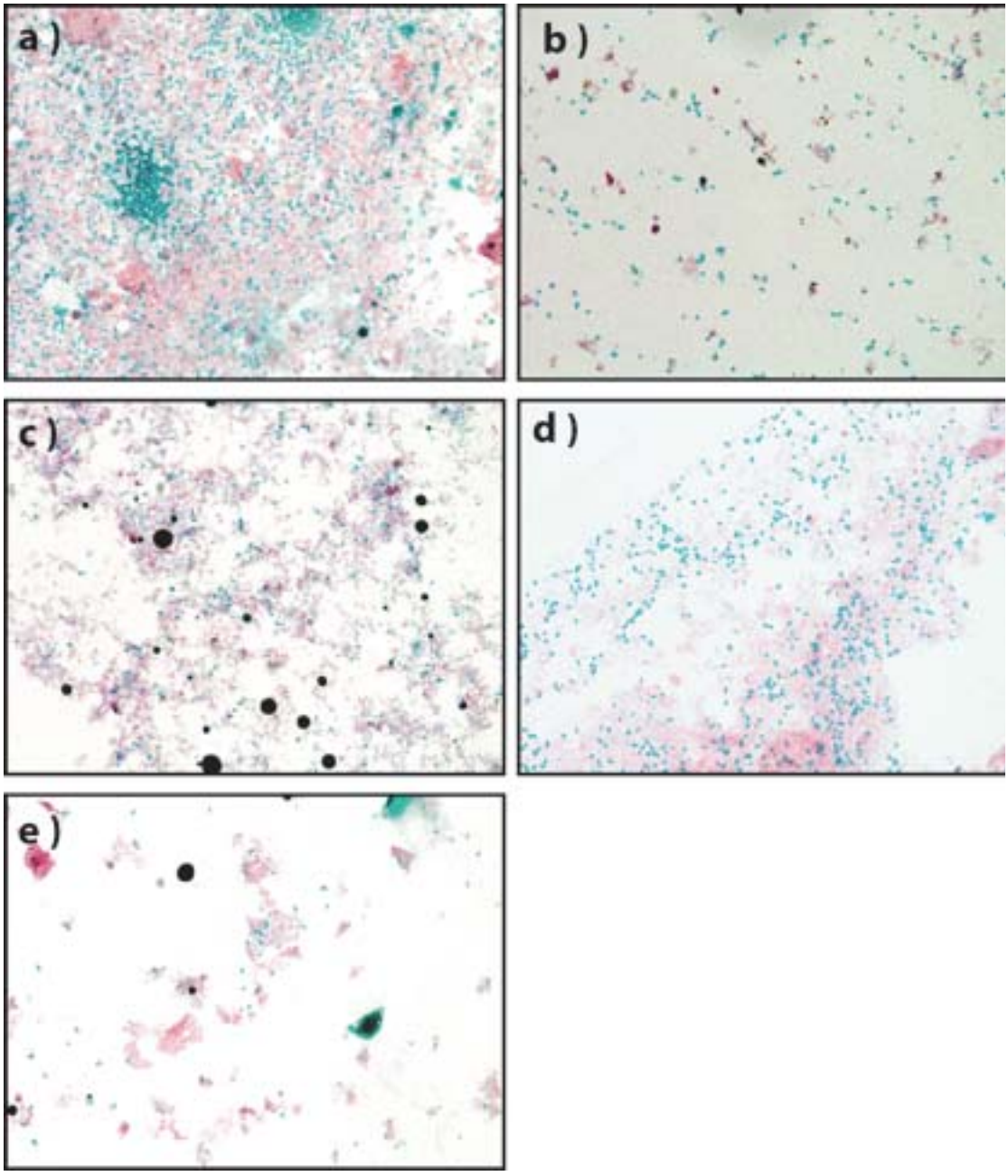

Figure 21 : Light microscopy images of *A.flavithermus* CM spores from different phases of the two=phase separation method; a) crude suspension-BEFORE b) pure spore layer c) crude suspension-AFTER d) phosphate buffer e) PEG phase

Since these spores are still viable, it is worth mentioning that these spores are still able to be purified using similar technique if the aim is to maximize the amount of purified spores from a crude suspension. Since the aim of this run is to purify spores from their vegetative cells and debris, the other layers were discarded.

In the initial imaging, spores tend to clustered together and this would provide some difficulties during AFM force-volume imaging when the interest is on a single spore. A small amount of 0.1% Polysorbate 20 (*Tween*) was added to the purified sample to separate the spores. Since adding different chemicals could influence the state of the

spore surface which is what the main interest in the project, only the minimum amount of Polysorbate 20 is added to the spore suspension.

3.3 Spore size comparison of different species

A side study during the purification process is to measure the size of spores of these different species. Figure 22 shows a boxplot of three species measured. The average spore size of *A.flavithermus* CM, *G.stearothermophilus* ATCC 2641 and *B.subtilis* are 1.47±0.17 μm, 1.89±0.13 μm and 1.39±0.06 μm respectively.

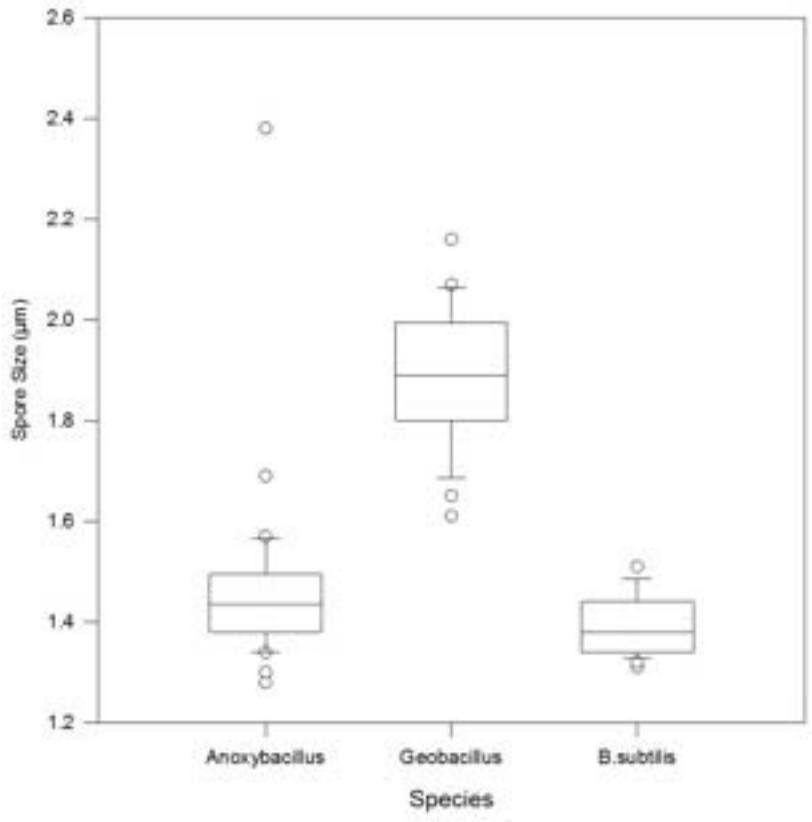

Figure 22 : Boxplot of endospore sizes on various thermophilic species.

From the boxplot, *G.stearothermophil*us ATCC 2641 spores are significantly larger than the other species particularly *A.flavithermus* CM and a t-test analysis had proven that its spores are significantly larger than *A.flavithermus* CM(t-stat =10.36, t-crit =1.67, P <0.001). Comparing spores of these thermophiles with a well-studied *B.subtilis* shows a significant size difference with the *G.stearothermophilus* ATCC 2641 (t-stat =17.62, t-crit = 1.67, P<0.001) and *A.flavithermus* CM (t-stat = 2.32, t-crit = 2, P=-.024). However, if the confidence interval required at 98% or higher, the spore size difference between *B.subtilis* and *A.flavithermus* CM is not significant.

3.4 Summary

The main point of these trials is to determine the viability and effectiveness on the sample's preparation technique for AFM topography and force-curve imaging. The substrate of interest for the whole project is stainless steel as it is used as standard in most milk powder plant and it was found that bacterial spores were loosely bound to the substrate and were easily peeled off from the substrate when applied with small sheer and lateral forces.

The results of these trials helped to understand the behavior of the spores with stainless steel substrate. Relative to the substrate, a thermophilic spore can be considered hydrophobic as it does not adhere or attached well on a hydrophilic substrate and shows low interaction force with the silicon tip which is also hydrophilic.

Apart from that, these trials also reveals that the dairy strains do not produce a lot of spores and certain strains need a longer maturing period to form spores or does not produce any spore at all. Hence, each of the strains needs to be monitored and extracted properly to ensure an efficient spore formation and ultimately a successful AFM study.

In summary, a two-phase separation is crucial to further purified the spores and glass substrate is selected over stainless steel disc to fix the spores onto. This situation seems counter intuitive but the lateral force exist in a milk powder manufacturing plant is not similar to the force of a sharp AFM tip on a scanning mode. The force produce by a continuous stream of flowing milk is not sufficient to overcome the spores' adhesion force on a stainless steel surface.

These procedures did not alter the aim of the study as the main interest is only the force between spores and AFM tip.Findings in this chapter eventually helped design the the next experimental methods and parameter to monitor the force acting on the surface of the spores.

3.5 From Force-Curve to Force-Volume imaging

In measuring the interaction of biological molecules, AFM has some unique advantages. It is very sensitive allowing measurement to a very small force interaction in the pN range. It also has the availability to selectively and finely control any molecules of interest without requiring a bulk amount of samples.

The initial idea to determine the adhesion force on the spore surface is by obtaining simple force-curves from spore samples using normal standard contact probe. This method involves approaching a fixed spore on a substrate with a probe and compute the adhesion force value acting on the area covered by the probe. This method was used in Trial 1 (section 3.1.2).

Since an endospore is fairly small (less than 2 micron length), a spore must be located at first using the topography imaging mode in a wide scan area (10x10 micron). To ensure the probe lands on the spore surface in Force-imaging mode, it needs to be in a small scan area (1x1micron) to avoid measuring other entities such as debris or the substrate itself. Figure 23 shows on how small scan area effects the accuracy of the force imaging.

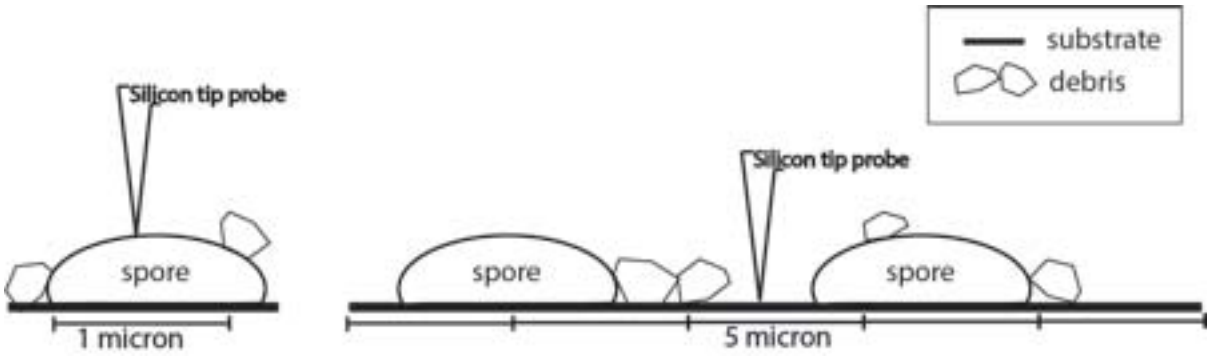

Figure 23 : The hit rate for probe to measure spore surface is higher in a smaller scan area (left) compared to a larger scan area (right)

These procedures are tedious, time consuming and it is worsen as samples tend to drift when the Imaging mode is switch into Force mode. It also only provides the force value on the small area where the probe landed, not the overall value of the whole surface area.

Driven by occurring difficulties and guided by the same ambition, an initiative was found on using a probe with a plateau tip. The idea was to approach a spore sample with a flat surface area that equally similar with the surface area of a spore. As the result, the adhesion force exerted by spore on the probe would be an equivalent value to the spores adhered to the stainless steel. Figure 24 shows the correlation between contact surface when normal tip and plateau tip is used. With that in mind, a stainless steel or chromium coated type plateau probe would be ideal for this condition.

However, this probe has an Achilles' heel in which it is impossible to scan an area to locate the spore that is crucial before proceeding to force mode as explained before. The flat tip will not provide the precise images which is similar behaviour with a broken silicon tip. Pre-visualization using the images generated from the scan sometimes could determine the location of the spores, but it is hardly accurate.

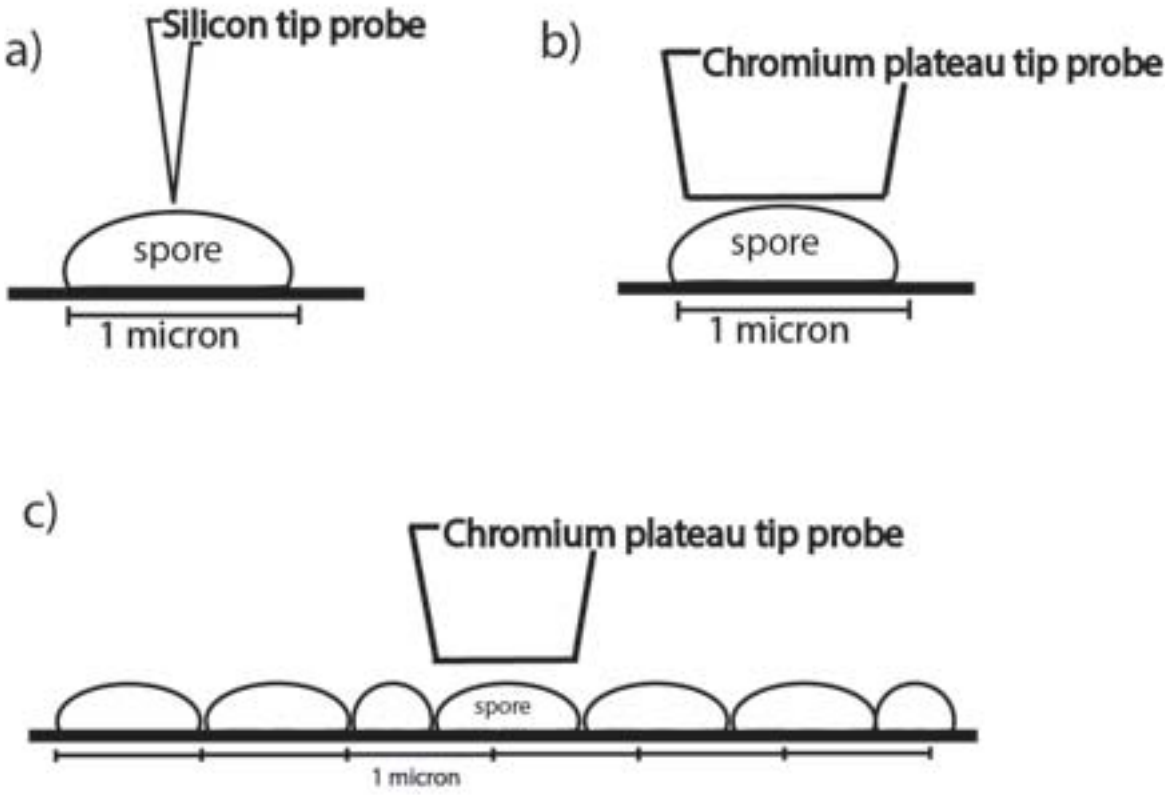

Figure 24 : Surface area measured using a silicon tip (a) and pleateau tip (b). Closely packed purified spores for an easy force measurement (c).

With this problem at hand, preparing a monolayer of highly purified spores that are closely packed on a substrate would remove the initial imaging procedure to locate the spores. In theory, spores that are packed closely and without any debris on the monolayer would provide the best chance for a probe to obtain a perfect contact with the spore surface as represented in Figure 24. Purification methods of spore suspensions were explained in section 3.2.2.

Another possible method using the idea on obtaining the overall adhesion force of the whole surface area is to use a custom spore probe which is made using the spore of interest as the tip of the probe. This type of bespoke probe was done in few literatures especially (Bowen *et al.*, 2000) which immobilize individual spore on a tipless cantilever. With this method, the stainless steel substrate will be the surface of interest while the force mode will provide the elusive adhesive force between the spore and stainless steel surface. Figure 25 shows where an individual spore is mounted on a V-shape tipless cantilever and the probe –substrate setup when in the AFM.

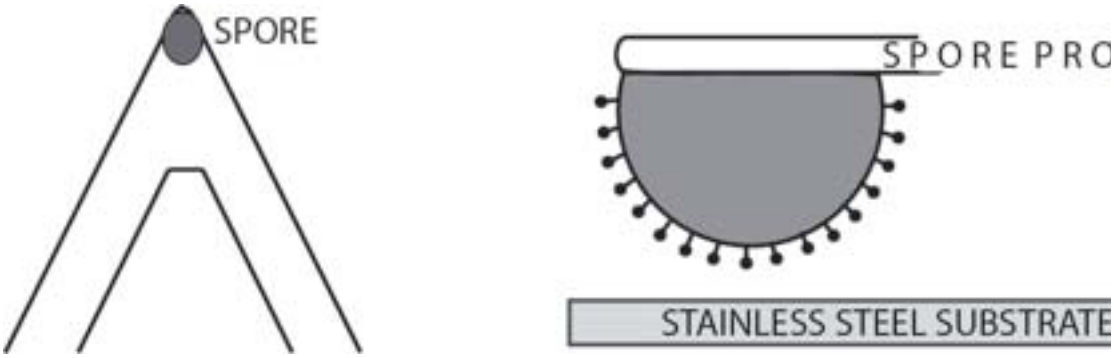

Figure 25 : A spore mounted on a tipless cantilever (left) and setup to measure adhesion force between the surfaces of spores and stainless steel (right).

This method could provide the best result but the tip has to be freshly prepared to avoid desiccation on the spore surface. Besides, even with the aid of a micromanipulator system, an extreme dexterity is required to attach a single spore onto the cantilever while avoiding the glue used from contaminating the surface that will be measured.

These three force spectroscopy methods discussed earlier are categorized as one-dimensional force imaging where only a specific intermolecular force is measured. Another major force spectroscopy technique offered with an AFM is force-mapping spectroscopy. As described in section 2.4.4, it involves a compilation of individual force curve over a specified area.

The major advantage of this technique is it could provide a massive amount of data on the interaction between the surface of the spore and the probe in just a single scan. Besides, the ability to specify a scan area provides the opportunity to obtain the force curve values of the whole spore surface exposed to the probe. In theory, this part will be likely to adhere to the stainless steel surface in the dairy plant. These individual adhesive forces in overall will give a value that should be equal or close to value obtained with a spore probe technique. Figure 26 shows a representation on the possibility to obtain adhesion force from a spore surface using Force-Volume technique

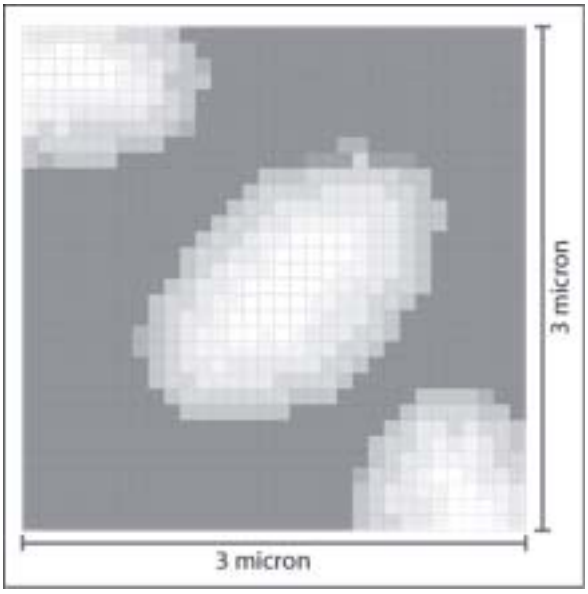

Figure 26 : 32x32 grid map on a 3x3 μm scan area. It should provide an enough scanning area to obtain a complete data from a whole spore.

A down side on this technique is the slow imaging speed even when the force map is produced with a reduced resolution, normally 64x64 grid map. In order to make each run reasonably short, a 32x32 grid map is at an acceptable value. In addition, a larger grid area requires a probe with a wider tip to ensure the adhesive force of each area is fully measured. In fact, a normal silicon probe could only measure an area of 10x10 nm at most. Hence, determining the adhesive force value between two surfaces requires a significant extrapolation if a small resolution scan is done.

4 Force-Volume imaging of *A.flavithermus* CM & *G. stearothermophilus* ATCC 2641 – Results and discussion

A.flavithermus strain CM was chosen because this is a latest strain derived from milk powder that is less studied. Besides, this strain has a faster growth and sporulation cycle in the laboratory. Since *Geobacillus* group is also a common thermophile found in milk powder and is vastly studied in the literature, using a *G.stearothermophilus* strain as a replicate for comparison with the *A.flavithermus* is beneficial.

Hence, *G.stearothermophilus* strain ATCC 2641 was chosen in this study instead of other strains derived from milk powder (P3 &D1) that were studied earlier in chapter 3. It was chosen as it produces the most spores compare to other *Geobacillus* strains. For best comparison, it is recommended that a dairy strain is used since *A.flavithermus* CM is also a dairy strain.

To gain a better understanding of how *A.flavithermus* CM spores adhere or attach on a stainless steel surface, force-volume measurement using an AFM is a good method. In this experimental setup, all imaging and force-volume measurements were done in air using fresh prepared samples (less than 6 hours old). Secondly, standard silicon tips of the same make (CSG 11/Au) were used throughout the study. A preliminary run was set up to establish the best instrumentations that should be used for future AFM run as describes in section 4.1.

4.1 Force-Volume imaging of *Anoxybacillus flavithermus* CM with various tips

The aim of this trial is to determine the suitable silicon tip that is optimally responsive with the adhesion force acting on the spore surface. In this situation, the goal is to find a type that is stiff enough to show a decent deflection value when encounter with an adhesion force on the spore surface. Although a much softer tip will have a higher sensitivity during scanning, it also has a larger deflection at an identical adhesion force which tends to exceed the measurement range of the AFM's photodiode. On the other side, a stiffer tip might not able to show a significant deflection value of the adhesion force resulting in a greater error on the final adhesion force value. As mentioned in section 2.4, both long and short tips' spring constant are 0.03 N/m and 0.1 N/m respectively.

The average distances of tip's deflection to adhesive force with the spore are 54.78±30 nm and 28.83±9.4 nm for the soft and stiff tip respectively. Ultimately, the adhesive force values between the tip and spore registered by these two different tips are between 1.943 nN to 2.543 nN.

Height and deflection imaging shows smooth and clean images indicating each tip is able to handle the fast scan rate up to 5 Hz. As the image height was pre-set to 800 nm in this trial and as the tip scans along, the area with higher elevation shows up in the images brighter. Meanwhile, area that exceeds the set values of 800 nm will be off the height scale and will be represented with a bright white area. The identified spores tend to exceed 800 nm values especially in the middle section of the spore which displays a bright white area in the image. This ‘blown highlight’ area has no collectible data as every force-curve values are off the scale. This situation will be common when a softer tip is use due to the smaller spring constant characteristic. As shows in Figure 27 where the central area of the spore exceeded the pre-set height does not contain any useful deflection values.

Since force-volume imaging relies on approach-retract sequence to generate a single force-curve graph, an area with lack of this available height will not provide a readout as the piezo had reached its maximum extension peak. With a stiffer tip, a ‘blown highlight’ is still partially salvageable as seen in Figure 28 where a decent deflection height can still be obtained. However, these values might not be accurate. Hence, it is recommended to use a larger height value of 1.5 to 2 μm for the best result in both imaging and force-volume modes.

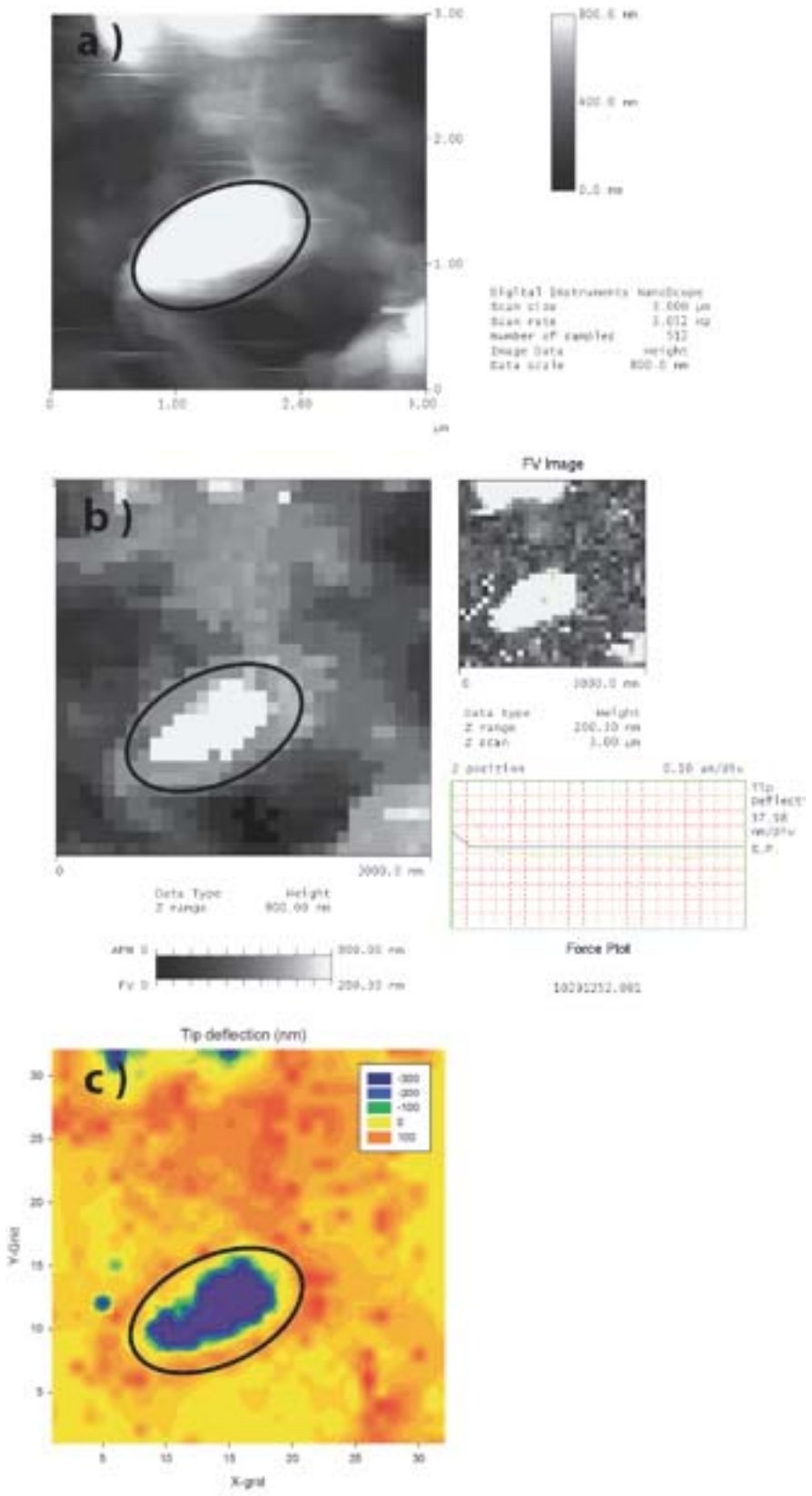

Figure 27 : *A.flavithermus* CM spores imaging using a soft CSG11/Au probe (0.03 N/m). a) Deflection b) Height & elasticity grid c) Adhesion Force's deflection

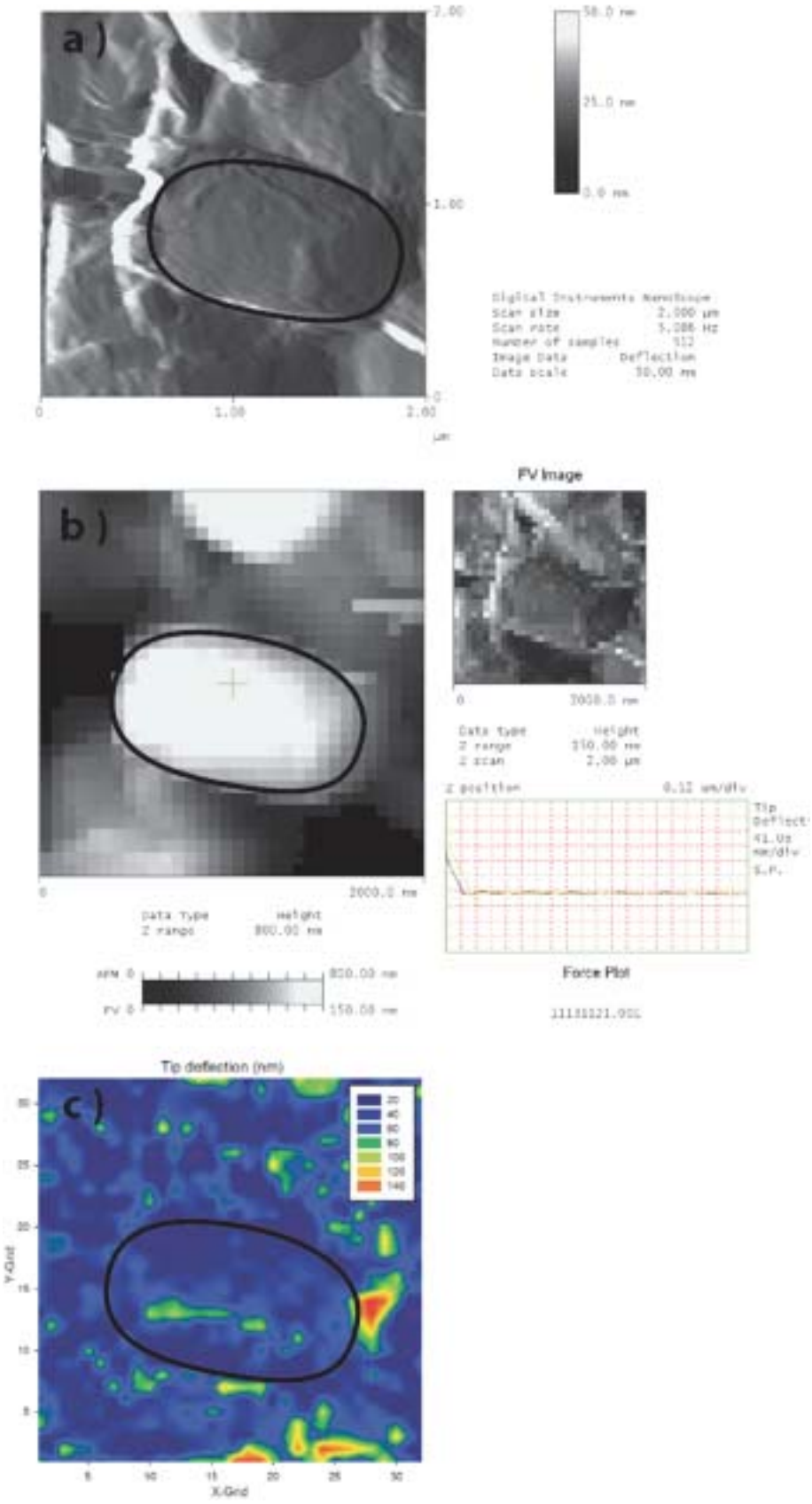

Figure 28 : *A.flavithermus* CM spores imaging using a soft CSG11/Au probe (0.1 N/m). a) Deflection b) Height & elasticity grid c) Adhesion Force's deflection

4.2 Imaging & Force-Volume of *Anoxybacillus flavithermus* CM

Once the preliminary run to determine the optimal methodology to measure the adhesion force was completed (Section 4.1), various runs under the pre-determined condition were carried out to record the force-volume readouts. This section will cover the results obtained from *A.flavithermus* CM samples. In total, 11 final spores were finalize for statistical evaluation while the best 5 images are presented in this report to provide a better understanding for the reader.

4.2.1 Imaging results

Sets of images below (Figure 29-33) show the deflection image of a single *A.flavithermus* CM spore and the bottom image show an adhesion force map of the surface. Circled area in both images is the area covered by the spore.

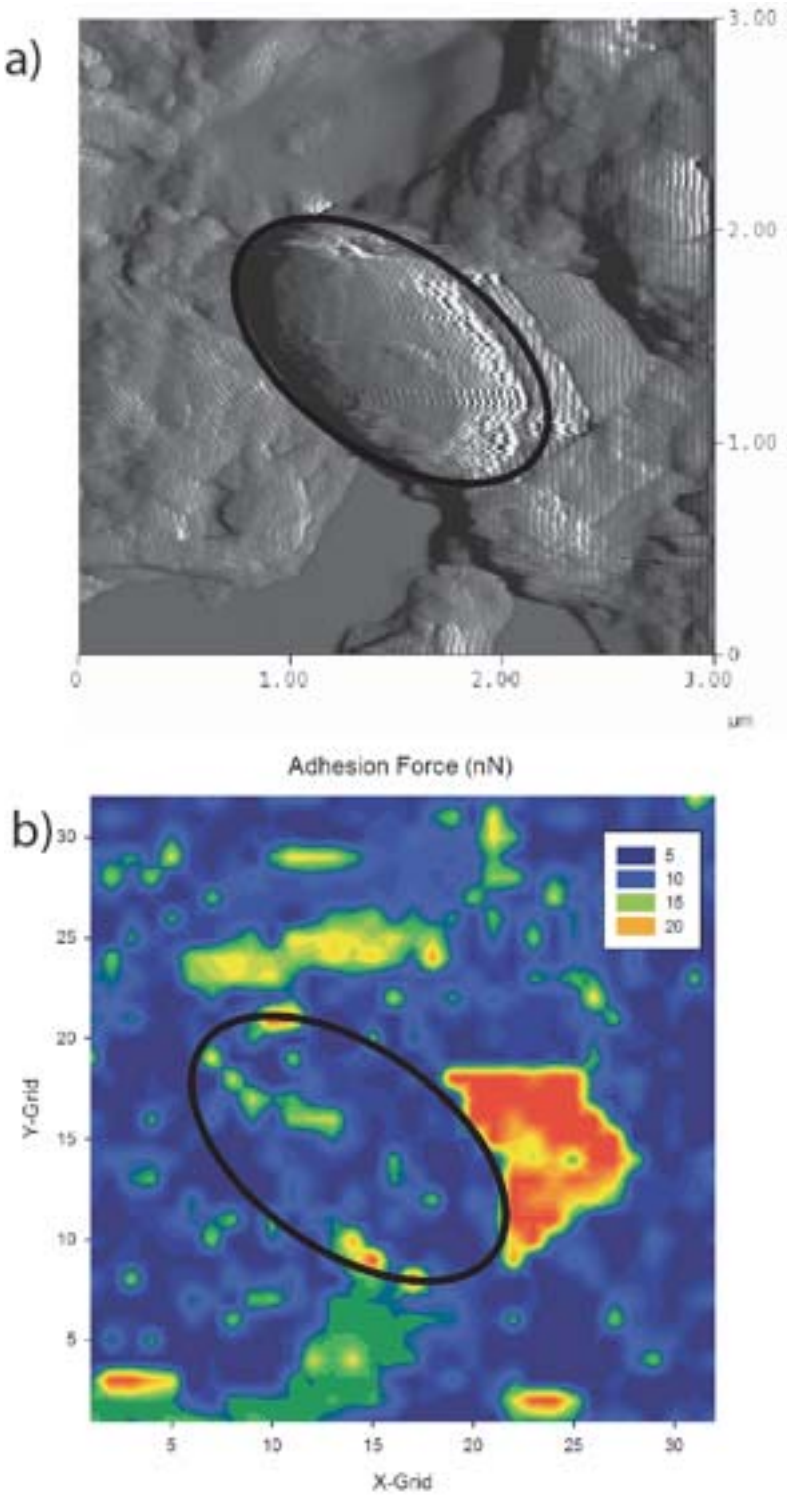

Figure 29 : *A.flavithermus* CM, Sample 1. 32x32 grid covering 4µm length.

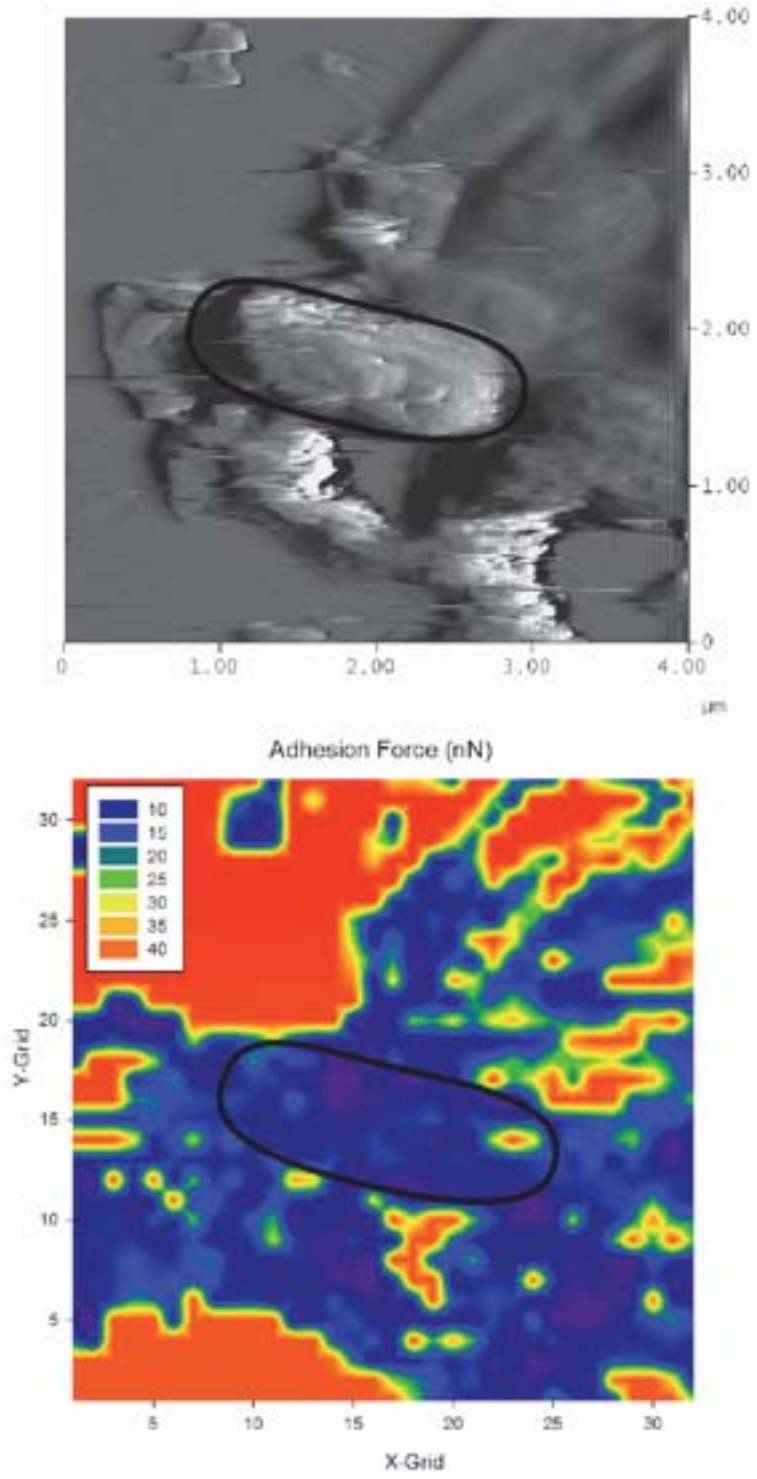

Figure 30 : *A.flavithermus* CM, Sample 2. 32x32 grid covering 4µm length.

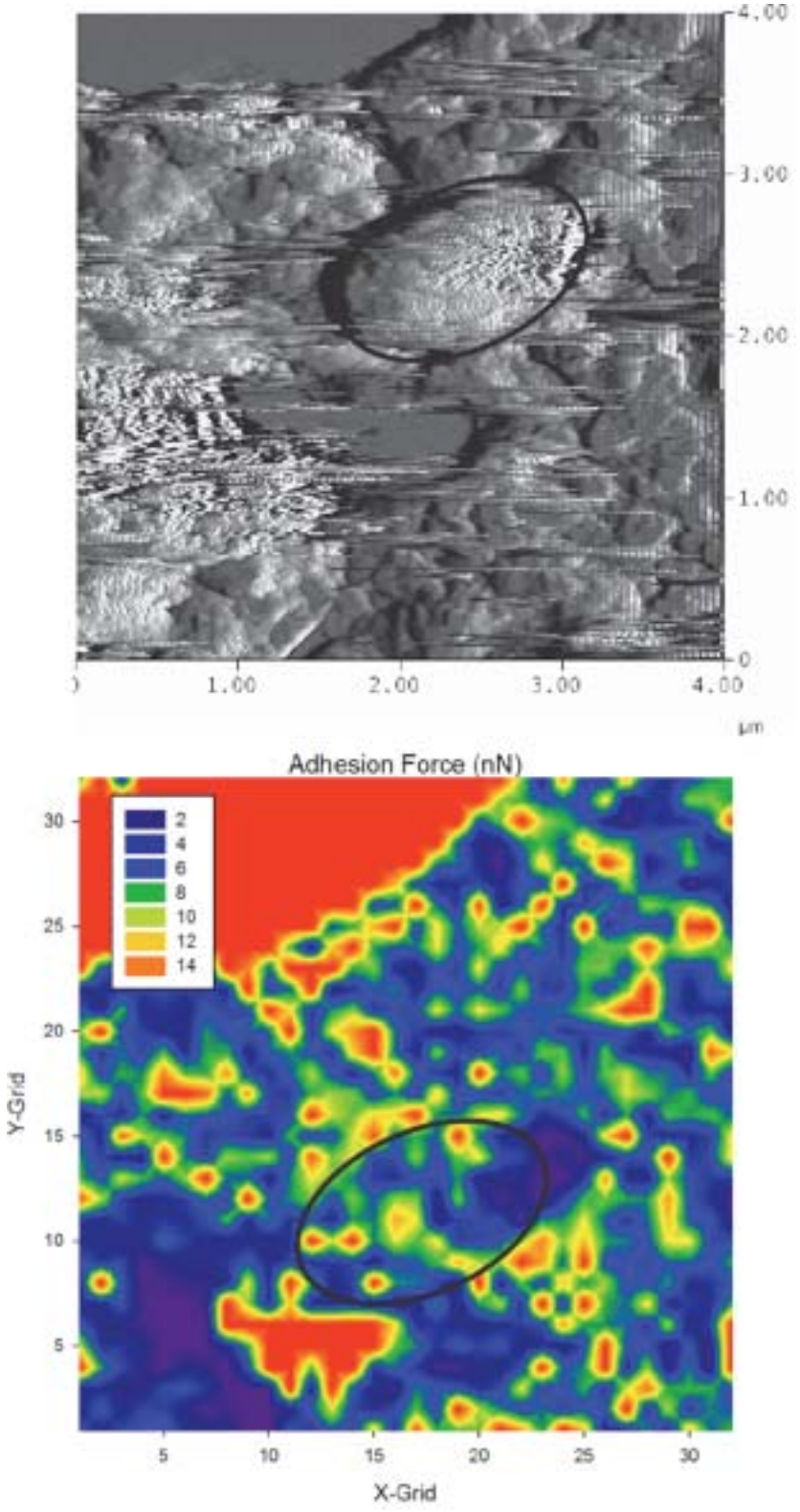

Figure 31 : *A.flavithermus* CM sample 3. 32x32 grid covering 4µm length.

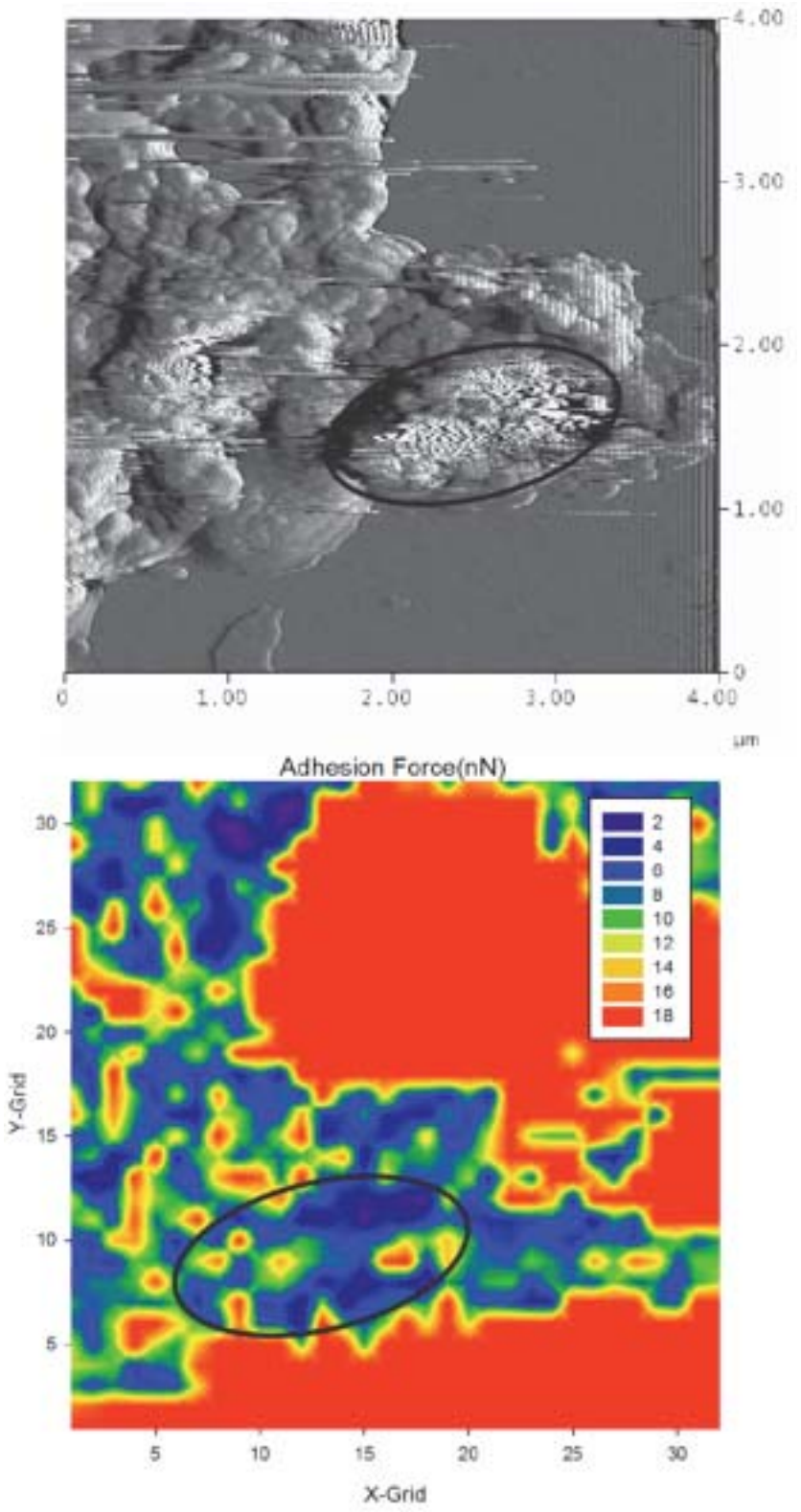

Figure 32 : *A.flavithermus* CM sample 4. 32x32 grid covering 4µm length.

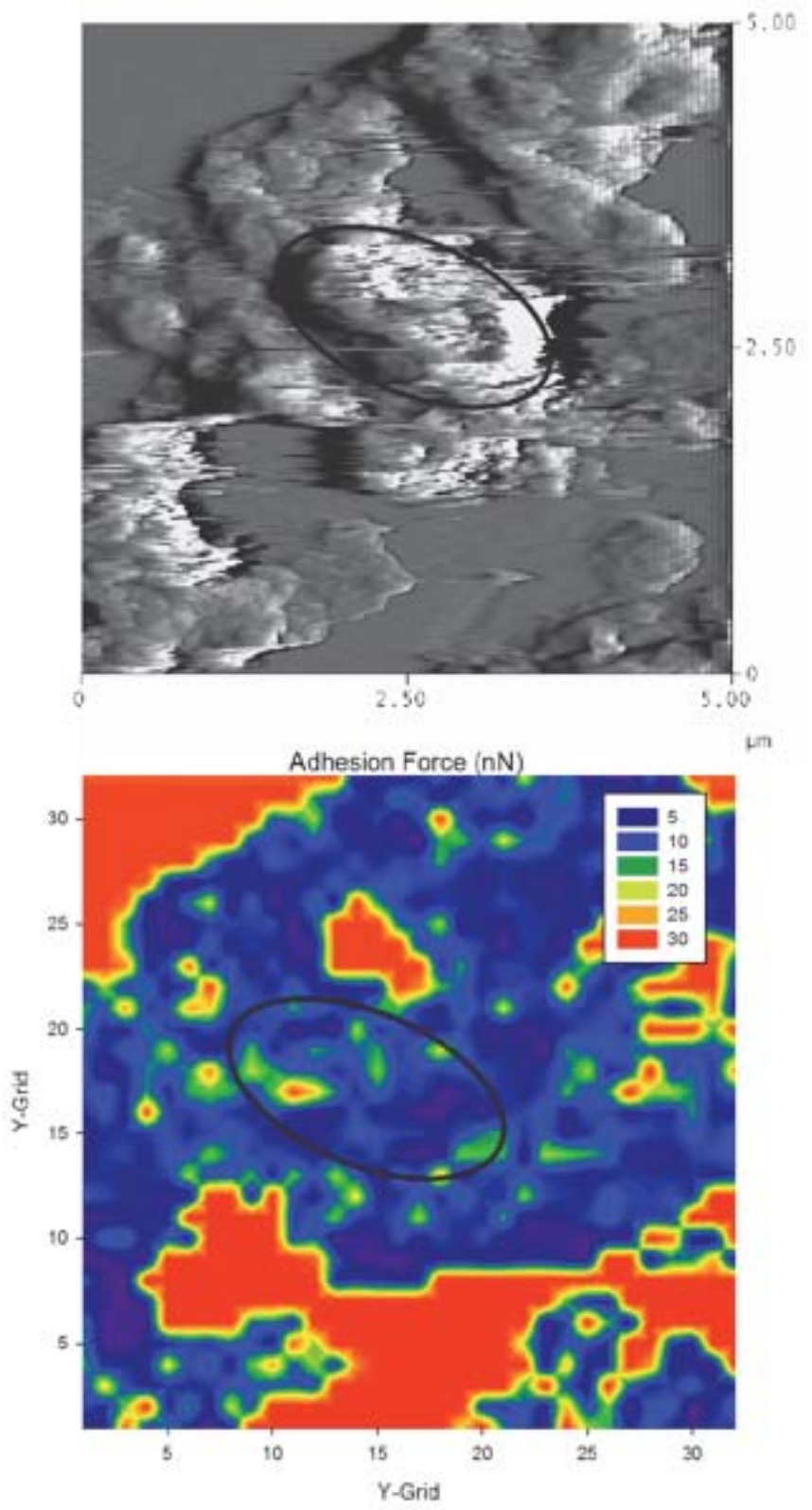

Figure 33 : *A.flavithermus* CM sample 5. 32x32 grid covering 5µm length.

4.2.2 Statistical analysis

A total of 812 adhesive force values from 11 *A.flavithermus* CM spore samples were obtained and Figure 34 shows a boxplot generated. The mean value of adhesive force measured is 3.9 ± 1.9 nN. Other values can be obtained from the Descriptive Statistics table below.

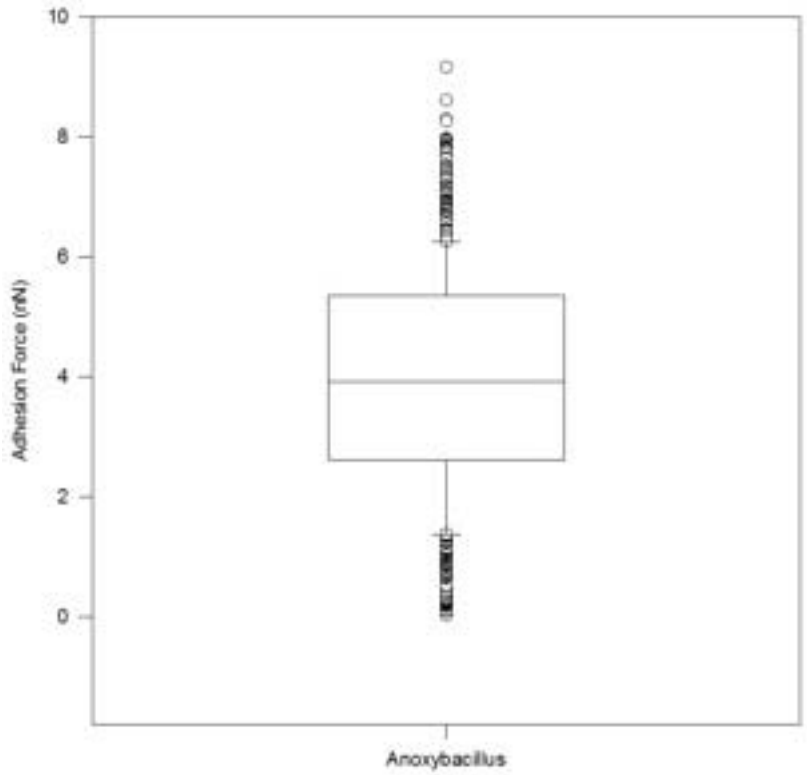

Figure 34 : Boxplot on adhesion forces of AFM tip with A.*flavithermus* CM spore surface.

Descriptive Statistics:

Data source: Data 1 in (Adhesion)Anoxy-Geo.JNB

Column	Size	Missing	Mean	Std Dev	Std. Error	C.I. of Mean
Anoxybacillus	812	0	3.928	1.876	0.0658	0.129

Column	Range	Max	Min	Median	25%	75%
Anoxybacillus	9.143	9.162	0.0184	3.924	2.615	5.351

Column	Skewness	Kurtosis	K-S Dist.	K-S Prob.	SWilk W	SWilk Prob
Anoxybacillus	0.0198	-0.598	0.0328	0.038	0.990	<0.001

Column	Sum	Sum of Squares
Anoxybacillus	3189.763	15384.657

4.3 Imaging & Force-Volume of *Geobacillus stearothermophilus* ATCC 2641

This section will cover the results obtained from *G.stearothermophilus* ATCC 2641 samples. In total, 16 final spores were finalize for statistical evaluation while the best 5 images are presented in this report to provide a better understanding for the reader.

4.3.1 Imaging results

Sets of images below (Figure 35-39) show the deflection image of a single *G.stearothermophilus* ATCC 2641 spore and the bottom image show an adhesion force map of the surface. Circled area in both images is the area covered by the spore.

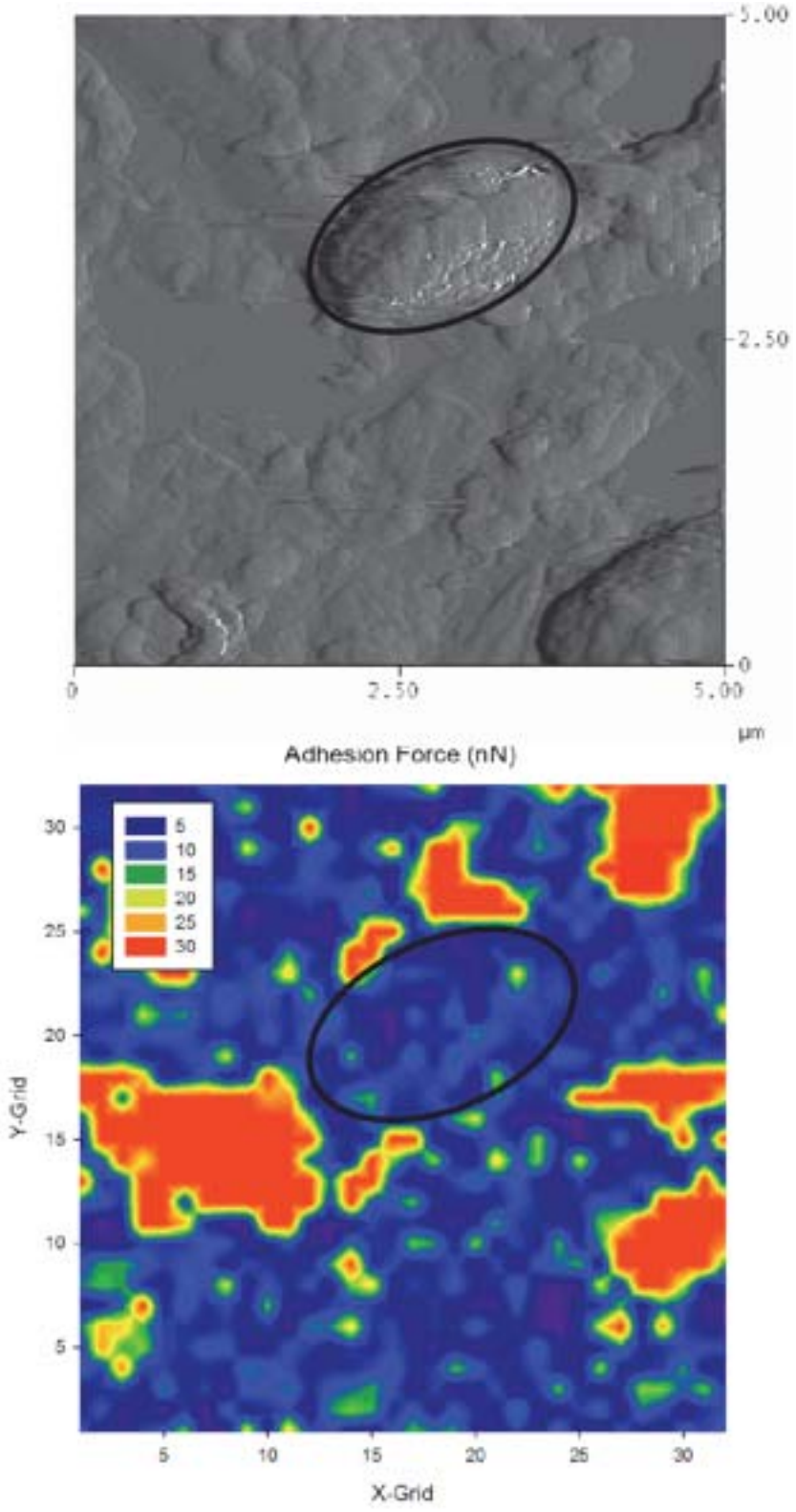

Figure 35 : *G.stearothermophilus* ATCC 2643, Sample 1. 32x32 grid covering 5µm length.

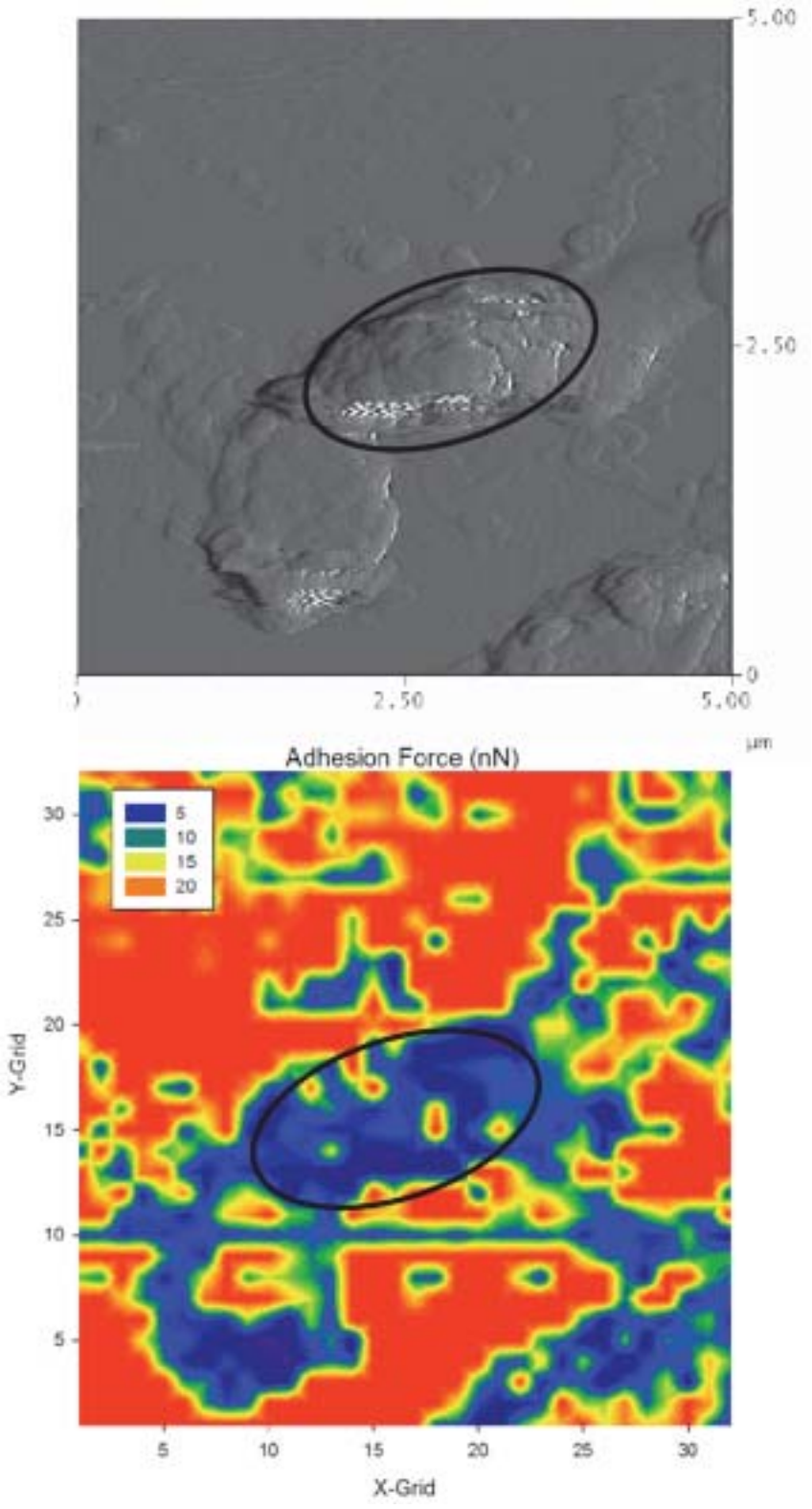

Figure 36 : *G.stearothermophilus* ATCC 2641, Sample 2. 32x32 grid covering 5µm length.

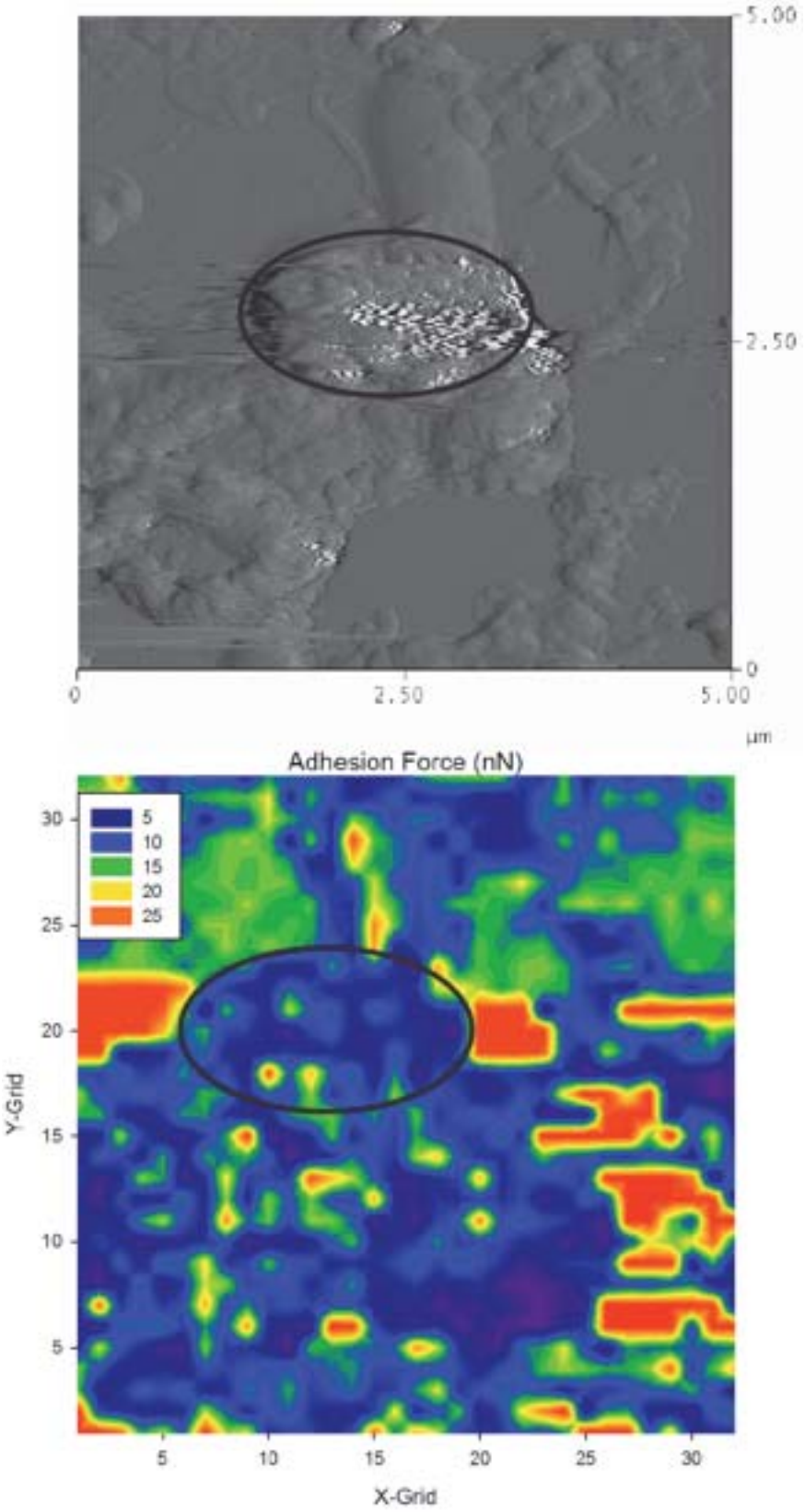

Figure 37: *G.stearothermophilus* ATCC 2641, Sample 3. 32x32 grid covering 5µm length.

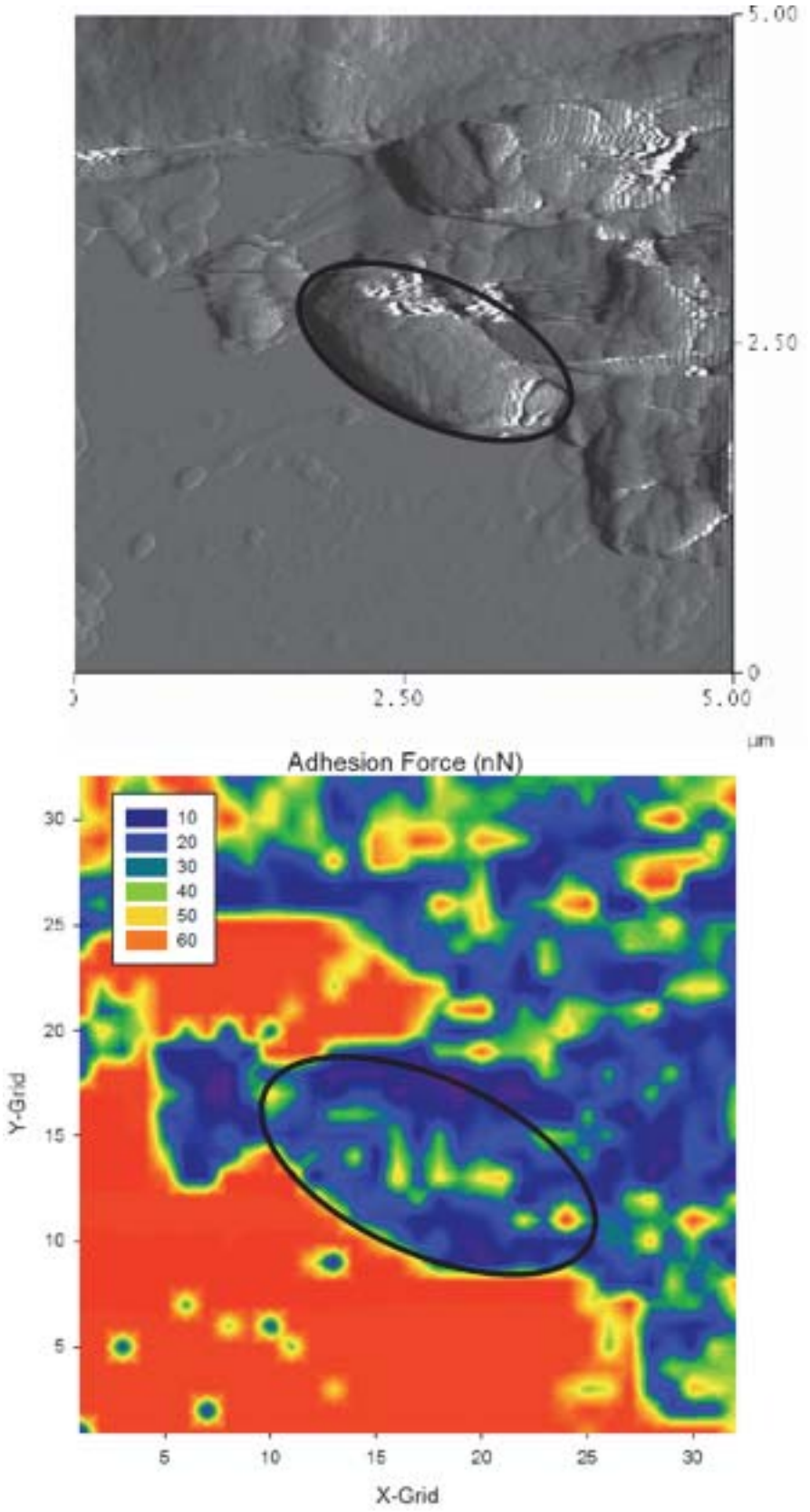

Figure 38 : *G.stearothermophilus* ATCC 2641, Sample 4. 32x32 grid covering 4µm length.

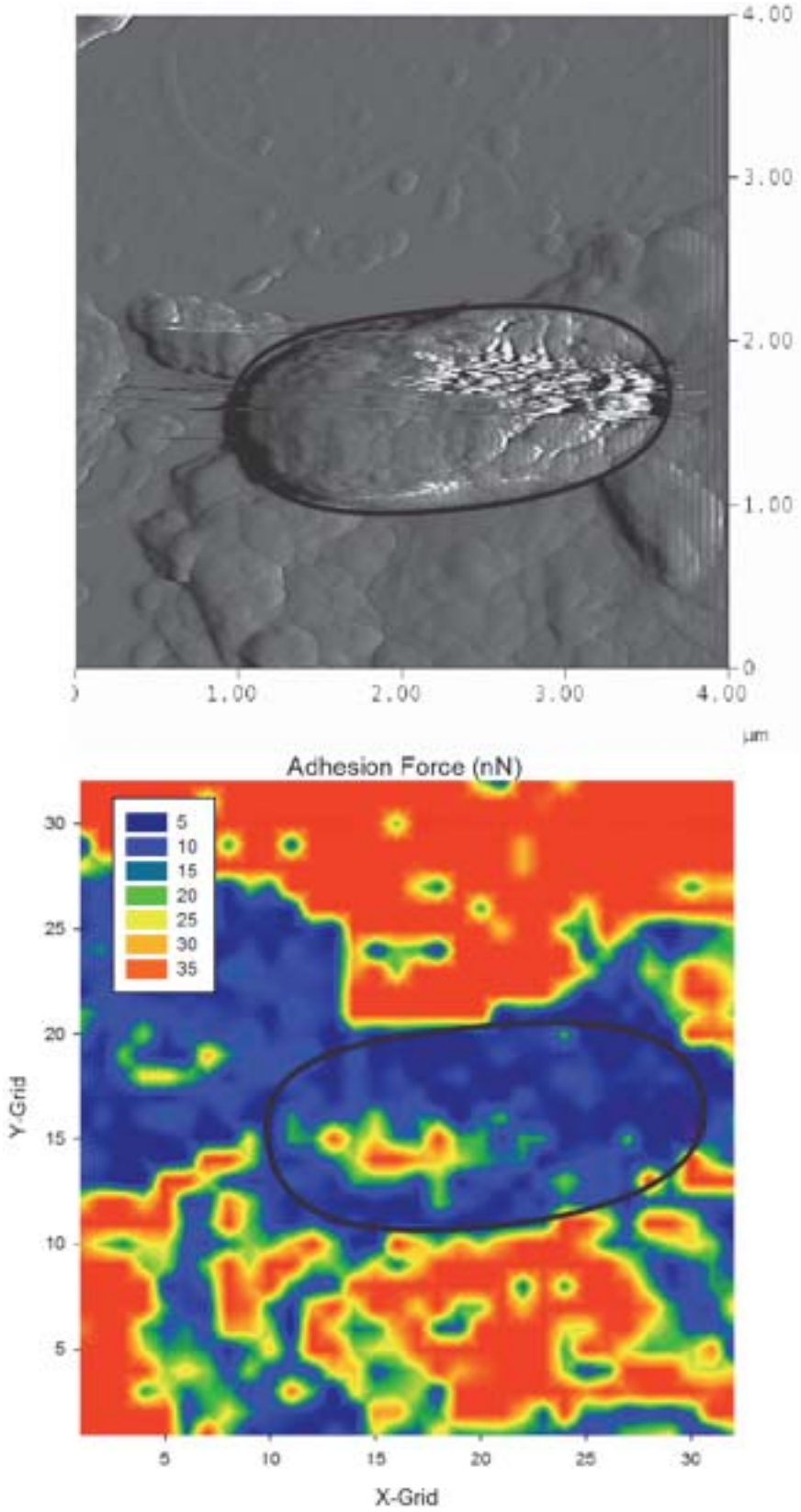

Figure 39 : *G.*stearothermophilus ATCC 2641 sample 5. 32x32 grid covering 4μm length.

4.3.2 Statistical analysis

A total of 832 adhesive force values from 16 samples of *G.stearothermophilus* ATCC 2641 spore samples were obtained and Figure 40 shows a boxplot generated. The mean value of adhesive force measured is 3.6 ± 2.6 nN. Other values can be obtained from the Descriptive Statistics table below.

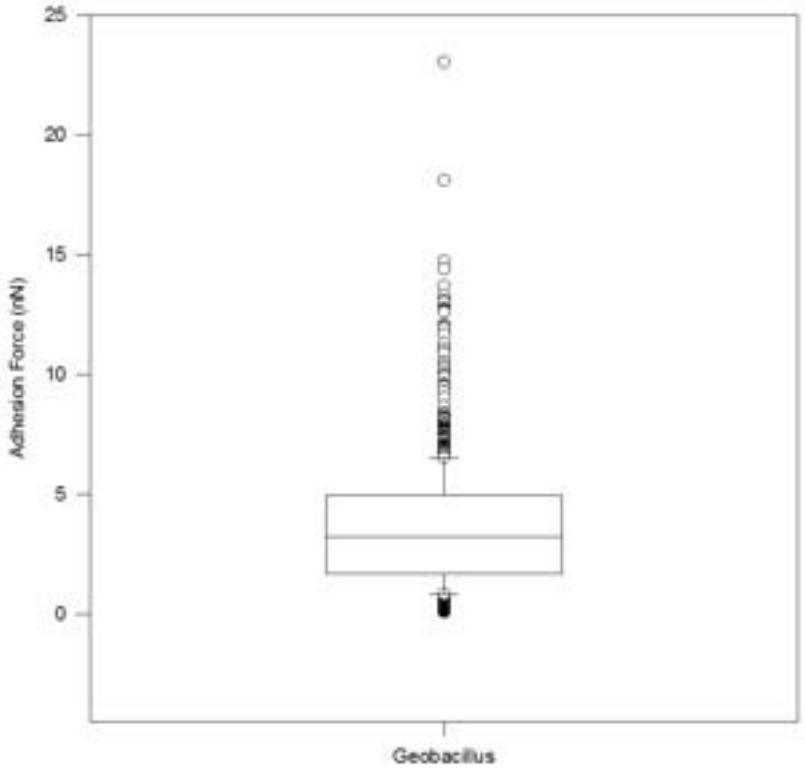

Figure 40 : Boxplot on adhesion forces of AFM tip with *G.stearothermophilus* ATCC 2641 spore surface.

Descriptive Statistics:

Data source: Data 1 in (Adhesion)Anoxy-Geo.JNB

Column	Size	Missing	Mean	Std Dev	Std. Error	C.I. of Mean
Geobacillus	832	0	3.616	2.641	0.0915	0.180

Column	Range	Max	Min	Median	25%	75%
Geobacillus	22.948	23.036	0.0872	3.235	1.668	4.951

Column	Skewness	Kurtosis	K-S Dist.	K-S Prob.	SWilk W	SWilk Prob
Geobacillus	1.727	5.993	0.0922	<0.001	0.882	<0.001

Column	Sum	Sum of Squares
Geobacillus	3008.737	16675.067

4.4 Imaging & Force-Volume of clean glass substrate

Similar AFM method used on spores was used to image and measure the force acting on clean glass surface that was used as the substrate to fix the spores in place for AFM imaging.

4.4.1 Imaging results

Sets of images below (Figure 40 & 41) show the deflection image (Top) and adhesion force map of the surface (Bottom) from a clean glass substrate.

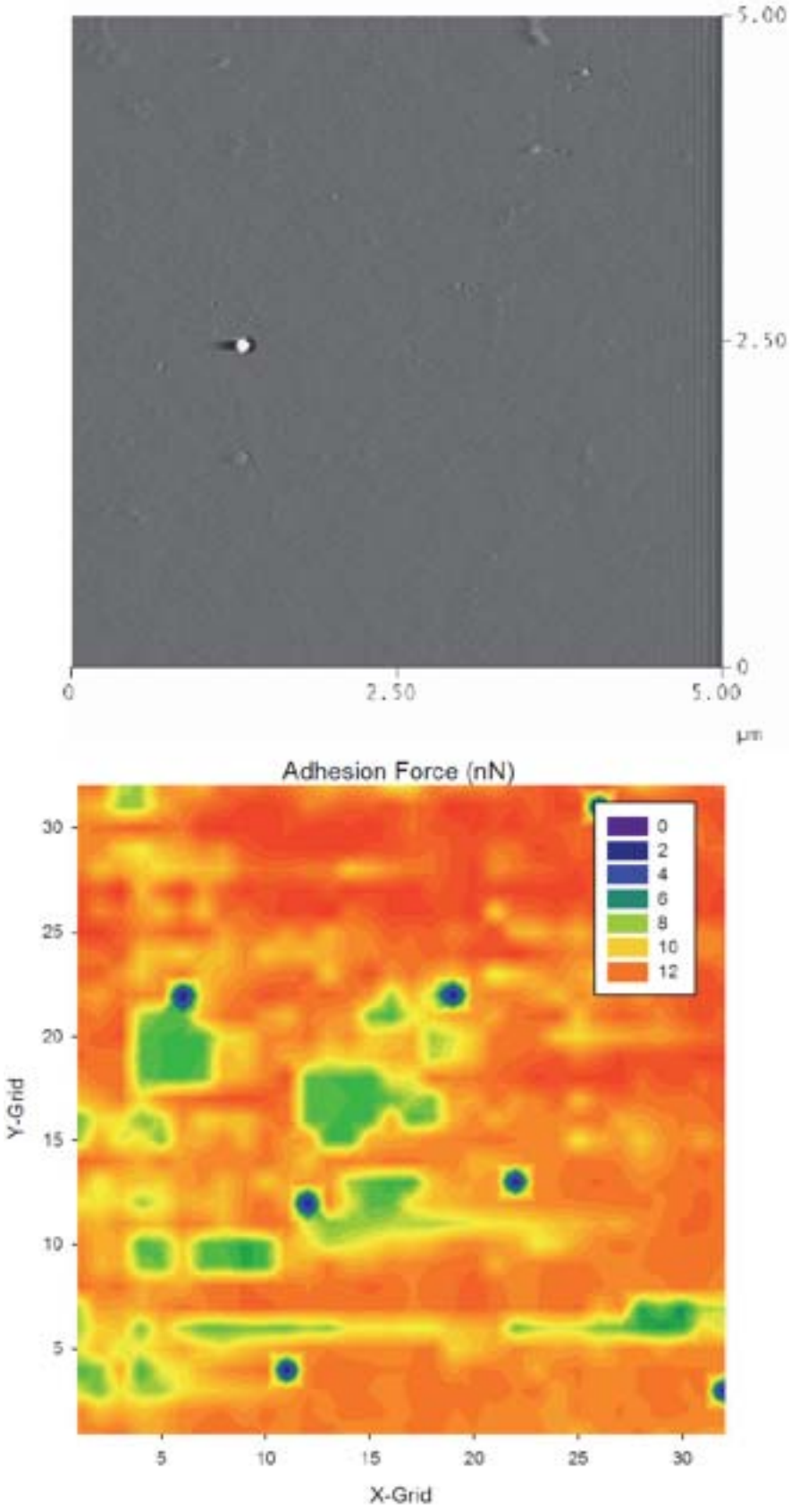

Figure 41 : Clean glass sample 1. 32x32 grids covering 5 μm lengths. (Top; Deflection, Bottom; Adhesion force map)

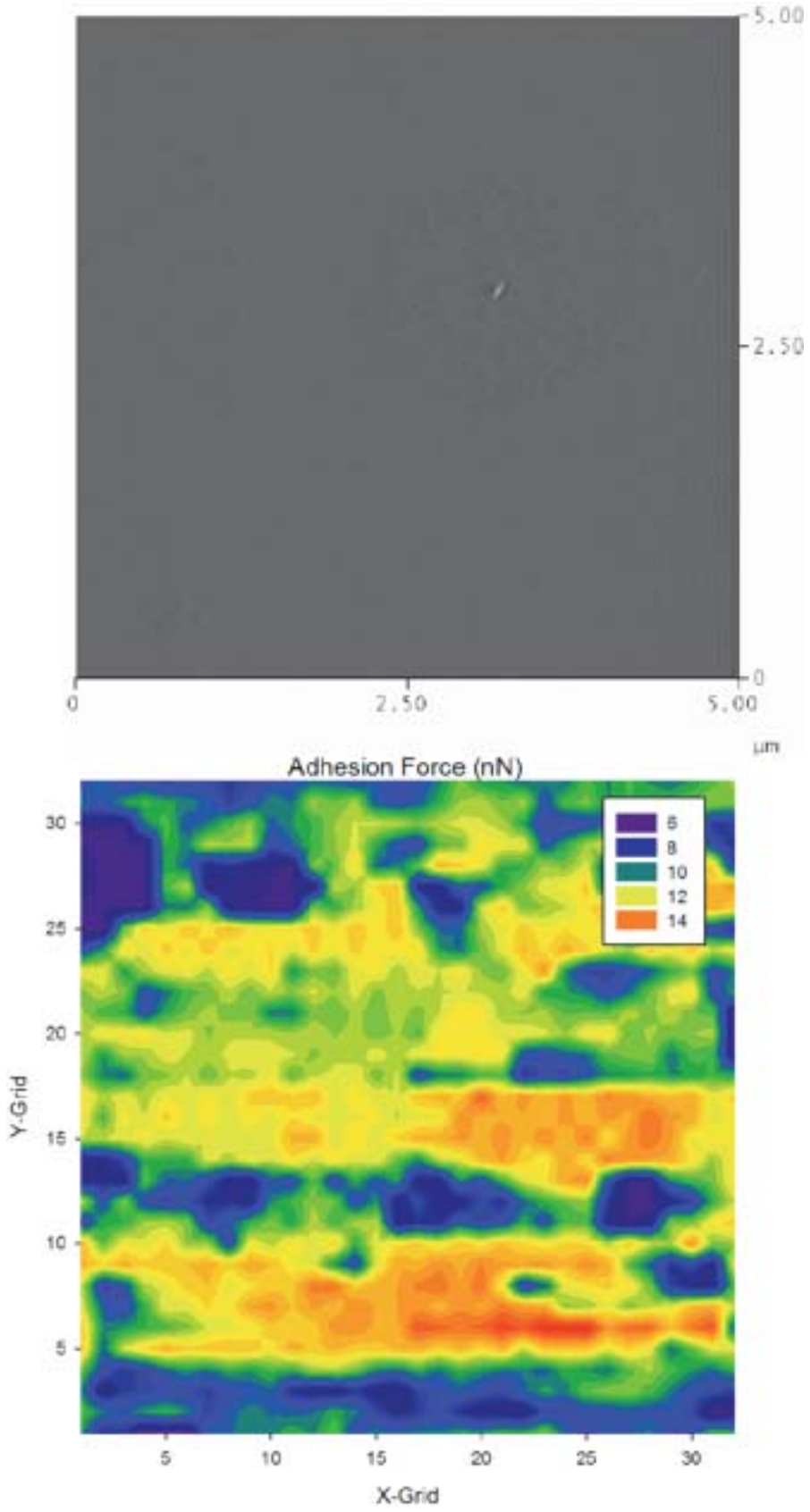

Figure 42 : Clean glass sample 2.32z32 grids covering 5μm lengths. (Top; Deflection, Bottom; Adhesion force map)

4.4.2 Statistical analysis

A total of 1912 adhesive force values from 6 clean glass samples were obtained and Figure 43 shows a boxplot generated. The mean value of adhesive force measured is 12.9±3.6 nN. Other values can be obtained from the Descriptive Statistics table below.

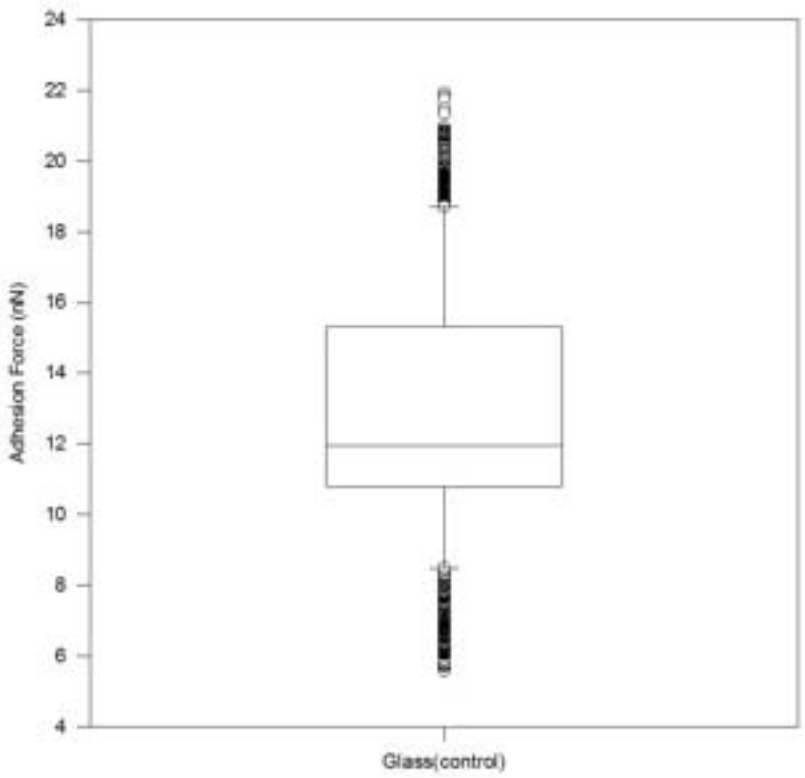

Figure 43 : Boxplot on adhesion forces of AFM tip with clean glass substrate.

Descriptive Statistics:

Data source: Data 1 in (Adhesion)Glass-control-Glass.JNB

Column	Size	Missing	Mean	Std Dev	Std. Error	C.I. of Mean
Glass(control)	1912	0	12.894	3.628	0.0830	0.163

Column	Range	Max	Min	Median	25%	75%
Glass(control)	16.321	21.906	5.585	11.966	10.793	15.309

Column	Skewness	Kurtosis	K-S Dist.	K-S Prob.	SWilk W	SWilk Prob
Glass(control)	0.388	-0.537	0.121	<0.001	0.955	<0.001

Column	Sum	Sum of Squares
Glass(control)	24653.443	343033.472

4.5 Discussion

4.5.1 Adhesion force between *A.flavithermus* CM & *G.stearothermophilus* ATCC 2641

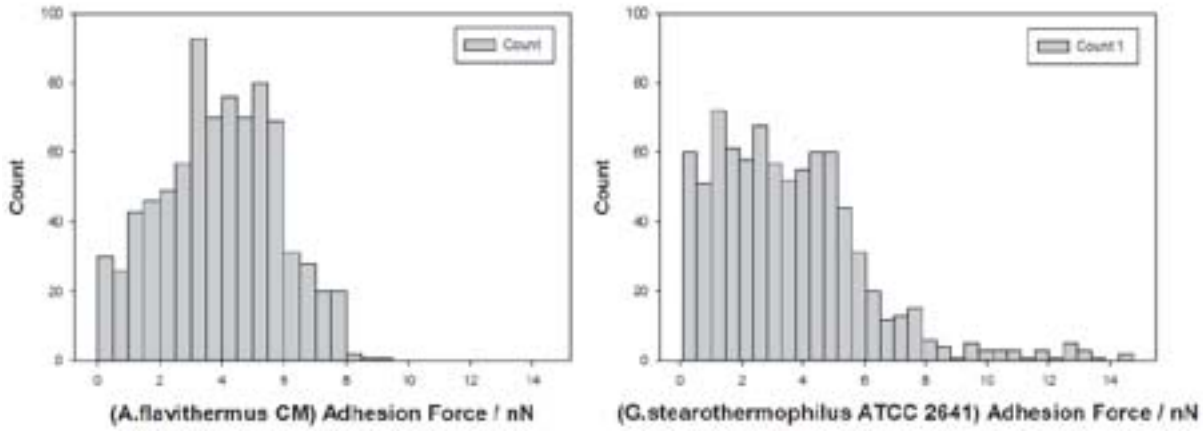

Figure 44: Histogram of adhesion force on A.*flavithermus* CM spores (left) and G.s*tearothermophilus* ATCC 2641 spores (right)

Figure 44 shows histograms on statistic distribution of adhesive force for both *A.flavithermus* CM and *G.stearothermophilus* ATCC 2641. Both histograms were built from a cumulative of 812 and 832 adhesive force values of *A.flavithermus* and *G.stearothermophilus* respectively.

The cumulative values of *A.flavithermus* CM are close to symmetrically distributed with a larger distribution on the smaller force value. Meanwhile, *G.stearothermophilus* ATCC 2641shows a positively skewed histogram with force values recorded up to the 14 nN scale. However in both histograms, most data are clustered in the 0-6 nN adhesion force region.

With that been said, a t-test analysis on both species dictates that the population mean on adhesion force of *A.flavithermus* CM is significantly higher than *G.stearothermophilus* ATCC 2641 (t-stat = -2.7, t-crit = 1.96, P= 0.007). However, if the demand require a confidence interval of 99.5% the difference in adhesion force is not significant. Although it is a relatively small difference in adhesive force (refer section 4.2.2 & 4.3.2), a higher standard deviation from *G.stearothermophilus* led to the significant difference in statistical analysis.

4.5.2 Adhesion force between thermophilic spores & glass substrate

During AFM imaging & force measurement, it was first observed that there is a significant difference on the force values between spore samples and glass substrates used.

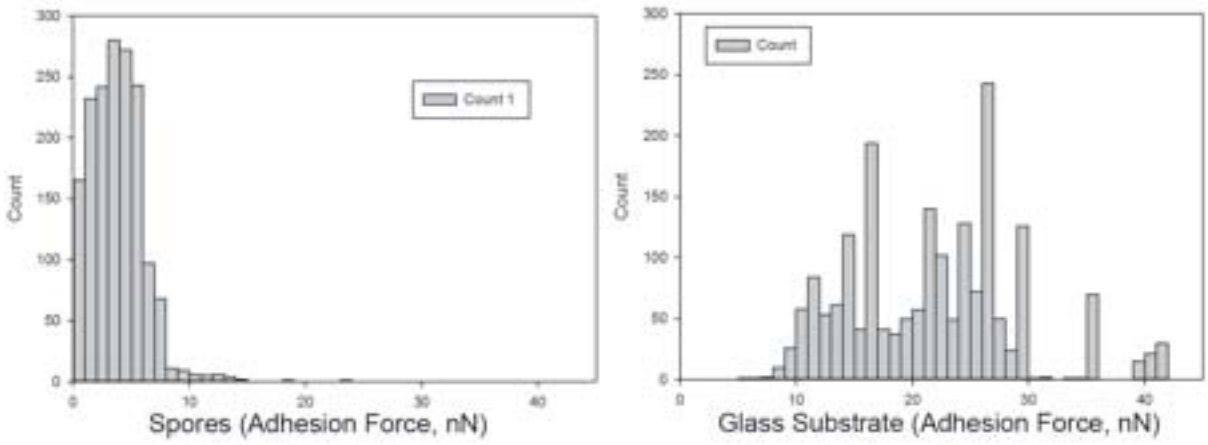

Figure 45 : Histogram of adhesion force on spores (left) and glass substrates (right)

Figure 45 shows histograms on statistic distribution of adhesive force on spores of both species and exposed glass substrate area of the samples imaged. Both histograms were built from a cumulative of 1644 and 1910 adhesive force values of spores and glass substrate.

By comparing the histograms, adhesion force values of the glass substrate with the AFM tip are mostly above the adhesion values recorded on spores. Statistical analysis shows the average adhesion force value of the spores is just 3.8±2.3 nN while a much higher average value of 21.8± 7.3 nN for the glass substrate. A t-test analysis also agrees that the AFM tip has a significantly higher interaction with the glass substrate than spores of both species (t-stat = 96.6, t-crit = 1.65, P = <0.001).

Meanwhile, comparing the difference with individual species also suggest the similar conclusion on both *A.flavithermus* CM (t-stat = 82.2, t-crit =1.645, P=<0.001) and *G.stearothermophilus* (t-stat=55.5, t-crit =1.645, P=<0.001).

4.5.3 Adhesion force between clean glass substrate & sample glass substrate

In theory, using the similar glass substrate and AFM tip of the same make would provide an equal force reading as the similar force acting on the identical material. A control test run was done to differentiate if there is any difference between a clean glass substrate and the one prepped with a spore suspension.

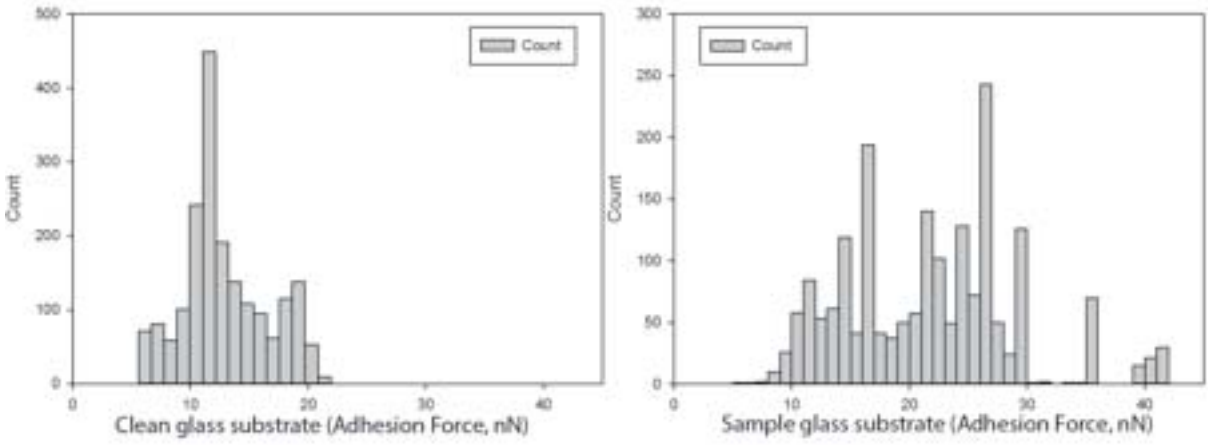

Figure 46 : Histogram of adhesion forces measured on clean glass surface (left) and glass substrate layered with spores (right)

Figure 46 shows the statistic distribution over a cumulative of 1912 and 1910 adhesive force value from 6 clean glass and 21 glass substrates respectively. The mean values for both substrates can be referred from section 4.4 and 4.5.2.

Forces measured from the clean sample shows tightly distributed values while substrate used in spore imaging has a diverse force range. The mean adhesion force value on both substrate shows a significant difference testifying that these same materials does not have the similar adhesive force value with the silicon tip. Although both values seem agreed with each other, t-test analysis shows that the adhesion force value measured from the sample glass substrate is significantly higher than the clean glass substrate (t-stat = -48, t-crit = 1.96, P= < 0.001).

4.5.4 Determining spore hydrophobicity to capillary effect

The cantilever used in the whole experiment is the high resolution Contact Silicon Cantilevers series 11 (CSG11). The single crystal silicon cantilever is doped with boron to avoid electrostatic charges that would affect the imaging. The original tip was made from pure silicon crystal but due to its instability in air, it is easily oxidised into silicon oxide. Silicon is relatively hydrophobic while its oxide is hydrophilic. Theoretically, a hydrophilic tip will have a higher adhesion force when in contact with a hydrophilic surface and shows a weaker force or none at all with hydrophobic surface.

Since all imaging was done in air, the annoying capillary effect will exist between the tip and measured surface in all samples. This minute amount of water that formed between the tip-sample regions will eventually give a higher adhesion value if it interacts with a hydrophilic surface. On the other hand when the tip interacts with a hydrophobic surface, the repulsion forces will render a lower total adhesion force compared to both hydrophilic surfaces. Figure 47 shows the graphical interpretation between two situations.

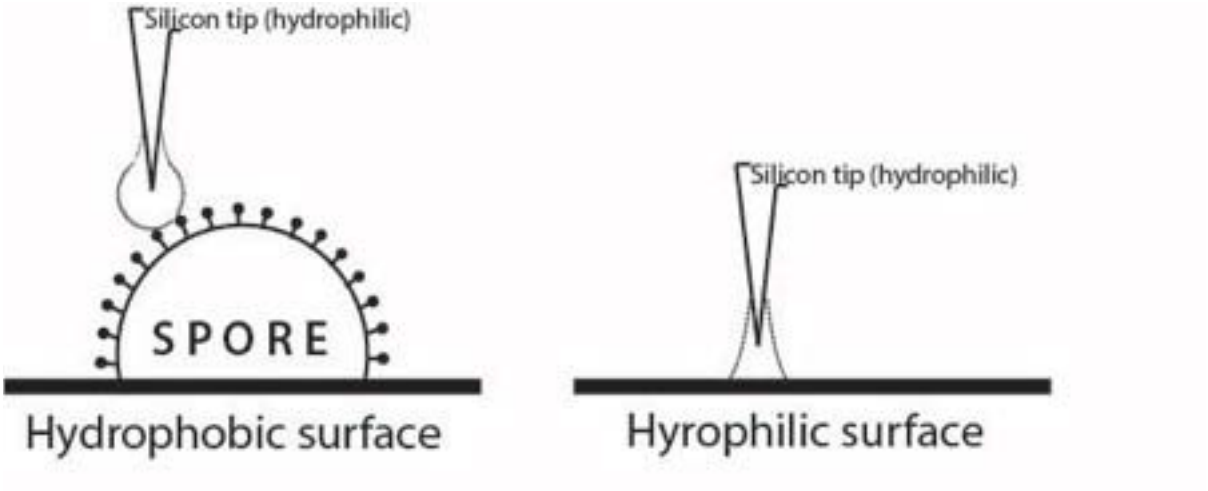

Figure 47 : Interpretation on low capillary force between hydrophilic tip - hydrophilic spores (left) and tip-glass substrate which is both hydrophilic (right)

(Bowen et al., 2002) had measured the adhesion force of *B.mycoides* with both hydrophilic and hydrophobic glass surface with an average value of 7.4±3.7 nN and 49.4±14.4 nN respectively. The result is eventually in agreement that a hydrophobic spore has a lower total adhesion forces when in contact with a hydrophilic surface. This higher value compared to what obtained in this experiment is presumed due to bigger contact area of the spore in contact with the surface. With a normal tip amount of surface interact can be control while it varies with spore tip due to size variation of spores and each spore is relatively much bigger than manufactured tip.

From the interaction results of silicon tip between spores and clean hydrophilic glass, the average adhesion values of both spores are significantly lower than value recorded with glass; *G.stearothermophilus* ATCC 2641 (3.6 ± 2.6 nN), *A.flavithermus* CM (3.9 ± 1.9 nN) & clean glass (14.1 ± 3.7 nN). This further suggests that spores are hydrophobic relative to glass and with a wide force gap between these surfaces, the capillary effects does not give a great impact on the measurement of the spores. Since hydrophobic surface have a repulsive interaction force with the hydrophilic silicon tip, low adhesion force is observed on both spore species when measured.

4.5.5 AFM silicon tip relative to stainless steel use in dairy plant

Stainless steel could varies in its hydrophobicity as a clean stainless steel has a surface contact angle of 25^{o} while treated with nitric acid renders it hydrophobic with surface contact angle as high as 60^{o}. It was shown that a highly hydrophobic *B.cereus* had the least adhered spore count on the untreated stainless steel and the highest count on oxidised hydrophobic stainless steel (Rönner *et al.*, 1990).

Since hydrophilic silicon tip is used in this experiment and considering untreated stainless steel is used in milk powder production industry, the behaviour of the two spore species should behave similar with these different materials. Since *G.stearothermophilus* spores have a low hydrophobicity value, it does not have a significant difference in adhesion between hydrophobic and hydrophilic surface (Rönner *et al.*, 1990). It does show an adhesive force during the experiment and

even a weak force, it does able to adhere to a hydrophilic surface. Hence, it should able to adhere on stainless steel surface as well.

Since *A.flavithermus* CM has a higher adhesion force with the silicon tip than *G.stearothermophilus* ATCC 2641, it has a higher chance to adhere to stainless steel. Hence, a spore count over a stainless steel surface in a spray dryer should have a higher value of *A.*flavithermus than *G.stearothermophilus*.

4.6 *Anoxybacillus flavithermus* CM : The Findings

A study shows low adhesion (0-5%) on *G.stearothermophilus* spores using the Hydrophobic Interaction Chromatography (HIC) test and with that, test on hydrophobic glass surface shows very low adherence (less than 100 spores/mm^2) compared to a very hydrophobic species (Rönner *et al.*, 1990).

The hydrophobicity of *A.flavithermus* spores has not been well characterized except a study on the vegetative cells that shows a higher adhesion (15-25%) than *G.stearothermophilus* spores using same HIC method (Palmer *et al.*, 2010). Spores have been characterized on having better adherence than its vegetative cells (Parkar *et al.*, 2001; Rönner *et al.*, 1990) and hence, testing *A.flavithermus* CM on hydrophobic glass surface in theory should give a higher spore count than *G. stearothermophilus* ATCC 2641.

The average adhesion force of *A.flavithermus* CM is higher compared to *G.stearothermophilus* ATCC 2641 suggesting that it has a lower hydrophobicity factor. The results from two sample t-test analysis had rejected the hypothesis that *A.flavithermus* CM shows similar adhesion force values with *G.stearothermophilus* ATCC 2641. This result agrees with(Parkar *et al.*, 2001) that a strain of *A.flavithermus* CM has a lower spore count values than most of G.stearothermophilus strains tested using MATH test. Hydrophilic Silicon Nitride tips were used in air and in theory, the hydrophobic surface will repel the interaction resulting a low adhesion force.

However, (Rönner *et al.*, 1990) also shows that *B. subtilis* has a lower hydrophobicity but has a higher adherence number than *G. stearothermophilus* (250 spores/mm^2). This shows that hydrophobicity does not directly influence the adhesive force of spores with a surface substrate as also agrees by others (Parkar *et al.*, 2001). Besides, its spores were even observed having 'string-like' structures on the spore surface but it does not affect the adhesion factor (Seale, Bremer, Flint, & McQuillan, 2010).

4.6.1 Adhesion force of *A.flavithermus* CM on stainless steel surface

In a Force-Volume mode of 32x32 grid resolution that measures a 3 μ x 3 μ square sample surface scans an area of 9 μm^2. Thus, a single pixel measured is roughly an area of 0.01 μm^2. Meanwhile, a CSG 11 silicon probe has a tip that could only measure a force in 0.0004 μm^2 area by simplifying the probe's end as a square with width of 20 nm as shown in Figure 48. Since only one force curve recorded in each pixel, the total adhesion value on each pixel needs to be extrapolated from the original single adhesion value. (Vadillo-Rodriguez *et al.*, 2004) also had validated that

adhesion force from a bacterium coated probe is significantly larger than standard sharp probe.

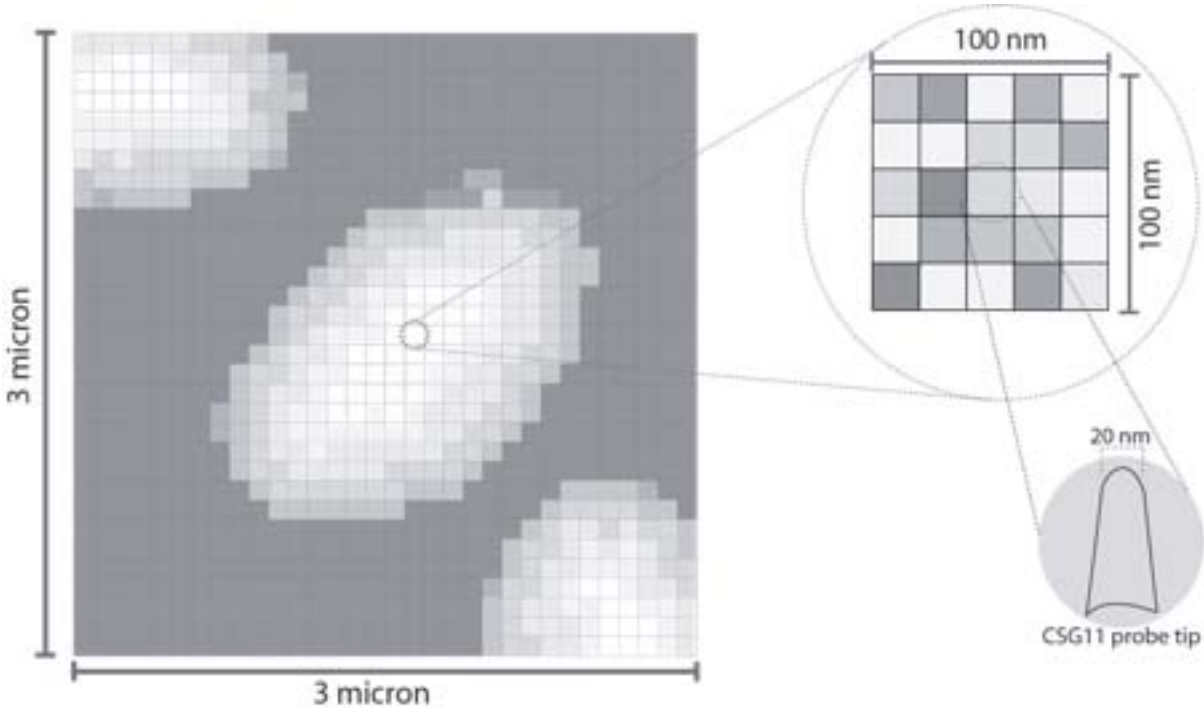

Figure 48 : A representative model in relation to the theoretical scanning area of an AFM probe.

To compile the overall value of the adhesion force on the spore surface, the simplest option is to use the height image of the FV mode and determine the area of the spore itself. The product of the amount of pixel and the average adhesion force value on a single pixel is the estimated adhesion force on a spore surface ($F_{ad'total'} = X_{pixels} F_{ad'pixel'}$). From eleven spore samples of *A.flavithermus* CM and *G.stearothermophilus* ATCC 2641, the adhesive force of a spore surface on a stainless steel are 14.0±2.8 μN and 18.0±3.1 μN respectively.

Although *G.stearothermophilus* has a smaller adhesive force with the silicon tip surface than *A.flavithermus* (Section 4.5.1), its significantly larger spore provides bigger contact area with the surface that contributes to a higher total adhesive force.

5 General Discussion

5.1 Summary

The aim of this study was to determine the adhesion force of thermophilic bacilli spores in milk powder manufacturing plant. The theoretical idea to achieve the aim is by measuring the adhesion force on the spores using force measurement methods available from an Atomic Force Microscopy (AFM). A few species were initially studied with, and the species *A.flavithermus* CM was given the spotlight interest due to minimal amount of studies of this species available in the literature. At the start of the study, the magnitude of adhesion force on *A.flavithermus* CM was not well defined. Although some studies have been done to study and measure the adhesion of spores on stainless steel, but the results were diversely spread (Bowen *et al*., 2000; Parkar *et al*., 2001; Rönner *et al*., 1990). This study has now narrowed the view on determining the adhesion force of a spore typically dairy thermophile *A.flavithermus* CM.

The results from the early trial were on the general behaviour of how spores adhere to a stainless steel substrate when developing a spore surface/spore lawn. It was found that a higher concentration or longer immersion period in a spore suspension tend to create a spore lawn with multiple layers. The spores are also loosely bound to the adjacent surfaces available and were easily dislodged upon the raster scan action of the AFM. For a proper AFM force imaging during the study, a well-defined & sturdily adhered monolayer is preferable for the best result.

Under the microscope, strains predominantly found in the dairy manufacturing plant do not produce a significant amount of spores compared to laboratory strains. Dairy strains' spore suspension (A.*flavithermus* CM, G.*stearothermophilus* P3 & G.*stearothermophilus* D1) have a small spore-to-debris ratio compared to the laboratory strains (G.*stearothermophilus* ATCC 2641 & *B.subtilis*). This situation causes a challenging situation to image and measure a specific spore under the AFM due to the interrupting debris.

The two-phase separation technique using Polyethylene Glycol (PEG) and phosphate buffer was used to purify the spores from other debris. The chemicals do not harm or significantly alter the surface of interest in the study and this similar technique had successfully separated the unwanted debris in various literature (Sacks & Alderton, 1961; Seale *et al*., 2008). Purifying the original suspension eventually provide a better spore-to-debris ratio that would provide a higher reliability in every monolayer developed. A tweak was added by adding a small amount of 0.1% polysorbate 20 in the purified suspension that provide a better imaging & measurement chances during AFM session.

For AFM analysis, various force measurement methods are possible to measure the adhesion force on the spores. The AFM force analysis standard does use the approach and retract single force-curve technique using either sharp tip or plateau tip cantilever for a specific localized reading or a single large surface area respectively.

Meanwhile, another specific approach is to use a bespoke spore probe to measure the adhesion force on the whole area in contact with specific substrate of interest.

In this spore study, the AFM force-volume technique was used with the CSG 11/Au sharp tip in all adhesion runs involving two spore species (*A.flavithermus* CM & *G.stearothermophilus* ATCC 2641) and clean glass slide as the control substrate. In the interest of this study, this is an ideal technique that measures the whole exposed sample's surface in a single scan cycle. It also mapped both height and force values simultaneously providing a redundancy in reference later in the post-processing. For an optimum measurement, the AFM sharp tip was paired with a stiff cantilever (0.1 N/m) that provides a better leeway from excessive deflection on the surface. Besides, the piezo height value was recommended to be pre-set at 2μm to achieve an accurate reading of the force mapping.

Relative to the AFM silicon tip, spores of both species were found to be hydrophobic with a small adhesion force value from 1-6.2 nN. It is relatively small compared to the hydrophilic glass surface that has a value range of 10.4-17.8 nN with this tip. Since untreated stainless steel is also hydrophilic (Rönner *et al.*, 1990) just as the silicon AFM tip, the adhesion force study that was done can be considered theoretically similar.

It was demonstrated that the attractive force from a hydrophilic surface are not significant on *A.flavithermus* CM and *G.stearothermophilus* ATCC 2641 spores. This suggests the agreement that spores of these species are hydrophobic relative to the silicon tip. *G.stearothermophilus*' spore was found to have a larger hydrophobic factor than the *A.flavithermus* when it shows a significantly smaller adhesion force with the hydrophilic AFM tip. However, a larger spore size factor in *G.stearothermophilus* provides it a higher magnitude to the total adhesion force with the stainless steel.

The result from this study will provide the dairy industry an extra sight on quantitative value of the adhesion force of thermophilic spores in dairy plant, typically in milk powder production. The fight against bacterial adhesion problem starts upon the initial contact of spores on stainless steel surface after the pasteurization stage. Once these few or even a single spore had adhered firmly on the surface, it will grow into biofilm layers. At this stage, it will be a harder effort to remove the contaminants.

Two key facts are important to battle this situation. Upon contact with the surface of stainless steel, an *A.flavithermus* CM spore could adhere to the surface with a force up to 16.8 μN while a *G.stearothermophilus* ATCC 2641 spore had a stronger force as high as 21.1 μN. Besides, a lone spore adheres better on surface compared to clustered spores. Secondly, using different materials with an opposite hydrophobicity factor than the spores is not a significant approach as spore's hydrophobicity does not dictates the magnitude of its adhesion. With that been said, the degree of adhesion on surface is greatly rely on the size of spore's surface area in contact with it.

5.2 Future Directions

This study had opened the first insight to the quantitative value of a dairy thermophilic strain on stainless steel surface. This will eventually lead to higher chances for further studies to narrow the search for better results on how these thermophilic species could thrive in the milk powder production plant.

5.2.1 Improving the methodology of Force-Volume imaging on spores

Currently, a major iteration was done to obtain the total adhesion force from a single spore as the sharp tip only covers a fraction of area in each specified grid. A flatter tip with larger contact area would be best but it lacks the imaging precision in finding the small and elusive spores.

The most ideal solution lies in the electronics technology that had seen a rapid progress in the past decade. With the advance of microprocessors, a bigger processing power promises a faster scan rate exceeding the current 32x32 grid scan. This so called high-speed AFM technique (Ando *et al.*, 2002; Ando *et al.*, 2001) could provide a better in-depth review of the spore in study.

5.2.2 Multiple dairy strains study

Instead of *A.flavithermus* CM, there are other numerous dairy thermophiles that were discovered in a milk powder processing plant. With these strains in a single study, an overall understanding can be achieved on how they generally behave in a dairy manufacturing plant. With this in mind, a proper method to maximize spore count from these low spore yielding strains is required.

5.2.3 The effect of milk processing variables on the spore's adhesion behaviour

There are many variables occur in an operation of manufacturing milk powder that might influence the magnitude of adhesion force. Examples of these variables are pH, casein's concentration and surfactant. Studying spores with these variables would provide a better representation to what really happens in the milk powder production plant. For a stable imaging and measurement with an AFM, these conditions have to be tested under liquid environment using a fluid cell module. Spore studies under these variables could provide a further understanding in their relationship with the adhesion factor.

5.2.4 Study of spore-substrate's interaction with different substrates

Current study mainly focuses on stainless steel since most of the equipment and pipeline are made from. However, different approach is possible to find out how spores behave to other different materials feasible for the plant. Materials that have an antimicrobial property such as copper or silver alloys could be an interesting subject for a study.

6 Bibliography

Adriano, O. H., & Charles, P. M. (2007). Structure, Assembly, and Function of the Spore Surface Layers. *Annual Review of Microbiology, 61*.

Albrecht, T. R., & Quate, C. F. (1987). Atomic Resolution Imaging of A Nonconductor by Atomic Force Microscopy. *Journal of Applied Physics, 62*(7), 2599-2602. doi: 10.1063/1.339435

Allen, S., Davies, J., Dawkes, A. C., Davies, M. C., Edwards, J. C., Parker, M. C., . . . Williams, P. M. (1996). In situ observation of streptavidin-biotin binding on an immunoassay well surface using an atomic force microscope. *FEBS Letters, 390*(2), 161-164. doi: http://dx.doi.org/10.1016/0014-5793(96)00651-5

Ando, T., Kodera, N., Maruyama, D., Takai, E., Saito, K., & Toda, A. (2002). A high-speed atomic force microscope for studying biological macromolecules in action. *Japanese Journal of Applied Physics Part 1-Regular Papers Short Notes & Review Papers, 41*(7B), 4851-4856. doi: 10.1143/jjap.41.4851

Ando, T., Kodera, N., Takai, E., Maruyama, D., Saito, K., & Toda, A. (2001). A high-speed atomic force microscope for studying biological macromolecules. *Proceedings of the National Academy of Sciences of the United States of America, 98*(22), 12468-12472. doi: 10.1073/pnas.211400898

Arnal, L., Serra, D. O., Cattelan, N., Castez, M. F., Vázquez, L., Salvarezza, R. C., . . . Vela, M. E. (2012). Adhesin Contribution to Nanomechanical Properties of the Virulent Bordetella pertussis Envelope. *Langmuir, 28*(19), 7461-7469. doi: 10.1021/la300811m

Ash, C., Farrow, J. A. E., Wallbanks, S., & Collins, M. D. (1991). Phylogenetic heterogeneity of the genus Bacillus revealed by comparative analysis of small-subunit-ribosomal RNA sequences. *Letters in Applied Microbiology, 13*(4), 202-206. doi: 10.1111/j.1472-765X.1991.tb00608.x

Baldwin, B., & Pearce, D. (Ed.). (2002). *Milk Powder*. Boca Raton: CRC Press.

Beldüz, A. O., Dülger, S., Demirbağ, Z., & Ertürk, Ö. (2000). Isolation and Characterisation of Bacillus flavothermus Strains from an Hot Spring of North-EastTurkey. *Biologia, 55*(3), 10.

Benoit, M. (Ed.). (2002). *Cell Adhesion Measured by Force Spectroscopy on Living Cells* (Vol. 68). USA: Elsevier Science.

Binnig, G., Gerber, C., Stoll, E., Albrecht, T. R., & Quate, C. F. (1987). Atomic Resolution with Atomic Force Microscope. *Europhysics Letters, 3*(12), 1281-1286. doi: 10.1209/0295-5075/3/12/006

Binnig, G., Quate, C. F., & Gerber, C. (1986). Atomic Force Microscopy. *Physical Review Letters, 59*(9), 930.

Bowen, W. R., Fenton, A. S., Lovitt, R. W., & Wright, C. J. (2002). The measurement of Bacillus mycoides spore adhesion using atomic force microscopy, simple counting methods, and a spinning disk technique. *Biotechnology and Bioengineering, 79*(2), 170-179. doi: 10.1002/bit.10321

Bowen, W. R., Lovitt, R. W., & Wright, C. J. (2000). Direct Quantification of Aspergillus niger Spore Adhesion in Liquid Using an Atomic Force Microscope. *Journal of Colloid and Interface Science, 228*(2), 428-433. doi: http://dx.doi.org/10.1006/jcis.2000.6969

Boyd, R. D., Verran, J., Jones, M. V., & Bhakoo, M. (2002). Use of the Atomic Force Microscope To Determine the Effect of Substratum Surface Topography on Bacterial Adhesion. *Langmuir, 18*(6), 2343-2346. doi: 10.1021/la011142p

Bremer, P. J., Seale, R. B., Flint, S., Palmer, J., Fratamicl, P. M., Annous, B. A., & Gunther, N. W. (2009). Biofilms in dairy processing. *Biofilms in the food and beverage industries*, 37. doi: 10.1533/9781845697167

Burgess, S. A., Brooks, J. D., Rakonjac, J., Walker, K. M., & Flint, S. H. (2009). The formation of spores in biofilms of Anoxybacillus flavithermus. *Journal of Applied Microbiology, 107*(3), 1012-1018. doi: 10.1111/j.1365-2672.2009.04282.x

Burgess, S. A., Lindsay, D., & Flint, S. H. (2010). Thermophilic bacilli and their importance in dairy processing. *International Journal of Food Microbiology, 144*(2), 215-225. doi: 10.1016/j.ijfoodmicro.2010.09.027

Campbell, G. A., & Mutharasan, R. (2006). Method of Measuring Bacillus anthracis Spores in the Presence of Copious Amounts of Bacillus thuringiensis and Bacillus cereus. *Analytical Chemistry, 79*(3), 1145-1152. doi: 10.1021/ac060982b

Cappella, B., & Dietler, G. (1999). Force-distance curves by atomic force microscopy. *Surface Science Reports, 34*(1-3), 1-+. doi: 10.1016/s0167-5729(99)00003-5

Carrera, M., Zandomeni, R. O., Fitzgibbon, J., & Sagripanti, J. L. (2007). Difference between the spore sizes of Bacillus anthracis and other Bacillus species. *Journal of Applied Microbiology, 102*(2), 303-312. doi: 10.1111/j.1365-2672.2006.03111.x

Chaudhuri, O., Parekh, S. H., Lam, W. A., & Fletcher, D. A. (2009). Combined atomic force microscopy and side-view optical imaging for mechanical studies of cells. *Nature Methods, 6*(5), 383-U392. doi: 10.1038/nmeth.1320

Choquet, D., Felsenfeld, D. P., & Sheetz, M. P. (1997). Extracellular Matrix Rigidity Causes Strengthening of Integrin Cytoskeleton Linkages. *Cell, 88*(1), 39-48.

Church, B. D., & Halvorson, H. (1959). Dependence of the heat resistance of bacterial endospores on their dipicolinic acid content. *Nature, 183*, 2.

Dague, E., Alsteens, D., Latgé, J.-P., & Dufrêne, Y. F. (2008). High-Resolution Cell Surface Dynamics of Germinating Aspergillus fumigatus Conidia. *Biophysical Journal, 94*(2), 656-660. doi: http://dx.doi.org/10.1529/biophysj.107.116491

Dai, J., Liu, Y., Lei, Y., Gao, Y., Han, F., Xiao, Y., & Peng, H. (2011). A new subspecies of Anoxybacillus flavithermus ssp. yunnanensis ssp. nov. with very high ethanol tolerance. *FEMS Microbiology Letters, 320*(1), 72-78. doi: 10.1111/j.1574-6968.2011.02294.x

De Clerck, E., Vanhoutte, T., Hebb, T., Geerinck, J., Devos, J., & De Vos, P. (2004). Isolation, characterization, and identification of bacterial contaminants in semifinal gelatin extracts. *Appl Environ Microbiol, 70*(6), 3664-3672.

de Hoon, M. J. L., Eichenberger, P., & Vitkup, D. (2010). Hierarchical Evolution of the Bacterial Sporulation Network. *Current Biology, 20*(17), R735-R745. doi: http://dx.doi.org/10.1016/j.cub.2010.06.031

Domke, J., Dannöhl, S., Parak, W. J., Müller, O., Aicher, W. K., & Radmacher, M. (2000). Substrate Dependent Differences in Morphology and Elasticity of Living Osteoblasts Investigated by Atomic Force Microscopy. *Colloids and Surfaces B: Biointerfaces, 19*(4), 367-379. doi: http://dx.doi.org/10.1016/S0927-7765(00)00145-4

Dufrene, Y. F. (2008). Towards Nanomicrobiology Using Atomic Force Microscopy. *Nat. Rev. Macro., 6*(9), 7.

Dufrêne, Y. F. (2000). Direct Characterization of the Physicochemical Properties of Fungal Spores Using Functionalized AFM Probes. *Biophysical Journal, 78*(6), 3286-3291.

Dufrêne, Y. F., Boonaert, C. J. P., van der Mei, H. C., Busscher, H. J., & Rouxhet, P. G. (2001). Probing molecular interactions and mechanical properties of microbial cell surfaces by atomic force microscopy. *Ultramicroscopy, 86*(1–2), 113-120. doi: http://dx.doi.org/10.1016/S0304-3991(00)00079-6

Dupres, V., Alsteens, D., Pauwels, K., & Dufrene, Y. F. (2009). In Vivo Imaging of S-Layer Nanoarrays on Corynebacterium glutamicum. *Langmuir, 25*(17), 9653-9655. doi: 10.1021/la902238q

Eaton, P. J., & West, P. (2010). *Atomic force microscopy / Peter Eaton, Paul West*: Oxford : Oxford University Press, 2010.

Emerson, R. J., & Camesano, T. A. (2004). Nanoscale investigation of pathogenic microbial adhesion to a biomaterial. *Applied and Environmental Microbiology, 70*(10), 6012-6022. doi: 10.1128/aem.70.10.6012-6022.2004

Faille, C., Jullien, C., Fontaine, F., Bellon-Fontaine, M.-N., Slomianny, C., & Benezech, T. (Writers). (2002). Adhesion of Bacillus spores and Escherichia coli cells to inert surfaces: role of surface hydrophobicity [Article], *Canadian Journal of Microbiology*: Canadian Science Publishing.

Faille, C., Lequette, Y., Ronse, A., Slomianny, C., GarÃ©naux, E., & Guerardel, Y. (2010). Morphology and physico-chemical properties of Bacillus spores surrounded or not with an exosporium: Consequences on their ability to adhere to stainless steel. *International Journal of Food Microbiology, 143*(3), 125-135.

Firtel, M., & Beveridge, T. J. (1995). Scanning probe microscopy in microbiology. *Micron, 26*(4), 347-362. doi: 10.1016/0968-4328(95)00012-7

Flint, S., Palmer, J., Bloemen, K., Brooks, J., & Crawford, R. (2001). The growth of Bacillus stearothermophilus on stainless steel. *Journal of Applied Microbiology, 90*(2), 151-157. doi: 10.1046/j.1365-2672.2001.01215.x

Flint, S. H., Brooks, J. D., & Bremer, P. J. (1997). The influence of cell surface properties of thermophilic streptococci on attachment to stainless steel. *J Appl Microbiol, 83*(4), 508-517.

Fotiadis, D. (2012). Atomic force microscopy for the study of membrane proteins. *Current Opinion in Biotechnology, 23*(4), 510-515. doi: 10.1016/j.copbio.2011.11.032

Gad, M., & Ikai, A. (1995). Method for immobilizing microbial cells on gel surface for dynamic AFM studies. *Biophysical Journal, 69*(6), 2226-2233.

Galvez, A., Abriouel, H., Lopez, R. L., & Ben Omar, N. (2007). Bacteriocin-based strategies for food biopreservation. *Int J Food Microbiol, 120*(1-2), 51-70.

Gautam, N., & Sharma, N. (2009). Bacteriocin : safest approach to preserve food products. *Indian Journal of Microbiology, 49*, 8.

Grossman, A. D., & Losick, R. (1988). Extracellular control of spore formation in Bacillus subtilis. *Proceedings of the National Academy of Sciences, 85*(12), 4369-4373.

Heinen, W., Lauwers, A. M., & Mulders, J. W. (1982). Bacillus flavothermus, a newly isolated facultative thermophile. *Antonie Van Leeuwenhoek, 48*(3), 265-272.

Helenius, J., Heisenberg, C.-P., Gaub, H. E., & Muller, D. J. (2008). Single-cell force spectroscopy. *Journal of Cell Science, 121*(11), 1785-1791. doi: 10.1242/jcs.030999

Helenius, J., Heisenberg, C. P., Gaub, H. E., & Muller, D. J. (2008). Single-cell force spectroscopy. *Journal of Cell Science, 121*(11), 1785-1791. doi: 10.1242/jcs.030999

Higginbottom, C. (1953). 501. The effect of storage at different relative humidities on the survival of micro-organisms in milk powder and in pure cultures dried in milk. *Journal of Dairy Research, 20*(01), 65-75. doi: doi:10.1017/S0022029900006713

Holo, H., Faye, T., Brede, D. A., Nilsen, T., Ødegård, I., Langsrud, T., . . . Nes, I. F. (2002). Bacteriocins of propionic acid bacteria. *Lait, 82*(1), 59-68.

Husmark, U., & Rönner, U. (1992). The influence of hydrophobic, electrostatic and morphologic properties on the adhesion of Bacillus spores. *Biofouling, 5*(4), 335-344. doi: 10.1080/08927019209378253

Ito, K. A. (1981). Thermophilic organisms in food spoilage: flat-sour aerobes. *Journal of Food Protection, 44*(2).

Kalogridou-Vassiliadou, D. (1992). Biochemical Activities of Bacillus Species Isolated from Flat Sour Evaporated Milk. *Journal of Dairy Science, 75*(10), 2681-2686. doi: 10.3168/jds.S0022-0302(92)78030-8

Kennedy, J., & Thorley, M. (2000). Guidebook to the Extracellular Matrix, Anchor, and Adhesion Proteins, 2nd Edition Thomas Kreis & Ronald Vale (Eds.). *Bioseparation, 9*(1), 56-56. doi: 10.1023/a:1008192324993

Koshikawa, T., Yamazaki, M., Yoshimi, M., Ogawa, S., Yamada, A., Watabe, K., & Torii, M. (1989). Surface hydrophobicity of spores of Bacillus spp. *J Gen Microbiol, 135*(10), 2717-2722.

Kristensen, T. J. (2010). Milk Powder Technology *Evaporation & Spray Drying*

Lau, P. C. Y., Lindhout, T., Beveridge, T. J., Dutcher, J. R., & Lam, J. S. (2009). Differential Lipopolysaccharide Core Capping Leads to Quantitative and Correlated Modifications of Mechanical and Structural Properties in Pseudomonas aeruginosa Biofilms. *Journal of Bacteriology, 191*(21), 6618-6631. doi: 10.1128/jb.00698-09

Li, J., Cassell, A. M., & Dai, H. J. (1999). Carbon nanotubes as AFM tips: Measuring DNA molecules at the liquid/solid interface. *Surface and Interface Analysis, 28*(1), 8-11. doi: 10.1002/(sici)1096-9918(199908)28:1<8::aid-sia610>3.0.co;2-4

Medalsy, I., Hensen, U., & Muller, D. J. (2011). Imaging and Quantifying Chemical and Physical Properties of Native Proteins at Molecular Resolution by Force–Volume AFM. *Angewandte Chemie International Edition, 50*(50), 12103-12108. doi: 10.1002/anie.201103991

Meyer, E. (1992). Atomic Force Microscopy. *Progress in Surface Science, 41*.

Milk Powder Production. (n.d.). Retrieved from www.dairyconsultant.co.uk/pdf/milk_powder_production.pdf website:

Misevic, G. N., Karamanos, Y., & Misevic, N. J. (2008). Atomic Force Microscopy Measurements of Intermolecular Binding Forces (Vol. 522, pp. 143-150).

Morris, V. J., Kirby, A. R., & Gunning, A. P. (1999). *Atomic force microscopy for biologists / V J Morris, A R Kirby, A P Gunning*: London : Imperial College Press, c1999.

Müller, D. J., Baumeister, W., & Engel, A. (1999). Controlled unzipping of a bacterial surface layer with atomic force microscopy. *Proceedings of the National Academy of Sciences, 96*(23), 13170-13174. doi: 10.1073/pnas.96.23.13170

Nazina, T. N., Tourova, T. P., Poltaraus, A. B., Novikova, E. V., Grigoryan, A. A., Ivanova, A. E., . . . Ivanov, M. V. (2001). Taxonomic study of aerobic thermophilic bacilli: descriptions of Geobacillus subterraneus gen. nov., sp. nov. and Geobacillus uzenensis sp. nov. from petroleum reservoirs and transfer of Bacillus stearothermophilus, Bacillus thermocatenulatus, Bacillus thermoleovorans, Bacillus kaustophilus, Bacillus thermodenitrificans to Geobacillus as the new combinations G. stearothermophilus, G. th. *Int J Syst Evol Microbiol, 51*(Pt 2), 433-446.

Nicolaus, B., Lama, L., Esposito, E., Manca, M. C., di Prisco, G., & Gambacorta, A. (1996). “Bacillus thermoantarcticus” sp. nov., from Mount Melbourne, Antarctica: a novel thermophilic species. *Polar Biology, 16*(2), 101-104. doi: 10.1007/s003000050034

Nold, S. C., Kopczynski, E. D., & Ward, D. M. (1996). Cultivation of aerobic chemoorganotrophic proteobacteria and gram-positive bacteria from a hot spring microbial mat. *Appl Environ Microbiol, 62*(11), 3917-3921.

Nugaeva, N., Gfeller, K. Y., Backmann, N., Düggelin, M., Lang, H. P., Güntherodt, H.-J., & Hegner, M. (2007). An Antibody-Sensitized Microfabricated Cantilever for the Growth Detection of Aspergillus niger Spores. *Microscopy and Microanalysis, 13*(01), 13-17. doi: doi:10.1017/S1431927607070067

Ohnesorge, F., & Binnig, G. (1993). True atomic resolution by atomic force microscopy through repulsive and attractive forces. *Science, 260*(5113), 1451-1456. doi: 10.1126/science.260.5113.1451

Palmer, J. S., Flint, S. H., Schmid, J., & Brooks, J. D. (2010). The role of surface charge and hydrophobicity in the attachment of Anoxybacillus flavithermus isolated from milk powder. *Journal of Industrial Microbiology & Biotechnology, 37*(11), 1111-1119. doi: 10.1007/s10295-010-0758-x

Parkar, S. G., Flint, S. H., & Brooks, J. D. (2003). Physiology of biofilms of thermophilic bacilli—potential consequences for cleaning. *Journal of Industrial Microbiology & Biotechnology, 30*(9), 553-560. doi: 10.1007/s10295-003-0081-x

Parkar, S. G., Flint, S. H., Palmer, J. S., & Brooks, J. D. (2001). Factors influencing attachment of thermophilic bacilli to stainless steel. *Journal of Applied Microbiology, 90*(6), 901-908. doi: 10.1046/j.1365-2672.2001.01323.x

Pearce, K. N. (1996). Milk Powder. Retrieved from http://nzic.org.nz/ChemProcesses/dairy/3C.pdf website:

Pikuta, E., Cleland, D., & Tang, J. (2003). Aerobic growth of Anoxybacillus pushchinoensis K1(T): emended descriptions of A. pushchinoensis and the genus Anoxybacillus. *Int J Syst Evol Microbiol, 53*(Pt 5), 1561-1562.

Pikuta, E., Lysenko, A., Chuvilskaya, N., Mendrock, U., Hippe, H., Suzina, N., . . . Laurinavichius, K. (2000). Anoxybacillus pushchinensis gen. nov., sp nov., a novel anaerobic, alkaliphilic, moderately thermophilic bacterium from manure, and description of Anoxybacillus falvithermus comb. nov. *International Journal of Systematic and Evolutionary Microbiology, 50*, 2109-2117.

Prickett, P. S. (1928). Thermopilic and thermoduric microorganisms with special reference to species isolated from milk. *NY State Agr. Exp. Sta. Bull., 147*, 58.

Ronimus, R. S., Parker, L. E., Turner, N., Poudel, S., Rückert, A., & Morgan, H. W. (2003). A RAPD-based comparison of thermophilic bacilli from milk powders. *International Journal of Food Microbiology, 85*(1–2), 45-61. doi: 10.1016/s0168-1605(02)00480-4

Ronimus, R. S., Rueckert, A., & Morgan, H. W. (2006). Survival of thermophilic spore-forming bacteria in a 90+ year old milk powder from Ernest Shackelton's Cape Royds Hut in Antarctica. *Journal of Dairy Research, 73*(02), 235-243. doi: doi:10.1017/S0022029906001749

Rönner, U., Husmark, U., & Henriksson, A. (1990). Adhesion of bacillus spores in relation to hydrophobicity. *Journal of Applied Microbiology, 69*(4), 550-556. doi: 10.1111/j.1365-2672.1990.tb01547.x

Rosenberg, M., & Kjelleberg, S. (1986). Hydrophobic interaction: role in bacterial adhesion. [Review]. *Advances in Microbial Ecology, 9*, 353-393.

Russell, A. D. (1982). The bacterial spore *The Destruction of Bacterial Spores* (pp. 29). London: Academic Press Inc.

Sacks, L. E., & Alderton, G. (1961). Behavior of bacterial spores in aqueous polymer two-phase systems. *J Bacteriol, 82*, 331-341.

Scott, S. (2005). *The growth of thermophilic bacteria in powder plant and the formation of spores in biofilms of the dairy thermophile Anoxybacillus flavithermus.* Massey University, Palmerston North.

Seale, R. B., Bremer, P. J., Flint, S. H., & McQuillan, A. J. (2010). Characterization of spore surfaces from a Geobacillus sp. isolate by pH dependence of surface charge and infrared spectra. *Journal of Applied Microbiology, 109*(4), 1339-1348. doi: 10.1111/j.1365-2672.2010.04760.x

Seale, R. B., Flint, S. H., McQuillan, A. J., & Bremer, P. J. (2008). Recovery of spores from thermophilic dairy bacilli and effects of their surface characteristics on attachment to different surfaces. *Applied and Environmental Microbiology, 74*(3), 731-737. doi: 10.1128/aem.01725-07

Setlow, P. (1995). Mechanisms for the Prevention of Damage to DNA in Spores of Bacillus Species. *Annual Review of Microbiology, 49*.

Stapelfeldt, H., Nielsen, B. R., & Skibsted, L. H. (1997). Effect of heat treatment, water activity and storage temperature on the oxidative stability of whole milk powder. *International Dairy Journal, 7*(5), 331-339. doi: http://dx.doi.org/10.1016/S0958-6946(97)00016-2

Stephens, C. (1998). Bacterial sporulation: A question of commitment? *Current Biology, 8*(2), R45-R48. doi: http://dx.doi.org/10.1016/S0960-9822(98)70031-4

Suter, D. M., Errante, L. D., Belotserkovsky, V., & Forscher, P. (1998). The Ig Superfamily Cell Adhesion Molecule, apCAM, Mediates Growth Cone Steering by Substrate-cytoskeletal Coupling. *The Journal of Cell Biology, 141*(1), 227-240.

Tai, S. K., Lin, H. P., Kuo, J., & Liu, J. K. (2004). Isolation and characterization of a cellulolytic Geobacillus thermoleovorans T4 strain from sugar refinery wastewater. *Extremophiles, 8*(5), 345-349.

Touhami, A., Jericho, M. H., & Beveridge, T. J. (2004). Atomic force microscopy of cell growth and division in Staphylococcus aureus. *Journal of Bacteriology, 186*(11), 3286-3295. doi: 10.1128/jb.186.11.3286-3295.2004

Touhami, A., Jericho, M. H., Boyd, J. M., & Beveridge, T. J. (2006). Nanoscale characterization and determination of adhesion forces of Pseudomonas aeruginosa Pili by using atomic force microscopy. *Journal of Bacteriology, 188*(2), 370-377. doi: 10.1128/jb.188.2.370-377.2006

Tripathi, P., Beaussart, A., Andre, G., Rolain, T., Lebeer, S., Vanderleyden, J., . . . Dufrene, Y. F. (2012). Towards a nanoscale view of lactic acid bacteria. *Micron, 43*(12), 1323-1330. doi: 10.1016/j.micron.2012.01.001

Ubbink, J., & Schär-Zammaretti, P. (2005). Probing bacterial interactions: integrated approaches combining atomic force microscopy, electron microscopy and biophysical techniques. *Micron, 36*(4), 293-320. doi: http://dx.doi.org/10.1016/j.micron.2004.11.005

Vadillo-Rodriguez, V., Busscher, H. J., Norde, W., De Vries, J., Dijkstra, R. J., Stokroos, I., & Van Der Mei, H. C. (2004). Comparison of atomic force microscopy interaction forces between bacteria and silicon nitride substrata for three commonly used immobilization methods. *Appl Environ Microbiol, 70*(9), 5441-5446. doi: 10.1128/aem.70.9.5441-5446.2004

Verbelen, C., Christiaens, N., Alsteens, D., Dupres, V., Baulard, A. R., & Dufrêne, Y. F. (2009). Molecular Mapping of Lipoarabinomannans on Mycobacteria. *Langmuir, 25*(8), 4324-4327. doi: 10.1021/la900302a

Walstra, P., Geurts, T. J., Noomen, A., Jellema, A., & van Boekel, M. A. J. S. (1999). *Dairy Technology*. New York: Marcel Dekker, Inc.

Warth, A. D., & Strominger, J. L. (1972). Structures of Peptidoglycan from Spores of Bacillus subtilis. *Biochemistry, 11*, 7.

Wiencek, K. M., Klapes, N. A., & Foegeding, P. M. (1990). Hydrophobicity of Bacillus and Clostridium Spores. [Article]. *Applied and Environmental Microbiology, 56*(9), 2600-2605.

Yamashita, H., Taoka, A., Uchihashi, T., Asano, T., Ando, T., & Fukumori, Y. (2012). Single-Molecule Imaging on Living Bacterial Cell Surface by High-Speed AFM. *Journal of Molecular Biology, 422*(2), 300-309. doi: 10.1016/j.jmb.2012.05.018

Yildiz, F., & Westhoff, D. C. (1989). Sporulation and thermal resistance of Bacillus stearothermophilus spores in milk. *Food Microbiology, 6*(4), 245-250. doi: 10.1016/s0740-0020(89)80005-x

Zeigler, & Daniel, R. (2001). The Genus Geobacillus. *Bacillus Genetic Stock Center, 3*.